NOVEL MODEL SYSTEMS FOR IN VITRO NEUROTOXICITY TESTING

CHEMICAL STRESSORS AND NEUROTOXIC HAZARD OF EXTREMELY LOW FREQUENCY ELECTROMAGNETIC FIELDS

MARTJE DE GROOT • 2016

Novel model systems for *in vitro* neurotoxicity testing

Chemical stressors and neurotoxic hazard of extremely low frequency electromagnetic fields

Martina Wilhelmina Gijsberta Didyma Maria de Groot

2016

Novel model systems for *in vitro* neurotoxicity testing. Chemical stressors and neurotoxic hazard of extremely low frequency electromagnetic fields.

ISBN/EAN:978-90-393-6462-8

Layout and printing: Proefschrift-aio.nl
Illustrations: Thomas van de Loo
Cover design: Marlon van den Besselaar

The studies described in this thesis were performed at the Neurotoxicology Research Group, Toxicology Division, at the Institute for Risk Assessment Sciences (IRAS), Faculty of Veterinary Medicine, Utrecht University.

Novel model systems for *in vitro* neurotoxicity testing

Chemical stressors and neurotoxic hazard of extremely low frequency electromagnetic fields

Nieuwe modelsystemen voor het testen van neurotoxiciteit *in vitro*

Chemische stress en neurotoxiciteit van extreem laagfrequente elektromagnetische velden

(met een samenvatting in het Nederlands)

Proefschrift

ter verkrijging van de graad van doctor aan de Universiteit Utrecht op gezag van de rector magnificus prof. dr. G.J. van der Zwaan, ingevolge het besluit van het college voor promoties in het openbaar te verdedigen op donderdag 28 januari 2016 des middags te 4.15 uur

door

Martina Wilhelmina Gijsberta Didyma Maria de Groot

geboren op 1 oktober 1987 te Delft

Promotor: Prof. dr. M. van den Berg
Copromotor: Dr. R.H.S. Westerink

This study was supported by the Netherlands Organization for Health Research and Development (ZonMw grant number 85300003: Elektromagnetische Velden en Gezondheid).

At first glance it may appear too hard. Look again. Always look again.

- Mary Anne Rodmacher -

Table of contents

Chapter 1
General introduction 11

Chapter 2
Toxicological endpoints and applied methodologies 25

Part I: Models in *in vitro* neurotoxicity testing 39

Chapter 3
Chemically-induced oxidative stress increases the vulnerability of PC12 cells to rotenone-induced toxicity 41

Chapter 4
Don't judge a neuron only by its cover: neuronal function in *in vitro* developmental neurotoxicity testing 65

Chapter 5
Characterization of calcium responses and electrical activity in differentiating mouse neural progenitor cells *in vitro* 83

Part II: Neurotoxic effects of ELF-EMF *in vitro* 107

Chapter 6
Assessment of the neurotoxic potential of exposure to 50 Hz extremely low frequency electromagnetic fields (ELF-EMF) in naïve and chemically stressed PC12 cells 109

Chapter 7
In vitro developmental neurotoxicity following chronic exposure to 50 Hz extremely low frequency electromagnetic fields (ELF-EMF) in primary rat cortical cultures 133

Chapter 8
Summary, general discussion and conclusions 161

References 185
Nederlandse samenvatting 209
Dankwoord 219
About the author 227

Abbreviations

$[Ca^{2+}]_i$	intracellular calcium concentration
AB	Alamar Blue
AC	alternating current
ACh	acetylcholine
AD	Alzheimer's disease
ALS	amyotrophic lateral sclerosis
AM	acetoxymethyl
ANOVA	analyses of variance
AP	action potential
B	magnetic field flux density
Ca^{2+}	calcium
CFDA	5-carboxyfluorescein diacetate
CNS	central nervous system
DAPI	4′,6-diamidino-2-phenylindole
DC	direct current
DCF	2',7'-dichlorofluorescein
DEX	dexamethasone
DIV	days *in vitro*
DMSO	dimethylsulfoxide
DNT	developmental neurotoxicity
DR	depolarization ratio
E	electric field strength
E14	embryonic day 14
EDTA	ethylenediamine tetraacetic acid
ELF	extremely low frequency
ELF-EMF	extremely low frequency electromagnetic field
EMF	electromagnetic field
ER	endoplasmic reticulum
F_{340}	340 nm excitation wavelength
F_{380}	380 nm excitation wavelength
$FeSO_4$	iron(II) sulfate
G	Gauss
GABA	γ-aminobutyric acid
GFAP	glial fibrillary acidic protein
H_2-DCFDA	2',7'-dichlorodihydrofluorescein diacetate
Hz	Hertz

IARC	international agency for research on cancer
IC_{50}	50% Inhibitory concentrations
ICNIRP	international commission on non-Ionizing radiation protection
K^+	potassium
K_{d*}	dissociation constant of Fura-2
L-DOPA	L-3,4-dihydroxydopamine
MEA	multielectrode array
mISI	median interspike interval
mNPC	mouse neural progenitor cell
MSR	mean spike rate
Na^+	sodium
NPC	neural progenitor cell
NR	neutral red
NSC	neural stem cell
PBS	phosphate buffered saline
PC12	pheochromocytoma cell line
PD	Parkinson's disease
PFA	paraformaldehyde
PLL	poly-L-lysine
PND	postnatal day
R	F_{340}/F_{380} ratio
R_{max}	maximum ratio
R_{min}	minimum ratio
rms	root mean square
ROS	reactive oxygen species
rt	room temperature
SD	standard deviation
SN	substantia nigra
SEM	standard error of the mean
TR	treatment ratio
T	Tesla
V/m	volts per metre
VGCCs	voltage-gated calcium channels

CHAPTER 1

General introduction

1.1 Neuronal function

The main function of the nervous system is to send and receive signals; so-called neurotransmission. The (central) nervous system controls body systems via direct nervous control (e.g. the cardiovascular system) or indirect via input into glands (e.g. the endocrine system). To send and receive signals, neurons have a specialized structure (Figure 1). They contain dendrites to receive input from other neurons and an axon with axon terminals that connect the neuron to (an)other neuron(s) via synapses. When a neuron receives an excitatory chemical signal via its dendrites, it becomes activated and generates an electrical signal (action potential [AP]) via the opening of voltage-sensitive sodium and potassium channels. The AP then travels along the axon to reach the synapse at the axon terminal. In the synapse, the electrical signal triggers the opening of voltage-gated calcium channels (VGCCs). Subsequently, the signal is translated into a chemical signal via the release of neurotransmitters into the synaptic cleft, which in turn activate receptors on the membrane of the next cell. In the receiving cell, the chemical signal can be translated into an AP again or it can activate intracellular signaling pathways, provided a sufficient number of receptors is activated. Afterwards, degradation or reuptake of the neurotransmitter from the synaptic cleft terminates the signal transduction (reviewed in Westerink, 2006).

Neuronal signaling thus depends largely on the viability and structure of neurons as well as on proper regulation of the cellular and molecular mechanisms underlying neurotransmission, in particular intracellular calcium signaling.

1.1.1 Intracellular calcium signaling

Calcium ions (Ca^{2+}) impact nearly every aspect of cellular life. Changes in intracellular Ca^{2+}-concentrations ($[Ca^{2+}]_i$) are involved in many (sub) cellular processes, including proliferation, excitability, motility, plasticity, apoptosis, and gene transcription. $[Ca^{2+}]_i$ is therefore tightly regulated by influx, buffering, compartmentalization in cellular structures (e.g. endoplasmic reticulum [ER] and mitochondria) and extrusion mechanisms (reviewed in Berridge *et al*., 1999 and Clapham, 2007).

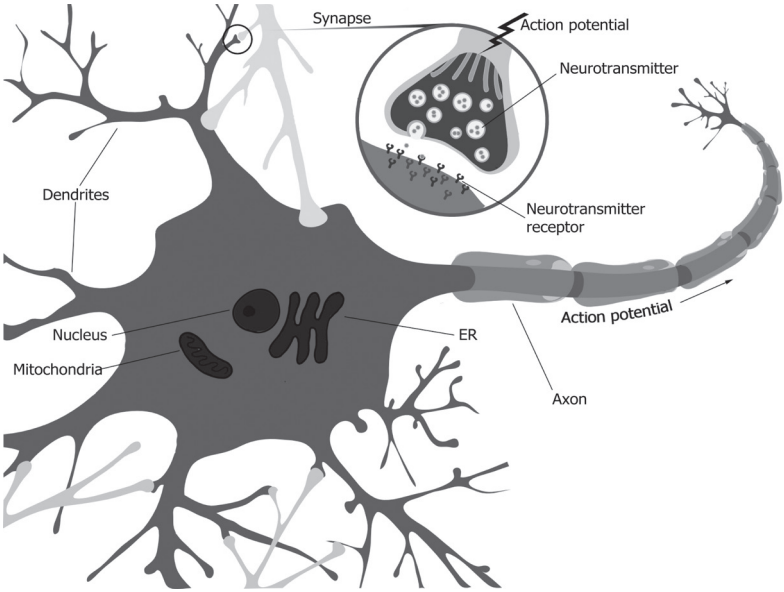

Figure 1. Schematic representation of neuronal structure and signaling. Abbreviations: ER, endoplasmic reticulum.

In neuronal cells, the influx of Ca^{2+} through voltage-gated channels is the classical trigger that activates the exocytotic release machinery and initiates vesicular neurotransmitter release (Westerink, 2006, Neher and Sakaba, 2008, Barclay *et al.*, 2005). $[Ca^{2+}]_i$ is thus essential for the regulation of neuronal communication, but it is also involved in neuronal differentiation, neurite outgrowth and axonal pathfinding (Rusanescu *et al.*, 1995, Neher and Sakaba, 2008, Arie *et al.*, 2009, Leclerc *et al.*, 2011).

1.1.2 Neurotoxicity of environmental insults

Both structurally and functionally, the nervous system is one of the most complex organ systems. The function of neuronal networks not only depends on proper intracellular signaling, but also on the presence of other neural cell types, including oligodendrocytes, microglia, and astrocytes (**Chapter 4**). The

nervous system is particularly sensitive to toxic insults and the regenerative capacity of nerve cells is limited. Any adverse effect on the chemistry, structure and function of the nervous system, induced by chemical (e.g. pesticides, heavy metals) or physical (e.g. ionizing radiation) influences is called neurotoxicity (Costa, 1998). Neurotoxicity following environmental exposures is often investigated *in vivo* (in accordance with regulatory guidelines), but can also be investigated using *in vitro* model systems. *In vitro* systems have the potential to improve understanding of basic physiological processes of neuronal cells and can be used to study the mechanisms underlying neurotoxic effects (Westerink, 2013). Different *in vitro* approaches to study the nervous system have been characterized and validated over the last decades (also see Costa *et al.*, 2011b and Walsh *et al.*, 2005).

Effects of chemical exposures have successfully been investigated *in vitro* and concentration-response relationships for neurotoxicity of a variety of chemicals have been established. Moreover, biological mechanisms underlying neurotoxicity have been (partially) unraveled using *in vitro* approaches. More difficulties arise when investigating physical exposures, especially when they have only limited energy and are therefore unlikely to cause direct effects on cell viability or function. A much investigated, and controversial, example of such a physical exposure involves electromagnetic fields (EMF), in particular extremely low frequency (ELF)-EMF.

1.2 Electromagnetic fields (EMF)

In modern day society, we use electricity on a daily basis and it is almost impossible to imagine life without it. Both in home and in occupational settings, we are surrounded by electricity. Whenever it is generated, transmitted, distributed or used, electromagnetic fields (EMF) exist, consisting of both an electric and a magnetic field.

An electric field is created by a difference in voltage and its strength (E) is expressed in volts per meter (V/m), whereas a magnetic field is created when electrical current flows and its flux density (B) is expressed in Tesla (T).

Alternatively, flux density can be expressed in Gauss (G), with 1 μT=10 mG (World Health Organization, 2007a). An electric field is even present without current flowing and when current starts to flow, it is constant. However, the magnetic field is not present without a current and its strength will vary with changes in power consumption. This current can either flow in one direction (direct current [DC]) or alternate (alternating current [AC]) and therefore generates static or time-varying fields, respectively. In practice, the generated field is a simple sinusoid or may be more complex, indicating the presence of harmonics (IARC Working Group, 2002). The strength of an electric field increases with increasing voltage, whereas a magnetic field increases with increasing current.

EMF are described by their frequency, wavelength or photon energy. These parameters are (inversely) proportional to one another, as described in the following formulas: $f=\frac{c}{\lambda}$; $f=\frac{E}{h}$; or $E=\frac{hc}{\lambda}$, where f is frequency, λ wavelength, E photon energy, c the speed of light in vacuum and h Planck's constant. With increasing frequency, photon energy increases directly proportional, whereas wavelength increases inversely proportional. The electromagnetic spectrum (Figure 2) covers the range of possible frequencies of electromagnetic waves. Types of EMF can be categorized by their frequency (expressed in Hertz [Hz]) and range from direct current to gamma rays.

Based on the energy the waves carry per quantum (the particles that carry the wave), EMF can be divided into non-ionizing or ionizing radiation. Ionizing waves carry so much energy that they can break bonds between molecules, whereas non-ionizing waves carry insufficient energy to break these bonds. As photon energy is directly proportional to frequency, the high frequency EMF are ionizing (e.g. x-rays and gamma-rays, Figure 2).

1.2.1 Extremely low frequency electromagnetic fields (ELF-EMF)

EMF with frequencies between 3 and 300 Hz are so-called extremely low frequency (ELF)-EMF (World Health Organization, 2007a). The exact frequencies depend on the definition, e.g. frequencies between 3–3000 Hz are also

referred to as ELF-EMF (IARC Working Group, 2002). Electric and magnetic fields in the ELF range are mostly associated with man-made sources, including high-tension power lines, electric power systems and electronic appliances for consumer and industrial use. The latter mostly operate at a frequency of 50 or 60 Hz (Europe and Northern America, respectively), also called power-frequency fields (IARC Working Group, 2002, World Health Organization, 2007b).

Power frequency electrical fields are able to cause well-defined biological responses through surface *electric* charge effects, ranging from perception to annoyance and spark discharges (World Health Organization, 2007b, National Radiological Protection Board, 2004). These effects are generally relatively subtle and transient. Electric fields and currents generated within the body by power frequency magnetic fields can, if sufficiently large, cause stimulation of nerves and muscles or affect other biological processes via interference with endogenous currents (World Health Organization, 2007b, National Radiological Protection Board, 2004, Santini *et al.*, 2009). Most of the epidemiological research on ELF-EMF has focused on the magnetic, rather than on the electric fields, although effects of the electric fields have been studied as well (Kheifets *et al.*, 2010b). The research presented in this thesis focused on effects of 50 Hz EMF magnetic fields.

Because of their low frequency, 50 Hz EMF are non-ionizing and unable to break bonds between molecules (Otto and von Muhlendahl, 2007). Moreover, they are not likely to induce thermal effects in humans (Pall, 2013, World Health Organization, 2007a), although their low frequency does enable the magnetic field to penetrate deep into tissues (e.g. muscle, heart or brain).

1.2.2 ELF-EMF and health effects

Already in the 1960s, researchers started gathering data on the health risks of ELF-EMF from studies of workers with high occupational exposure. Since then, a lot of research has been performed, including epidemiological and experimental *in vivo* and *in vitro* studies. Most profoundly, ELF-EMF exposure

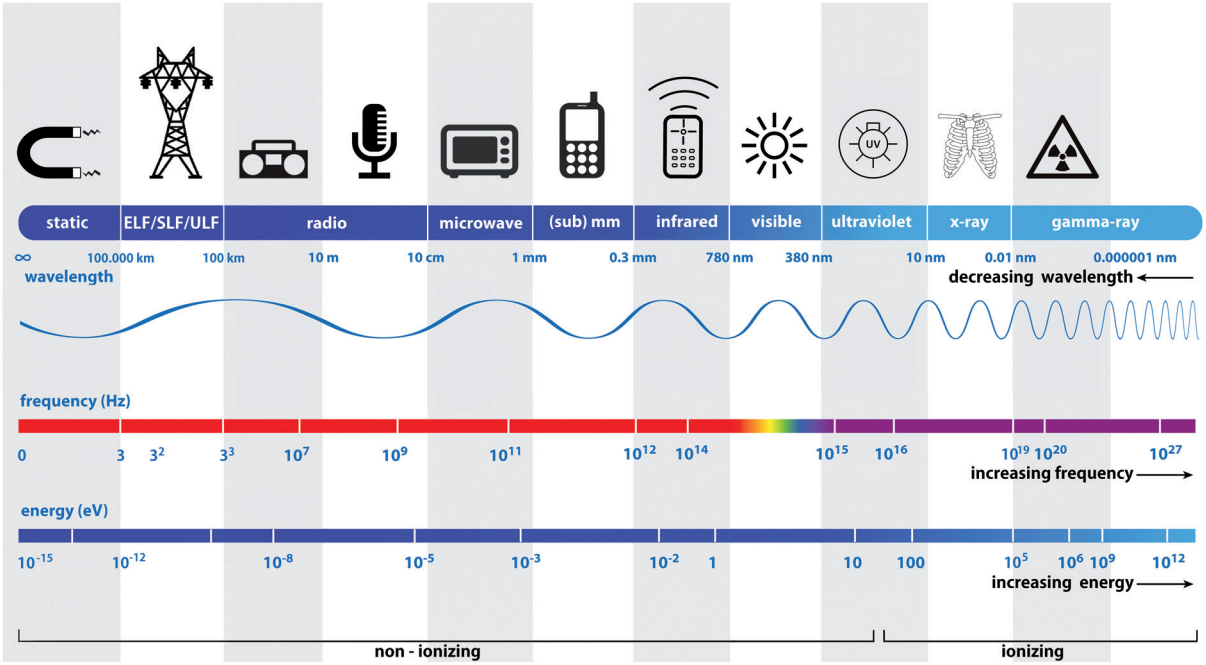

Figure 2. The electromagnetic spectrum depicting the range of possible frequencies of electromagnetic radiation, together with the associated wavelengths and energy. Abbreviations: ELF, extremely low frequency; ULF, ultra low frequency; SLF, super low frequency.

has been associated with an increased incidence of childhood leukemia. This was first suggested by Wertheimer and Leeper in 1979, who found an association between living near high-tension transmission lines and the incidence of childhood leukemia (Wertheimer and Leeper, 1979). This study led to increased scientific and societal interest concerning ELF-EMF health effects and resulted in more research into the potential (carcinogenic) effects of ELF-EMF. Since then, the association between ELF-EMF and childhood leukemia has been confirmed in several studies (Li et al., 1998, Li *et al.*, 2009, Ahlbom *et al.*, 2000, Greenland *et al.*, 2000, Hardell and Sage, 2008, Kheifets *et al.*, 2010a, Teepen and van Dijck, 2012), demonstrating a consistent (approximate) two-fold increase in childhood leukemia associated with average exposure to residential power-frequency magnetic field above 0.3 to 0.4 μT (World Health Organization, 2007b). However, it has also been suggested that the observed association can be due to selection bias, misclassification, chance or other confounding factors such as time or socioeconomic status (Kheifets and Shimkhada, 2005, Bunch *et al.*, 2014). Nonetheless, these epidemiological findings led to the classification of ELF-magnetic fields as a "possible human carcinogen" (group 2B) by the International Agency for Research on Cancer (IARC; IARC Working Group, 2002), a classification used to denote an agent for which there is limited evidence of carcinogenicity in humans and less than sufficient evidence for carcinogenicity in experimental animals (World Health Organization, 2002).

Since Wertheimer and Leeper, other health effects of ELF-EMF exposure have also been investigated, including effects on cardiovascular disorders, immunology and haematology and (other types of) cancer (Feychting *et al.*, 2005, World Health Organization, 2007a, IARC Working Group, 2002, National Institute of Environmental Health Sciences, 2002, International Commission on Non-Ionizing Radiation Protection, 2010, Ahlbom *et al.*, 2001). However, relatively few studies have focused on effects of the nervous system, which is surprising given the vulnerability of the nervous system. Moreover, its function depends on the use of electrical signals (see 1.1 Neuronal function) and it is therefore considered to be particularly sensitive to ELF-EMF.

In neurotoxicology it is well established that the developing nervous system (Rice and Barone, 2000) as well as the stressed or aging nervous system (Gandhi and Abramov, 2012, Lin and Beal, 2006) are especially sensitive for environmental insult. Moreover, the development of neuronal cells into functional neural networks is highly dependent upon electrical activity (van Oss and van Ooyen, 1997, Butz et al., 2009, van Ooyen, 1994) and many of the processes that define neuronal functionality and connectivity are modulated by electrical activity (e.g. gene expression, cell death, transmitter receptor function and expression, neurite outgrowth and neuron-glia interactions; Butz *et al.*, 2009). Disturbance of this spontaneous activity by external influences (like ELF-EMF) could disrupt normal network development and thereby alter neuronal network structure and/or function.

The studies that have been performed regarding ELF-EMF effects on different aspects of the nervous system's function (e.g. cognitive, behavioral and neuroendocrine responses), have mainly focused on degeneration, e.g., Alzheimer's disease and amyotrophic lateral sclerosis (for reviews see Feychting *et al.*, 2005, World Health Organization, 2007a, IARC Working Group, 2002, National Institute of Environmental Health Sciences, 2002, and International Commission on Non-Ionizing Radiation Protection, 2010). From these reports it becomes clear that these ELF-EMF studies are often hard to reproduce and that conclusions are often weakened by experimental shortcomings. Moreover, there is lack of biological plausibility for any of the associations (World Health Organization, 2007a). At present, there is insufficient evidence to conclude that ELF electric and/or magnetic fields affect neurobehavioral, neuroendocrine of neurodegenerative processes in a way that adversely impacts human health. However, it is also not possible to conclude that there is no effect of ELF-EMF on the nervous system.

In view of these uncertainties and given the high societal and scientific interest in the effects of ELF-EMF exposure, part of this thesis will focus on the potential effects of 50 Hz magnetic fields on the structure and function of neuronal cells *in vitro*. Using different and sensitive *in vitro* models for adult,

aging/stressed and developing neuronal cells, the potential neurotoxic effects of a variety of EMF exposure scenarios and field strengths could be thoroughly investigated. At the same time, the use of *in vitro* models allows for the investigation of the biological mechanisms underlying any observed effects.

1.3 Thesis outline

The research presented in this thesis aims at developing and characterizing novel *in vitro* models for neurotoxicity testing, with a special focus on developmental neurotoxicity testing (Part I) and to subsequently use some of these *in vitro* models to investigate the potential neurotoxicity of exposure to 50 Hz ELF-EMF *in vitro* (Part II).

The cell models, techniques and methods that were used in the different chapters of this thesis are summarized in **Chapter 2**. All of these models were carefully selected and characterized prior to being used to assess the neurotoxicity of external influences (i.e. chemical or physical). The first part of this thesis (**Chapter 3–5**) will focus on the evaluation and characterization of different *in vitro* neurotoxicity models.

The stressed or aging nervous system is associated with increased vulnerability, mitochondrial dysfunction, oxidative damage, and accumulation of mutations in mitochondrial DNA and/or reactive oxidative species (ROS; Gandhi and Abramov, 2012, Hung *et al.*, 2010, Lin and Beal, 2006, Raha and Robinson, 2000). To mimic stressed or aging neuronal cells, PC12 cells were pre-treated with different compounds that increase their production of ROS to obtain a chemically stressed phenotype. To assess if these phenotypes indeed show increased vulnerability to an external insult, these chemically stressed PC12 were functionally characterized in the presence or absence of a chemical exposure in **Chapter 3**.

Although working with cell lines like the (chemically stressed) PC12 cells has clear advantages, other (primary) cell models may be more suitable when investigating effects on the developing nervous system. In **Chapter 4**, the

focus is therefore on *in vitro* models and innovative experimental approaches for functional (developmental) neurotoxicity testing. It presents an overview of different cell models and endpoints to select when studying developmental neurotoxicity (DNT), with emphasis on the use of functional endpoints.

Primary cultures (e.g. rat cortical cultures) and stem- or progenitor cells are examples of suitable cell models to investigate DNT effects of ELF-EMF exposure. In **Chapter 5**, mouse neuronal progenitor cells are characterized as a model to study (functional) effects of external stimuli on the developing nervous system.

The second part of this thesis will focus on investigating the possible neurotoxic effects of extremely low frequency electromagnetic field (ELF-EMF) exposure, using a variety of exposure scenarios in different *in vitro* models for adult, stressed or aging and developing neuronal cells (**Chapter 3–5**).

Earlier studies indicated that ELF-EMF effects are often inconsistent and/or have small effect sizes. Moreover, it is hard to compare studies due to the use of different cell types, exposure systems, exposure durations and/or field strengths. Possibly the biggest limitation is the lack of knowledge on the molecular and cellular mechanisms underlying the presumed (neurotoxic) effects of ELF-EMF (Schuz *et al.*, 2009, Johansen, 2004). Also, potential vulnerable conditions, including stressed, aging or developing systems, are underrepresented in current (*in vitro*) ELF-EMF research. There is thus a clear need to study the effect of ELF-EMF exposure on neuronal development and function *in vitro*.

Due to its high energy demand and limited anti-oxidant systems, the nervous system is sensitive to oxidative stress and thus particularly vulnerable for external influences that negatively affect their oxidative status (e.g. tobacco smoke, alcohol and ionizing radiation). Oxidative stress has consequently been linked to neuronal cell death in several neurodegenerative diseases (Ruszkiewicz and Albrecht, 2015, Halliwell, 2006). Moreover, ELF-EMF

exposure has previously been linked to altered cellular anti-oxidant capacity in both *in vitro* and *ex vivo* neuronal models (Falone *et al.*, 2007, Falone *et al.*, 2008, Morabito *et al.*, 2010, Ciejka *et al.*, 2011, Di Loreto *et al.*, 2009, Park *et al.*, 2013). To investigate effects of acute and (sub-) chronic ELF-EMF exposure on membrane integrity, ROS production and calcium homeostasis in adult, stressed or aging neuronal cells, both naïve as well as chemically stressed PC12 cells were exposed to ELF-EMF in **Chapter 6**.

Chapter 7 describes research on effects of ELF-EMF exposure on the developing nervous system. As apparent from **Chapter 4** and **5**, mouse neural progenitor cells (mNPCs) are a state of the art model system. However, mNPCs are still being (functionally) characterized for their use in (developmental) neurotoxicology and they have some shortcomings compared to other developmental models, including robustness and throughput. Primary cortical cultures on the other hand have been investigated for several decades and are still widely used in the field of neurotoxicology. They have proven to be a valuable tool to study neuronal function and developmental neurotoxicity and are the current standard for studying neuronal signaling using the multielectrode array (MEA; Hogberg *et al.*, 2011). In **Chapter 7** primary rat cortical cultures were therefore used to assess effects of chronic, developmental ELF-EMF exposure on neuronal function.

At the end of this thesis the findings on ELF-EMF exposure (**Chapters 6** and **7**) will be summarized and placed in the context of available literature in the general discussion (**Chapter 8**).

CHAPTER 2

Toxicological endpoints and applied methodologies

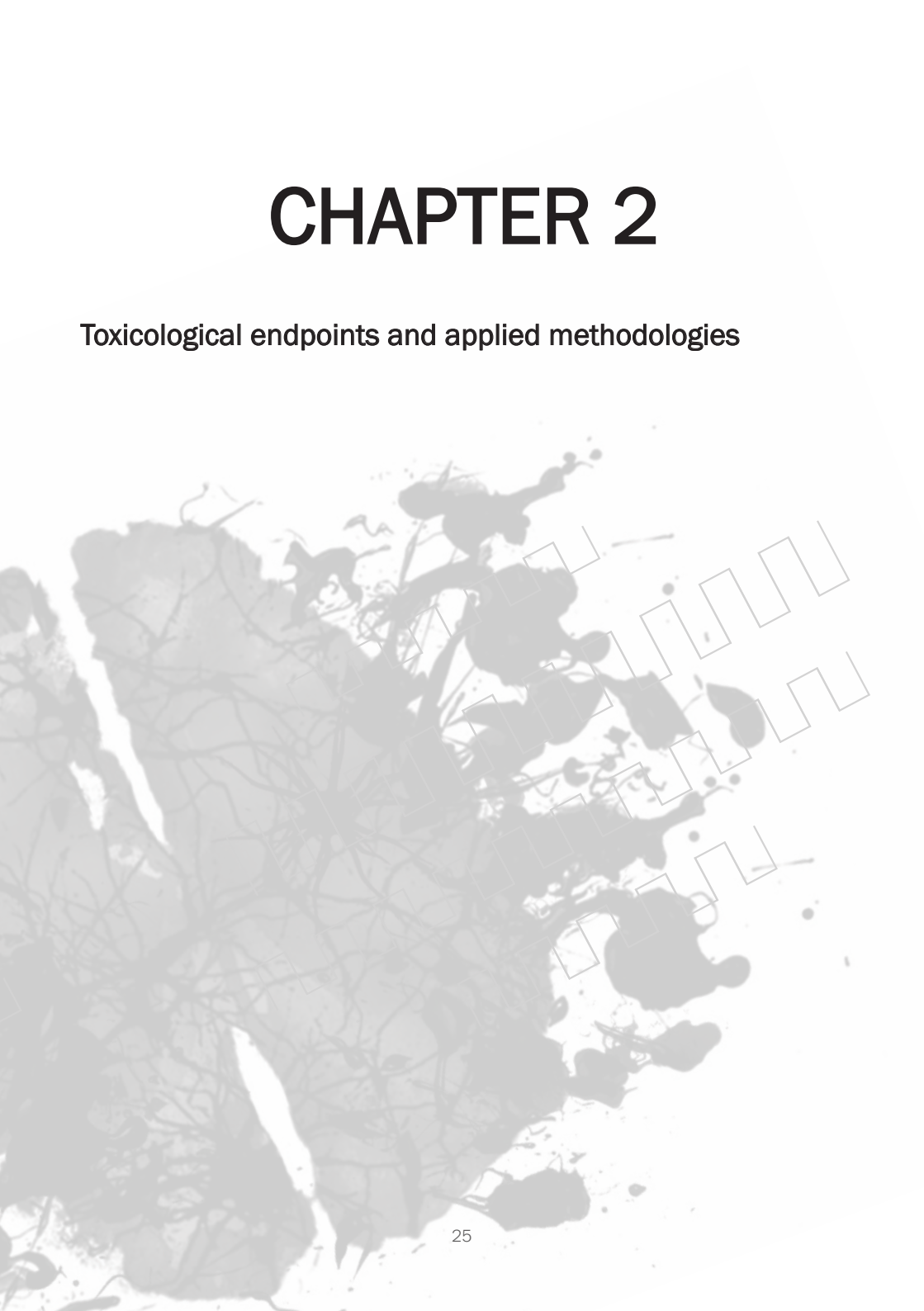

There are many *in vitro* approaches to study the nervous system that are more time- and cost effective than the conventional animal experiments. Additionally, *in vitro* approaches have the potential to provide insight into cellular and molecular mechanism underlying observed toxicities. Although these *in vitro* approaches serve a useful purpose, it is important to choose the appropriate approach, depending on the research question at hand, as each approach has its advantages and disadvantages (reviewed in Chapter 4). In the following chapters of this thesis, both *in vitro* cell lines and *ex vivo* primary cell cultures are characterized and used as models for (developmental) neurotoxicity testing of ELF-EMF exposure. The cell models used in this thesis (Chapter 2.1) are exposed to ELF-EMF (Chapter 2.2) and subsequently evaluated on a variety of endpoints (Chapter 2.3).

2.1 *In vitro* and *ex vivo* models

2.1.1 Pheochromocytoma (PC12) cell line (Chapter 3 and 6)

The pheochromocytoma (PC12) cell line is derived from a rat adrenal tumor (Greene and Tischler, 1976). PC12 cells divide rapidly, are easily cultured and well characterized, making them a popular model. Indeed, they are extensively being used in neuroscience, e.g. to study the molecular machinery underlying vesicular neurotransmitter release (exocytosis; Khvotchev *et al.*, 2007, Shin *et al.*, 2002, Westerink, 2004, Westerink and Ewing, 2008) and in neurotoxicology to study the effects of environmental pollutants on neuronal development, function and degeneration (Westerink and Ewing, 2008, Shafer and Atchison, 1991, Westerink, 2013).

PC12 cells contain functional voltage-gated calcium channels (VGCCs), predominantly the L-type, but also the N- and P/Q-type VGCCs, which account for ~20% of total Ca^{2+}-influx during depolarization (Dingemans *et al.*, 2010b, Heusinkveld *et al.*, 2010).

Although PC12 cells are chromaffin-derived cells, their Ca^{2+}-homeostasis resembles that of sympathetic neurons (Duman *et al.*, 2008). Comparable to neuronal cells, the main influx route for Ca^{2+} into PC12 cells is via VGCCs,

which open upon depolarization with potassium (K^+). The rapid influx of Ca^{2+} through VGCCs can trigger various intracellular processes, including neurotransmitter release.

PC12 cells can be differentiated or pre-treated with several (pharmacological) agents to modify their phenotype. For example, differentiation of naïve PC12 cells with dexamethasone (DEX) is known to enhance the synthesis and secretion of catecholamines (~99% dopamine), while cells maintain functional calcium homeostasis and neurotransmitter receptors function (Elhamdani *et al.*, 2002, Taylor and Peers, 1999, Westerink and Vijverberg, 2002, Taylor and Peers, 2000, Westerink *et al.*, 2002).

2.1.2 Mouse neural progenitor cells (Chapter 5)

Both the adult and embryonic nervous system contains populations of multipotent neural progenitor cells (NPCs) that are derived from cells of ectodermal lineage (Breier *et al.*, 2010). These multipotent progenitor cells can be applied to generate a heterogeneous neural culture containing neurons, astrocytes and oligodendrocytes, as progenitor cells already have some characteristics from the region from which they are isolated (Breier *et al.*, 2010, Davila *et al.*, 2004). mNPCs are typically characterized by the expression (RNA or immunoreactivity) of one or more phenotypic markers, such as β(III)-tubulin for neurons, nestin for stem/neural progenitor- and glial fibrillary acidic protein (GFAP) for glial cells (Breier *et al.*, 2010).

mNPCs can be cultured in the proliferation phase to proliferate and expand in suspended sphere form. Upon removal of certain growth factors, the cells stop dividing and differentiate into multiple cell types (Breier *et al.*, 2010, de Groot *et al.*, 2014a). Cultured neural progenitor cells can be used to imitate basic processes of brain development *in vitro*, which can be modulated by developmental neurotoxicants (Moors *et al.*, 2009). As such, this model can be used to tests chemicals for their ability to affect neuronal proliferation, migration, differentiation and apoptosis (Fritsche *et al.*, 2011).

Moreover, differentiated mNPCs have functional neuronal characteristics *in vitro* similar to neurons *in vivo* (see Chapter 5).

The use of stem- and progenitor cells in neurotoxicology is relatively new and they are still being characterized and validated. Nevertheless, they have great potential as a model for developmental neurotoxicity (DNT) testing (Fritsche *et al.*, 2011, Moors *et al.*, 2009).

2.1.3 Rat primary cortical cultures (Chapter 7)

For decades, cultures of dissociated primary neurons have been a popular research tool (Mains and Patterson, 1973, Dichter, 1978). Already in 1978, Dichter described using cells isolated from embryonic rat cortices to study the development of neuronal structure, function and synaptic connections *in vitro* (Dichter, 1978). At present, rat primary cortical cultures are still widely being used to study (developmental) neurotoxicity (Robinette *et al.*, 2011, Hogberg *et al.*, 2011).

Primary cortical cultures are well characterized and widely used in the field of (developmental) neurotoxicology. Similar to the NPCs, *ex vivo* cultures of cortical cells have been shown to contain different cell types (Hogberg *et al.*, 2011). Moreover, the most critical neurodevelopmental processes, such as progenitor cell commitment, proliferation and differentiation of astrocytes and maturation of neurons are present in these cultures (Hogberg *et al.*, 2011). When cultured on multielectrode array (MEA) plates (Chapter 2.3.3), cortical cultures develop spontaneous network activity with action potentials and organized patterns of action potential bursts (Robinette *et al.*, 2011).

2.2. Extremely low frequency (ELF)-EMF exposure systems

The different cell models used in this thesis were exposed to 50 Hz ELF-EMF using custom-made exposure apparatus (Immunent BV, Velthoven, The Netherlands). For acute exposure during Ca^{2+}-imaging (Chapter 6), block-pulsed ELF-EMF with a main frequency of 50 Hz (<10% harmonics) and

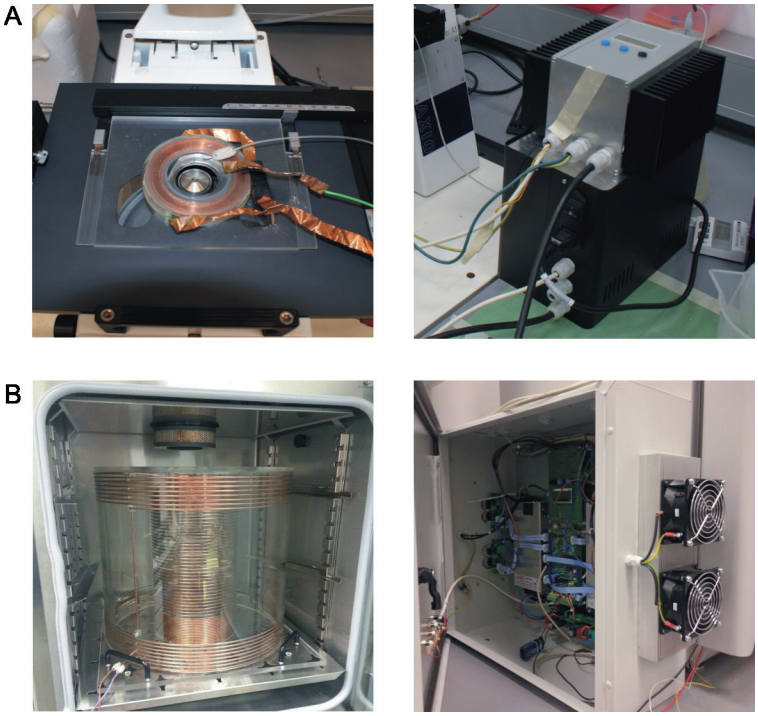

Figure 1. ELF-EMF exposure devices. **A.** Microscope-fitted copper coils (left) for ELF-EMF exposure during acute experiments and connected signal generator (right) with preprogrammed signals. **B.** Incubator-fitted copper coils (left) for (sub-) chronic exposure experiments and connected signal generator (right) with preprogrammed signals.

different intensities (1–1000 μT rms) were generated using a copper coil fitted to the stage of the fluorescence microscope (Figure 1A). For chronic and developmental exposure experiments (Chapter 6 and 7), ELF-EMF were generated using a copper coil fitted into an incubator (Figure 1B).

Both exposure systems consist of double copper wired solenoid coils connected to a signal generator with preprogrammed exposure protocol. The

copper coils consist of one continuous copper conductor, ensuring equal current in different coil components. Both systems generate AC and DC vertical field components with field strengths (B_{AC} and B_{DC}) in the range from 1 to 1000 µT. Field strengths were calibrated and monitored using an EMDEX II Tesla meter (Enertech Consultants, Campbell, California, USA) and the coil current was regularly monitored by a Tenma 72-7226 clamp meter (Tenma Test Equipment, Springboro, OH, USA).

To ensure similar treatment between exposed and control groups, cells in the control groups were sham-exposed by placing them in the switched-off microscope-fitted coil (approximately 0.2 µT, i.e. background ELF-EMF from the fluorescence microscope set-up) for acute experiments or in a second identical incubator (approximately 0.4 µT, i.e. background ELF-EMF generated by the incubator) for chronic experiments.

2.3 Toxicological endpoints

2.3.1 Measurements of cell stress, damage and death

Cell viability is often assessed to screen the potential of a certain exposure to cause cell death (cytotoxicity). Moreover, it can be assessed to exclude that exposure effects on other readouts are confounded by cytotoxicity.

Alamar Blue assay (Chapter 7)

The Alamar Blue (AB) assay has been used for over 50 years to assess cell viability and cytotoxicity in a range of biological and environmental systems and in a number of cell types (Rampersad, 2012). The Alamar Blue assay is based on the reduction of the non-toxic and non-fluorescent resazurin to the fluorescent resorufin by mitochondrial reductases (including complex 1) in viable cells. The read-out from the AB assay thus provides a measure of mitochondrial activity and is therefore an indicator of the cell's energy metabolism (Magnani and Bettini, 2000). As such the AB assay is used as a measure of cell viability. Under most circumstances, the AB assay does not require washing steps, thereby limiting potential confounding of the outcome by cell detachment. A potential disadvantage of the assay is that increases

in mitochondrial activity could mask true effects on cell viability. However, as resorufin is excreted from the cell and the cells do not need to be lysed prior to measurement, the AB assays allows for combination with a second independent assay for cell viability such as the CFDA-AM and/or NR assay.

CFDA-AM assay (Chapter 6 and 7)

5-Carboxyfluorescein diacetate (CFDA) is bound to an acetoxymethyl (AM) ester, making it a cell permeable non-fluorescent dye CFDA-AM. Once diffused into the cell the dye is de-esterified to fluorescent CFDA molecules by non-specific intracellular esterases. CFDA is not able to cross the cell membrane. Viable cells with an intact plasma membrane will readily take up and de-esterify the dye, whereas this process is hampered in damaged or death cells, making the CFDA assay a measure of membrane integrity and as such, cell viability.

Neutral red assay (Chapters 3 and 7)

The Neutral Red (NR) assay is one of the most used cytotoxicity assays, based on the ability of viable cells to incorporate and bind the NR dye in the lysosomes (Repetto *et al.*, 2008). Viable cells can passively take up the NR dye because of the steep pH gradient between the cytosol and lysosome interior. The integrity of the lysosomal pH correlates to cell viability and as such, the amount of dye incorporated in the lysosomes provides a measure of cell viability. Measuring the fluorescence of NR requires wash- and extraction steps, making this assay less suitable for cells with a weak attachment to culture material. When using strongly attached cells, the NR assay can be performed subsequent to the non-invasive combined AB and/or CFDA assay.

Oxidative stress (Chapter 3 and 6)

Cells constantly generate reactive oxygen species (ROS) during aerobic metabolism. At the same time, they use their antioxidant defense systems to prevent oxidative stress. Oxidative stress occurs when the generation of ROS overwhelms the natural antioxidant defenses and is implicated in a wide variety of pathological processes, including neurodegeneration.

ROS generation upon exposure to ELF-EMF was assessed using the cumulative fluorescent dye H_2-DCFDA. The cell-permeant 2',7'-dichlorodihydrofluorescein diacetate (H_2-DCFDA) is a chemically reduced form of fluorescein used as an indicator for ROS in cells. H_2-DCFDA passively transfers across the cell membrane to enter the cells. Upon cleavage of the acetate groups by intracellular esterases and subsequent oxidation by ROS, the non-fluorescent H_2-DCFDA is converted to the highly fluorescent 2',7'-dichlorofluorescein (DCF). DCF-based ROS assays such as the H_2-DCFDA assay detect a number of different radicals (Jakubowski and Bartosz, 2000) and provide thus a broad indication of oxidative stress.

2.3.2 Measurements of cellular morphology

Immunofluorescent staining of α-synuclein, β(III)-tubulin, GFAP and nestin (Chapters 3, 5 and 7)

Cellular morphology is essential in identifying the type, structure, and size of a cell or cellular network. It is often investigated using (fluorescent) microscopy. Additionally, the cells can be stained with fluorescent antibodies to detect certain target proteins in the cell (Chapter 3) or on the cell surface. Consequently, (immunofluorescent) staining can be used to distinguish between different cell types within heterogeneous cultures (Chapter 5), or to detect changes in morphology (neurite outgrowth, Chapter 7), e.g. after exposure to a certain treatment.

In Chapter 3, the expression of α-synuclein was invested in different chemically pre-treated PC12 phenotypes as a marker of dopaminergic neurodegeneration. α-Synuclein is an intracellular protein that is hypothesized to play a modulatory role in synaptic transmission and is implicated in the pathophysiology of neurodegenerative disorders (including Parkinson's disease [PD]; Luk *et al.*, 2012, Cookson, 2009).

In Chapter 5, the presence of multiple neuronal cell types in differentiating mNPCs was confirmed by staining the cells with specific and commonly used intracellular markers for developing neuronal cells (Gassmann *et al.*, 2012,

Moors *et al.*, 2009, Fritsche *et al.*, 2011, Breier *et al.*, 2010). To identify the presence of neurons, specific antibodies against class III β-tubulin (β(III)-tubulin) were used. β(III)-tubulin is a microtubule element found almost exclusively in neurons, making it possible to separate neurons from glial cells, which do not express this marker. Additionally, anti-glial fibrillary acidic protein (GFAP) was used to identify the presence of astrocytes. This is a class-III intermediate filament and is used as a cell-specific marker that distinguishes astrocytes from other glial cells during the development of neuronal cells. Lastly, nestin expression was assessed as a marker for nervous system-specific stem cells. It is a class VI intermediate filament protein that is expressed in stem cells of the (central) nervous system but not in mature neuronal cells.

In Chapter 7, anti-β(III)-tubulin antibodies were used to determine neurite length in primary cortical cultures, as it stains the microtubule in both the cell body and the neurites of the cortical neurons.

Alternatively, the presence of certain target proteins can be identified using flow cytometry analysis (FACS) or western blotting, making these techniques suitable to detect and quantify the presence of different cell types. However, as these techniques lack the sensitivity and spatial resolution of confocal microscopy they do not provide information on cell shape or neuronal (network) structure. We therefore considered confocal microscopy to be the most appropriate method.

2.3.3 Measurements of cellular function

Intracellular calcium homeostasis (Chapters 3, 5–7)

Changes in intracellular calcium concentrations ($[Ca^{2+}]_i$) were determined by measuring fluorescence of the high-affinity Ca^{2+}-responsive fluorescent dye Fura-2 AM. Because of the acetomethyl (AM) ester, Fura-2 AM crosses the cell membrane, allowing the cell to be loaded with Fura-2 AM in a non-invasive manner. During the incubation, intracellular non-specific esterases remove the AM group from the Fura-2 AM. The resulting Fura-2 present in the cytosol is Ca^{2+}-sensitive and no longer able to cross the cell membrane. As Fura-2

AM itself is also fluorescent, but not Ca^{2+}-sensitive, any excess Fura-2 AM is removed from the cells prior to the start of the experiments to assure only intracellular calcium is measured.

After loading and de-esterification, cells were placed on the stage of an inverted microscope to select a suitable region of cells. As Fura-2 is a dual wavelength dye, fluorescence of Ca^{2+}-bound Fura-2 was evoked by 340 and 380 nm excitation wavelengths (F_{340} and F_{380}) using a polychromator and subsequently collected at 510 nm with a digital camera. Due to the spectral shift upon binding Ca^{2+}, free $[Ca^{2+}]_i$ is positively associated with fluorescence evoked by F_{340} and negatively associated with fluorescence evoked by F_{380}. After subtraction of background fluorescence, the F_{340}/F_{380} ratio (R) was calculated as it directly correlates to $[Ca^{2+}]_i$.

During experiments, cells were continuously superfused with saline. Most of the experiments consisted of a baseline recording to measure basal $[Ca^{2+}]_i$, after which an increase in $[Ca^{2+}]_i$ was triggered by switching superfusion to saline containing a stimulus for several seconds to measure stimulation-evoked $[Ca^{2+}]_i$, followed by a recovery period in which $[Ca^{2+}]_i$ returned to baseline. For acute ELF-EMF exposure experiments (Chapter 6) cells were subsequently (sham-) exposed to ELF-EMF for 30 minutes and stimulated for a second time during this exposure.

At the end of each experiment, minimum and maximum ratios (R_{min} and R_{max}) were determined and used, together with K_{d*} (the dissociation constant of Fura-2, determined for the experimental set-up) to calculate $[Ca^{2+}]_i$ from R using a modified Grynkiewicz's equation (Grynkiewicz *et al.*, 1985, Deitmer and Schild, 2000): $[Ca^{2+}]_i = K_{d*} \times (R - R_{min})/(R_{max} - R)$.

Notably, the use of a dual wavelength dye like Fura-2 allows more accurate measurement of $[Ca^{2+}]_i$ compared to single wavelength dyes (e.g. Fluo-4) as the measurements are less dependent on parameters such as dye loading efficiency, the amount of available dye, dye leakage or photobleaching.

Spontaneous electrical activity (Chapter 5 and 7)

Electrophysiological methods can be used to analyze brain activity and neuronal function *in vitro* and *in vivo* (Obien *et al.*, 2015). However, traditional single-cell electrophysiology is very time-consuming and lacks throughput (despite recent improvements; Wood *et al.*, 2004, Dunlop *et al.*, 2008, Kodandaramaiah *et al.*, 2012), thereby hampering toxicological (screening) applications.

In the research performed in this thesis, the multielectrode array (MEA) technique was used to investigate the development of electrical activity in mNPCs (Chapter 5) and rat cortical cultures, as well as to study the effects of ELF-EMF thereon (Chapter 7). The MEA-based recording techniques date back to the early eighties (Gross *et al.*, 1982) and it has been improved ever since.

The MEA technique allows simultaneous and non-invasive recordings of local field potentials and extracellular action potentials at different locations in a population of neurons at millisecond time scale. It thus enables the investigation of (developmental or chemically-induced) changes in intercellular communication from excitable tissues *in vivo* or *in vitro* by providing spatial and temporal recordings of electrical activity (Obien *et al.*, 2015). Many different *in vitro* models can be cultured on MEAs, including hippocampal slices, primary mammalian dissociated cultures and stem cells. (Defranchi *et al.*, 2011). Most of the mammalian neuronal networks cultured on MEAs become spontaneously active and remain stably active for up to months (Gramowski *et al.*, 2004, Gross *et al.*, 1982, van Pelt *et al.*, 2004). Importantly, as MEA recordings are non-invasive and do not disrupt cellular integrity, it is possible to repeatedly record activity in the same cellular network over time.

Neurons grown on MEAs possess many characteristics of neurons *in vivo*, including (the development of) spontaneous activity with spiking, bursting, and plasticity (van Pelt *et al.*, 2004, Robinette *et al.*, 2011, van Pelt *et al.*, 2005, Pasquale *et al.*, 2008). Moreover, they are responsive to neurotransmitters and pharmacological agents (Gross *et al.*, 1997). MEA

recordings have also been successfully used to study and identify chemical-induced (developmental) neurotoxicity (McConnell *et al.*, 2012, Hogberg *et al.*, 2011, Wallace *et al.*, 2015, Robinette *et al.*, 2011, Defranchi *et al.*, 2011). MEAs are available as single or multiwell (12, 48, or 96) systems and have improved throughput compared to classical electrophysiological approaches. It has even been demonstrated that multiwell MEAs can provide sufficient throughput for compound screening while retaining the qualities of single well MEAs (McConnell *et al.*, 2012).

Thus, *in vitro* cultures of neurons grown on MEAs could provide a functional endpoint to assess developmental neurotoxicity (Robinette *et al.*, 2011, Hogberg *et al.*, 2011).

The models and techniques described in this chapter were carefully selected and characterized in Chapters 3–5. Next, these models and techniques were applied in Chapter 6 and 7 to investigate the (developmentally) neurotoxic potential of ELF-EMF exposure.

PART I:
MODELS IN IN VITRO NEUROTOXICITY TESTING

CHAPTER 3

Chemically-induced oxidative stress increases the vulnerability of PC12 cells to rotenone-induced toxicity

Martje W.G.D.M. de Groot and Remco H.S. Westerink

Neurotoxicology Research Group, Toxicology Division, Institute for Risk Assessment Sciences (IRAS), Faculty of Veterinary Medicine, Utrecht University, P.O. Box 80.177, NL-3508 TD Utrecht, The Netherlands

Neurotoxicology (2014). **43**: 102-109
DOI: 10.1016/j.neuro.2014.02.008

Abstract

In vitro models, including the widely used PC12 cell line, can increase insight into cellular and molecular mechanisms underlying neurodegenerative processes. An important determinant for the vulnerability of cells for chemical insults may be the endogenous level of oxidative stress. To test this hypothesis, we induced different degrees of cellular stress in PC12 cells by altering their ROS production using dexamethasone, L-dihydroxyphenylalanine (L-DOPA) and iron. These different PC12 models were subsequently used to investigate whether the degree of cellular stress could increase their susceptibility to environmental pollutants. The characteristics of these stressed PC12 cell subtypes and their vulnerability to the reference pesticide rotenone were investigated using a combination of biochemical (oxidative stress, cell viability, and α-synuclein expression) and functional (fluorescent calcium imaging) assays. Our combined data demonstrate that chemically-induced stress in PC12 cells increases the production of reactive oxygen species (ROS) and alters calcium homeostasis and α-synuclein expression. Moreover, L-DOPA and $FeSO_4$ pre-treated PC12 cells show increased vulnerability to rotenone-induced cytotoxicity. These chemically stressed cell models may therefore prove valuable to investigate how increased cellular stress influences neurotoxic outcome, for example in case of mixture toxicity.

Keywords: α-Synuclein; Oxidative stress; Fura-2 Ca^{2+}-imaging; Dexamethasone; Iron; L-DOPA.

1. Introduction

The etiology of (dopaminergic) neurodegeneration is largely unknown, although several genetic and environmental factors have been identified, including exposure to pesticides such as rotenone, paraquat, and maneb (Caudle *et al.*, 2012, Freire and Koifman, 2012, Shulman *et al.*, 2011, van der Mark *et al.*, 2012). Another important risk factor is aging, which is associated with increased vulnerability, mitochondrial dysfunction, oxidative damage, and accumulation of reactive oxidative species (ROS) and/or mutations in mitochondrial DNA (Gandhi and Abramov, 2012, Lin and Beal, 2006).

Due to its high energy demand and limited anti-oxidant systems, the nervous system is already sensitive to oxidative stress. This sensitivity is particularly profound in dopaminergic neurons due to the generation of reactive oxygen or nitrogen species via auto-oxidation or enzymatic degradation of dopamine or its precursor L-dihydroxyphenylalanine (L-DOPA; Asanuma *et al.*, 2003). Additionally, dopaminergic neurons of the Substantia Nigra (SN) have a high iron content that increases during aging (Snyder and Connor, 2009). Iron ions are known catalyzers of ROS and drive the conversion of milder ROS (e.g. H_2O_2) into free radical ROS (e.g. hydroxyl radicals; Halliwell, 2006), thereby further depleting anti-oxidant systems (Jiang *et al.*, 2006). Iron-dependent oxidative stress has consequently been linked to neuronal cell death in several neurodegenerative diseases, including Parkinson's Disease (PD; Caudle *et al.*, 2012, Bolognin *et al.*, 2009, Double *et al.*, 2000).

As increased oxidative stress and iron- or dopamine content are important risk factors contributing to degeneration of neuronal cells, we hypothesize that upregulation of these factors by chemical pre-treatment increases the vulnerability to subsequent (chemical) insults. We therefore differentiated pheochromocytoma (PC12) cells (Greene and Tischler, 1976) with dexamethasone (DEX), or pre-treated them with $FeSO_4$ or L-DOPA in an attempt to modulate the endogenous level of oxidative stress. These easily-cultured cells have been extensively used in neuroscience, e.g. to study the molecular

machinery underlying vesicular neurotransmitter release (exocytosis; Khvotchev *et al.*, 2007, Shin *et al.*, 2002, Westerink, 2004, Westerink and Ewing, 2008) and in neurotoxicology to study the effects of environmental pollutants on neuronal development, function and degeneration (Shafer and Atchison, 1991, Westerink and Ewing, 2008, Westerink, 2013). Differentiation of naïve PC12 cells with DEX is known to enhance the synthesis and secretion of catecholamines [~99% dopamine], while cells maintain functional calcium homeostasis and neurotransmitter receptors function, comparable to primary neurons (Elhamdani *et al.*, 2002, Taylor and Peers, 1999, Taylor and Peers, 2000, Westerink and Vijverberg, 2002, Westerink *et al.*, 2002). On the other hand, pre-treatment of PC12 cells with $FeSO_4$ or L-DOPA increases respectively their iron or dopamine content, thereby increasing ROS production.

In these differently treated PC12 models we investigated multiple endpoints relevant to cell death and the onset of neurodegeneration, including biochemical (cell viability, ROS production, and α-synuclein expression) and functional, dynamic endpoints critical for proper neuronal function (Ca^{2+}-homeostasis) to reveal if chemical stress increases neuronal vulnerability. Our combined data imply that chemically stressed PC12 cells may be a valuable tool to investigate how increased cellular stress influences neurotoxic outcome, for example in case of mixture toxicity.

2. Materials and methods

2.1 Chemicals

RPMI 1640, penicillin-streptomycin, PBS, Fura-2 AM and 2',7'-dichlorodihydrofluorescein diacetate (H_2-DCFDA) were obtained from Life Technologies (Bleiswijk, The Netherlands); all other chemicals were obtained from Sigma-Aldrich (Zwijndrecht, the Netherlands), unless described otherwise. Saline solutions for Ca^{2+}-imaging experiments, containing (in mM) 125 NaCl, 5.5 KCl, 2 $CaCl_2$, 0.8 $MgCl_2$, 10 HEPES, 24 glucose, and 36.5 sucrose (pH set at 7.3), were prepared with deionized water (Milli-Q®; resistivity >10 MΩ·cm). Stock solutions of 2 mM ionomycin and 0.001–100 mM rotenone (analytical

grade) were prepared in DMSO and kept at –20°C. $FeSO_4$ stock solution (10 mM) was prepared from $FeSO_4 \cdot 7H_2O$ in Milli-Q® containing 0.5% H_2SO_4 and kept at 4°C. DEX stock solution (10 mM) was prepared in ethanol and stored at –20°C. L-DOPA stock solutions (10 mM) were freshly prepared prior to each experiment in cold colorless RPMI 1640 without supplementation. Stock solutions of all compounds were diluted in RPMI 1640 culture medium without supplementation to obtain the desired concentrations just prior to the experiments (all solutions used in the cell viability and ROS experiments, including control experiments, contained a maximum of 1 µL DMSO/mL).

2.2 Cell culture

Rat pheochromocytoma (PC12) cells (Greene and Tischler, 1976) clone CRL-1721 (passage 18) obtained from ATCC (American Type Culture Collection, Manassas, VA, USA), were grown for a maximum of 10 passages in RPMI 1640 containing L-glutamine supplemented with 5% fetal calf serum and 10% horse serum (ICN Biomedicals, Zoetermeer, The Netherlands), 100 IU/mL penicillin, and 100 mg/mL streptomycin at 37°C in a 5% CO_2 atmosphere as described previously (Hendriks *et al.*, 2012, Hondebrink *et al.*, 2011a). Cells were subcultured one day prior to measurements of the intracellular calcium concentration ($[Ca^{2+}]_i$), cell viability, α-synuclein expression, or ROS production. For fluorescent imaging of $[Ca^{2+}]_i$, cells were seeded in 25 cm^2 flasks at a density of 7.5×10^6 cells/flask and subcultured in 35 mm diameter glass bottom dishes (MatTek, Ashland, MA, USA) at a density of 4.5×10^5 cells/dish. For measurement of cell viability, ROS production or α-synuclein expression, cells were seeded in 75 cm^2 flasks at a density of 22.5×10^6 cells/flask and subcultured in transparent 24-well plates (Greiner Bio-one, Solingen, Germany) for cell viability and ROS, or on glass coverslips for α-synuclein expression at a density of 6×10^5 cells/well or cover slip. All cell culture flasks, plates, coverslips and dishes were coated with poly-L-lysine (50 µg/mL).

2.3 Chemically stressed PC12 models

PC12 cells were differentiated and subcultured in supplemented culture medium containing 5 µM DEX for 3–5 days or subcultured and pre-treated with 100 µM L-DOPA or 10 µM $FeSO_4$ for 24 h prior to measurements to obtain the different chemically stressed PC12 subtypes (Figure 1).

2.4 Cell viability

Cell viability was assessed using a Neutral Red (NR) assay, as described previously (Heusinkveld *et al.*, 2010). Briefly, 24 h after subculturing, naïve PC12 cells were exposed to different concentrations of $FeSO_4$ or L-DOPA (up to 10 mM) in RPMI 1640 medium without supplementation to assess whether a 24 h pre-treatment with $FeSO_4$ or L-DOPA decreased cell viability in the NR assay. Alternatively, naïve, 5 µM DEX-differentiated and 10 µM $FeSO_4$ or 100 µM L-DOPA pre-treated PC12 cells were exposed to DMSO or 0.001–100 µM rotenone for 24 h to determine the vulnerability of the different PC12 models to the environmental pollutant rotenone (Figure 1).

2.5 Intracellular calcium imaging

Changes in $[Ca^{2+}]_i$ were measured in cells from the different chemically pre-treated models (Figure 1) using the Ca^{2+}-sensitive fluorescent ratio dye Fura-2 AM as described previously (Hendriks *et al.*, 2012, Heusinkveld and Westerink, 2011, Hondebrink *et al.*, 2012). After a 5 min baseline recording, cells were depolarized using high K^+-containing saline (100 mM) for 18 s (K1). 35 min after the first depolarization, cells were again depolarized with high K^+-containing saline (K2) to obtain a depolarization ratio (DR; see 2.8 Data analysis and statistics) and to investigate possible effects on the depolarization-evoked increase of $[Ca^{2+}]_i$ (Figure 4A for example recordings), whereas the average $[Ca^{2+}]_i$ during baseline was determined per cell to investigate effects on basal $[Ca^{2+}]_i$. Maximum and minimum ratios (R_{max} and R_{min}) were determined at the end of each recording by addition of ionomycin (final concentration 5 µM) and ethylenediamine tetraacetic acid (EDTA; final concentration 17 mM). Changes in F_{340}/F_{380} ratio (R), reflecting changes in $[Ca^{2+}]_i$, were further analyzed using a custom-made MS-Excel macro. Free cytosolic $[Ca^{2+}]_i$ was calculated from

the F_{340}/F_{380} ratios using Grynkiewicz's equation (Grynkiewicz *et al.*, 1985): $[Ca^{2+}]_i = K_{d*} \times (R - R_{min})/(R_{max} - R)$, where K_{d*} is the dissociation constant of Fura-2 AM determined in the experimental set-up.

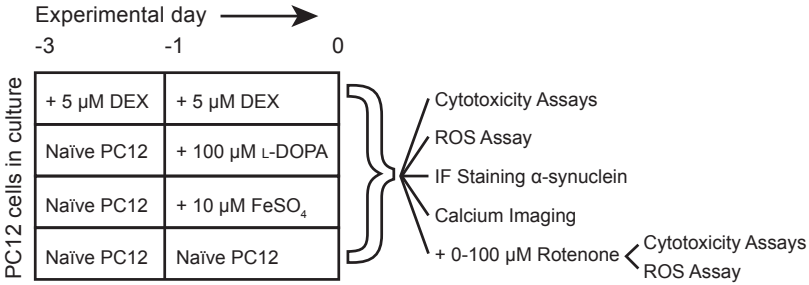

Figure 1. Schematic overview of differentiation and pre-treatment of the different PC12 models, including an overview of the experiments.

2.6 ROS measurements

Cumulative ROS production was assessed using the fluorescent dye H_2-DCFDA (protocol adapted from Heusinkveld *et al.*, 2010). Briefly, 2 h after subculturing of naïve and DEX-differentiated PC12 in 24-well plates, a subset of naïve cells was pre-treated with 10 µM $FeSO_4$ or 100 µM L-DOPA (Figure 1). After a 24 h pre-treatment, cells were incubated with 0.5 mL 1.5 µM H_2-DCFDA for 30 min at 37 °C and 5% CO_2. Subsequently, cells were exposed to 0.5 mL colorless RPMI 1640 without supplementation to determine basal ROS production over time in the different PC12 models. In a separate set of experiments, the different pre-treated PC12 models were exposed to DMSO or different concentrations of rotenone (0.001–100 µM; Figure 1) for 1 h in colorless RPMI 1640 without supplementation to assess changes in rotenone-induced ROS production. Fluorescence was measured spectrophotometrically at 480/530 nm (excitation/emission) at multiple time points on an Infinite M200 microplate reader equipped with a Xenon Flash light source (10 W; Tecan Trading AG, Männedorf, Switzerland) controlled by iControl software (version 7.1).

2.7 Immunofluorescent staining of α-synuclein

To assess the effects of differentiation with DEX or the different pre-treatments on intracellular α-synuclein expression in the different PC12 models, intracellular α-synuclein was labeled with specific fluorescent antibodies and visualized using confocal microscopy. Briefly, 2 h after subculturing of naïve and DEX-differentiated PC12 cells on glass coverslips in 24-well plates, a subset of naïve cells was pre-treated with 10 μM $FeSO_4$ or 100 μM L-DOPA (Figure 1). After 24 h, cells were fixed with 4% paraformaldehyde (PFA) in 0.1 M phosphate buffer (pH 7.4) for 30 min at room temperature. Subsequently, coverslips were quenched for PFA, permeabilized and incubated with blocking buffer (2% bovine serum albumin [BSA] and 0.1% saponin in PBS) containing 20 mM NH_4Cl for 20 min at room temperature. Each of the subsequent incubation steps was performed in blocking buffer. Next, coverslips were incubated with polyclonal sheep anti-rat antibody against α-synuclein (ab6162; Abcam, Cambridge, UK) at a 1:200 dilution for 45 min at room temperature. Subsequently, coverslips were washed three times and incubated with a fluorochrome-conjugated secondary antibody (Alexa488 donkey-anti-sheep; Life Technologies, Bleiswijk, The Netherlands) at a 1:200 dilution 30 min at room temperature in the dark. Nuclear staining was performed by incubating the coverslips with 4',6-diamidino-2-phenylindole (DAPI; Life Technologies, Bleiswijk, The Netherlands) at a concentration of 200 nM for 5 min at room temperature in the dark. The washing procedure was repeated and the coverslips were sealed with FluorSave™ (Calbiochem, San Diego, CA, USA). Immunostained coverslips were visualized using a Leica SPEII Confocal microscope (Leica DMI4000 equipped with TCS SPE-II) using a 40x oil immersion objective (N.A. 1.4–0.7) and captured using LAS AF software (version 2.6.0).

2.8 Data analysis and statistics

All data are presented as mean ± SEM from the number of wells or cells (*n*) indicated, derived from 3 to 8 independent experiments (*N*). Background-corrected data from each PC12 cell model in the cell viability assay are expressed as percentage of the respective nonexposed control. ROS data is

expressed as a percentage compared to the basal ROS production at t = 0 h and compared to the DMSO control of the respective model where applicable. For both cell viability and ROS data, wells that show effects two times SD above or below average are considered outliers (<7% for all experiments) and excluded from further analysis. Data from fluorescent microscopy are analyzed as effects on basal $[Ca^{2+}]_i$ and depolarization-evoked $[Ca^{2+}]_i$. Basal calcium is expressed as $[Ca^{2+}]_i$ (nM) during a 2.5 min interval prior to K1. Depolarization-evoked $[Ca^{2+}]_i$ is expressed as the amplitude of the depolarization-evoked increase in $[Ca^{2+}]_i$ (K1, in µM) as well as a depolarization ratio (DR): the amplitude of the second K^+-evoked increase in $[Ca^{2+}]_i$ (K2) expressed as a percentage of K1 per cell. Data from immunofluorescent imaging were analyzed as full preparation Z-stack images (0.5 µm/stack) using LAS AF Lite software (version 2.6.0). The intensity of fluorescently-labeled α-synuclein in each cell was quantified using a false color scale in Image J (version 1.46) and corrected for differences in cell area. Immunofluorescent data is presented as percentage of naïve PC12 cells. All statistical analyses were performed using SPSS 20 (SPSS, Chicago, IL, USA). One-way analyses of variance (ANOVA), followed by Bonferroni post hoc analyses to correct for multiple testing, were performed to investigate changes in α-synuclein expression and calcium homeostasis (K1 and DR) between the different PC12 models. Two-way ANOVA, followed by a Bonferroni corrected pairwise comparisons, were performed to investigate changes in ROS production or cell viability in the different PC12 models over time or with increasing rotenone concentration. p-values < 0.05 were considered statistically significant. IC_{50}s for rotenone on cell viability in the different PC12 models were calculated using a log-scale nonlinear fit in GraphPad Prism (version 6.01; GraphPad Software Inc., La Jolla, CA, USA).

3. Results

3.1 Increased ROS production in the different PC12 cell models

To exclude that the presented results are due to direct cytotoxicity resulting from chemical pre-treatment, effects of different concentrations of L-DOPA and $FeSO_4$ on cell viability were investigated using a NR assay. The data demonstrate that pre-treatment with 100 µM L-DOPA or 10 µM $FeSO_4$ for 24 h did not affect cell viability in PC12 cells (not shown).

To confirm our hypothesis that the production of ROS in PC12 cells is altered by differentiation with 5 µM DEX for 3–5 days or by a 24 h pre-treatment with 100 µM L-DOPA or 10 µM $FeSO_4$, ROS production was measured up to 24 h after pre-treatment in the different models using the fluorescent dye H_2-DCFDA. As H_2-DCFDA is a cumulative ROS sensitive dye and ROS are also produced during normal cell functioning, all PC12 cell models show a significant increase in cumulative ROS production over time from 1 h onwards, including naïve PC12 cells (two-way ANOVA: $p < 0.001$; and $p < 0.001$ compared to $t = 0.5$ h; Figure 2). However, PC12 cells differentiated with DEX or pre-treated with 100 µM L-DOPA or 10 µM $FeSO_4$ show a significantly higher ROS production after 24 h compared to naïve PC12 cells ($p < 0.001$ for all models; Figure 2). These data demonstrate that the different pre-treatments increase the ROS production and that the cells pre-treated with 10 µM $FeSO_4$ show the largest increase in basal ROS production ($p < 0.05$ compared to naïve, DEX-differentiated and L-DOPA pre-treated PC12 cells from $t = 3$ h onwards; Figure 2 and Table 1).

3.2 Alterations in α-synuclein expression in the different PC12 cell models

To evaluate if PC12 cells show an increase in α-synuclein expression after the different pre-treatments, immunostainings for α-synuclein were performed on the four PC12 cell phenotypes and corrected for differences in cell size (Figure 3A–D for representative images). Naïve PC12 cells ($n = 72$) express α-synuclein (Figure 3A and E) and both DEX-differentiated ($n = 38$) and L-DOPA

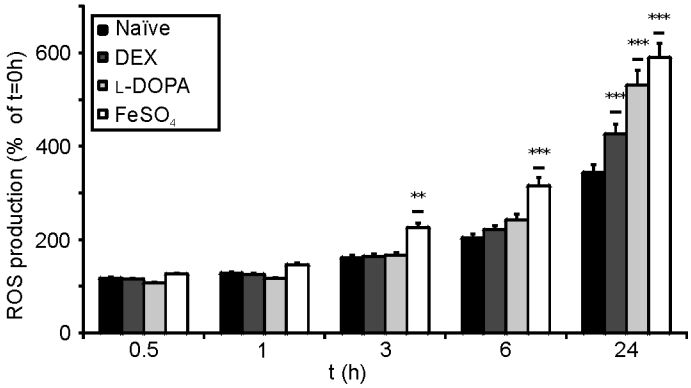

Figure 2. Bar graph illustrating the basal ROS production up to 24 h in the different pre-treated PC12 models. Basal ROS production increases over time in all PC12 models. After 24 h, all pre-treated PC12 models show a significantly higher basal ROS production compared to naïve PC12 cells. Data represent average ROS values (± SEM) compared to t = 0 h, from at least 32 wells from 8 separate experiments. $^{**}p < 0.01$ and $^{***}p < 0.001$ compared to naïve PC12 cells.

Table 1. Summary of the changes in cellular characteristics in the different chemically stressed PC12 models. Arrows indicate a relative increase (↑), decrease (↓) or no effect (=) in the presented parameters compared to naïve PC12 cells.

	ROS production t = 24 h	α-synuclein expression	Basal $[Ca^{2+}]_i$	1st evoked $[Ca^{2+}]_i$	DR (%)
Naïve	↑	=	=	=	=
5 µM DEX	↑↑	=	=	↓	=
100 µM L-DOPA	↑↑	=	=	↓↓	=
10 µM $FeSO_4$	↑↑	↑	=	↓	↑

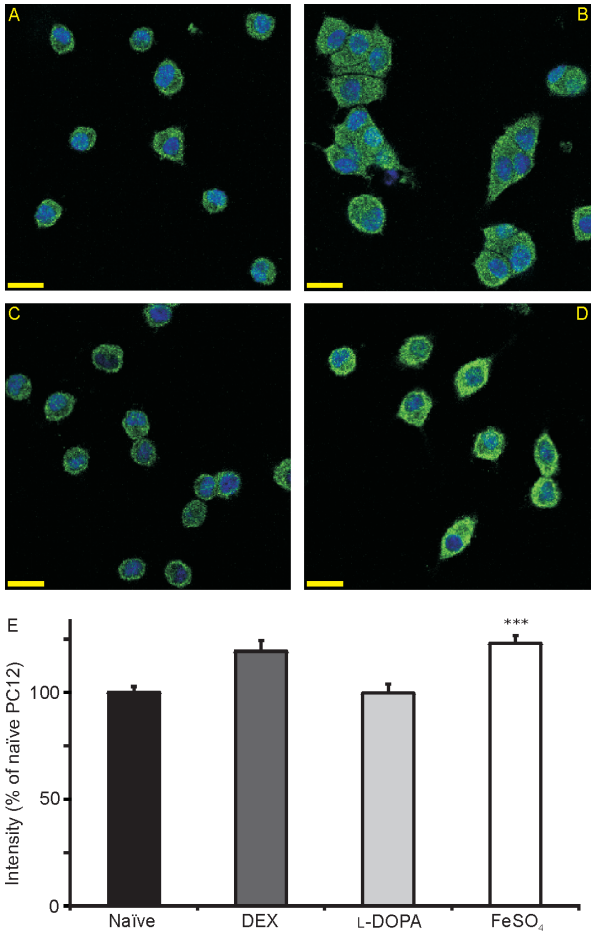

Figure 3. Representative confocal images of the different immunostained PC12 cell models. α-Synuclein expression (green) is comparable in naïve **A.**, DEX-differentiated **B.**, and L-DOPA pre-treated **C.**, PC12 cells, whereas $FeSO_4$ pre-treated **D.**, PC12 cells show a more intense α-synuclein staining. Nuclei were stained with DAPI (blue). Magnification: 40× oil immersion. Scale bar: 10 µm. **E.**, Bar graph illustrating the expression of α-synuclein in the different PC12 models. Data represent average fluorescent values corrected for cell area (± SEM) expressed as a percentage of naïve PC12 cells (n = 38–72 cells from 3 separate experiments). ***$p < 0.001$ compared to naïve PC12 cells.

(n = 60) pre-treated PC12 cells show an α-synuclein expression comparable to naïve PC12 cells (123.1 ± 6.7% and 120.6 ± 4.9%; respectively; Figure 3B, C and E). On the other hand, $FeSO_4$ pre-treated (n = 68) PC12 cells display a significant increase in α-synuclein expression (147.7 ± 6.5% [$p < 0.001$ compared to naïve PC12 cells] Figure 3D and E), demonstrating that $FeSO_4$ pre-treatment can affect α-synuclein expression (Figure 3 and Table 1).

3.3 Alterations in calcium homeostasis in the different PC12 cell models

To assess whether the different PC12 phenotypes maintain a functional calcium homeostasis and to reveal possible differences in calcium characteristics, single-cell fluorescent microscopy was used. Naïve PC12 cells (n = 114) show a low basal $[Ca^{2+}]_i$ of 102 ± 1 nM, which rapidly increases up to 2.1 ± 0.1 µM upon depolarization with high potassium-containing saline (Figure 4). After this first depolarization, superfusion was switched back to saline and $[Ca^{2+}]_i$ recovered to near basal values within minutes. Cells were depolarized again 35 min following the first depolarization to derive a DR (see 2.8 Data analysis and statistics). For naïve PC12 cells, the amplitude of the second depolarization-evoked increase in $[Ca^{2+}]_i$ amounted up to 1.7 ± 0.1 µM, yielding a DR of 79 ± 2% (illustrated by example traces in Figure 4A).

Calcium homeostasis in DEX-differentiated PC12 cells (n = 131) is comparable with calcium homeostasis in naïve PC12 cells with a low basal $[Ca^{2+}]_i$ of 105 ± 1 nM and a depolarization-evoked increase in $[Ca^{2+}]_i$ amounting to 1.9 ± 0.1 µM, which is only slightly lower than in naïve PC12 cells ($p < 0.01$). The amplitude of the second depolarization-evoked increase in $[Ca^{2+}]_i$ in DEX-differentiated PC12 cells amounted to 1.5 ± 0.1 µM, yielding a DR of 80 ± 2%, which is not significantly different from the naïve PC12 cells (Figure 4). PC12 cells pre-treated with 100 µM L-DOPA (n = 121) for 24 h also have a low basal $[Ca^{2+}]_i$ of 107 ± 1 nM. However, unlike naïve PC12 cells, L-DOPA pre-treated PC12 show only a modest increase in $[Ca^{2+}]_i$ upon depolarization, amounting to 0.7 ± 0.1 µM, which is significantly lower than in naïve PC12 cells ($p < 0.001$). The amplitude of the second depolarization-evoked increase in $[Ca^{2+}]_i$ in L-DOPA

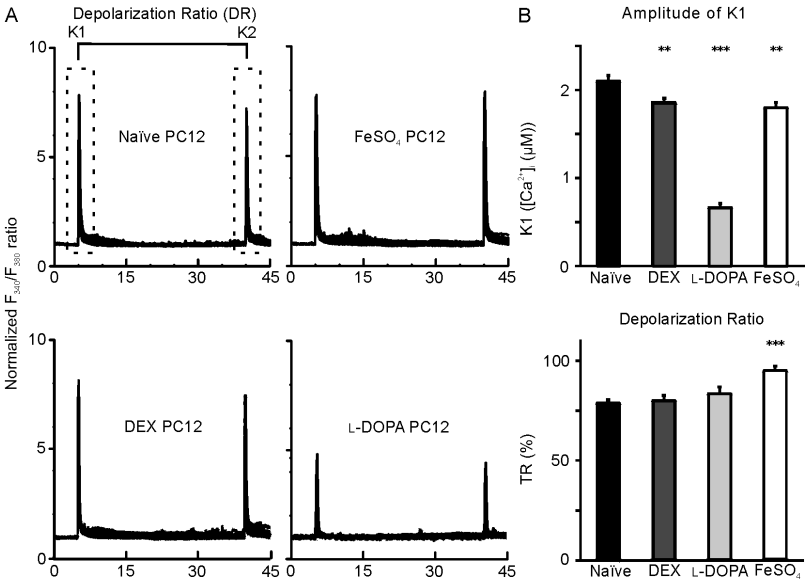

Figure 4. Chemically stressed PC12 cell models display functional but distinct Ca^{2+}-characteristics. **A.** Representative example traces of cytosolic $[Ca^{2+}]_i$ of individual PC12 cells from the different models. **B.** Bar graphs illustrating the decrease in the depolarization-evoked amplitude in $[Ca^{2+}]_i$ (K1, upper graph) by pre-treating the cells with DEX, L-DOPA or $FeSO_4$, and the increase in DR (lower graph) by pre-treating the cells with 10 μM $FeSO_4$. Data represent mean ± SEM from 100 to 131 cells from 7 to 8 separate experiments. $^{**}p < 0.01$ and $^{***}p < 0.001$ compared to naïve PC12 cells.

pre-treated PC12 cells amounted to 0.5 ± 0.0 μM, yielding a DR of 83 ± 3%, which is not significantly different from the naïve PC12 cells (Figure 4). PC12 cells pre-treated with 10 μM $FeSO_4$ (n = 100) for 24 h have low basal $[Ca^{2+}]_i$ of 109 ± 1 nM, comparable to naïve PC12 cells, and a slightly lower depolarization-evoked $[Ca^{2+}]_i$ of 1.8 ± 0.1 μM ($p < 0.01$ compared to naïve PC12 cells). Noteworthy, the second depolarization-evoked increase in $[Ca^{2+}]_i$ in $FeSO_4$ pre-treated PC12 cells amounts to 1.7 ± 0.1 μM, resulting in a significantly higher DR of 95 ± 2% ($p < 0.001$) compared to naïve PC12 cells (Figure 4).

DEX-differentiation for 3–5 days and chemical pre-treatment of the naïve PC12 cells with $FeSO_4$ or L-DOPA thus appears to cause marked differences in the amplitude of K1 and the DR between the different models, without affecting basal $[Ca^{2+}]_i$ (Figure 4 and Table 1).

3.4 Altered vulnerability of stressed PC12 cell models following rotenone exposure

To assess whether the different PC12 models indeed show altered vulnerability to rotenone, naïve, DEX-differentiated and PC12 cells pre-treated with 100 µM L-DOPA or 10 µM $FeSO_4$ were exposed to 0.001–100 µM rotenone for 24 h and effects on cell viability were assessed using a NR assay. The results demonstrate a clear concentration-dependent decrease in cell viability with increasing rotenone concentrations for all PC12 models (two-way ANOVA, $p < 0.001$; Figure 5). Naïve PC12 cells show a significant decrease in cell viability from 0.1 µM rotenone onwards ($p < 0.001$ compared to DMSO control). When comparing the results of the different stressed models to naïve PC12 cells, it is clear that from 0.01 to 10 µM rotenone DEX-differentiated PC12 cells show a smaller decrease in cell viability ($p < 0.01$ compared to naïve PC12 cells), indicative of decreased vulnerability, whereas L-DOPA pre-treated PC12 cells show a larger decrease in cell viability from 0.001 to 1 µM rotenone ($p < 0.01$ compared to naïve PC12 cells), demonstrating increased vulnerability. $FeSO_4$ pre-treated PC12 cells also show a larger decrease in cell viability at 0.001 µM rotenone but otherwise behave comparable to naïve cells ($p < 0.01$ compared to naïve PC12 cells; Figure 5).

This becomes more apparent when comparing the IC_{50}s for rotenone in the NR assay for the different PC12 phenotypes (Table 2). DEX-differentiated PC12 cells appear less vulnerable with an IC_{50} of 9.8 µM, which is 10 times higher than of naïve PC12 cells (0.9 µM). Moreover, L-DOPA pre-treated PC12 cell indeed appear more vulnerable with an IC_{50} for rotenone of 0.09 µM, whereas $FeSO_4$ pre-treated PC12 cells appear only slightly more vulnerable (IC_{50} of 0.6 µM).

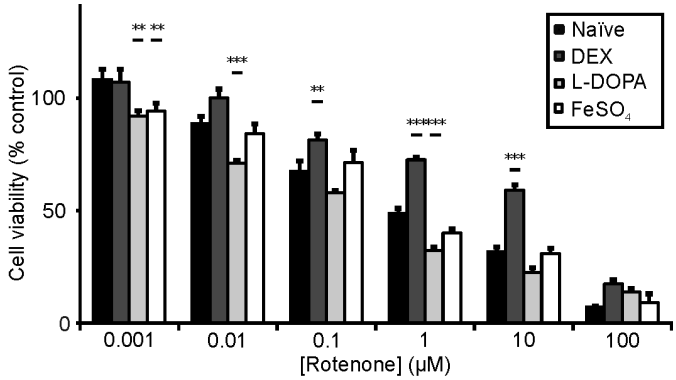

Figure 5. Effects of 24 h rotenone exposure on cell viability in the different PC12 cell models. Bar graph illustrating the effects of rotenone (0.001–100 μM) exposure on cell viability in naïve (black bars), DEX-differentiated (dark gray bars), L-DOPA (light gray bars), and $FeSO_4$ pre-treated (white bars) PC12 cells in the NR assay. Data represent mean ± SEM (from at least 12 wells from 4 to 10 independent experiments per condition). $^{**}p < 0.01$ and $^{***}p < 0.001$ as compared to naïve PC12.

Finally, we assessed whether differentiation with DEX or pre-treatment with $FeSO_4$ or L-DOPA also affects cumulative ROS production of PC12 cells in response to an environmental stressor. Exposure to rotenone for 1 h concentration-dependently increases ROS production in the different PC12 models (two-way ANOVA; $p < 0.001$; Figure 6). DEX-differentiated PC12 cells show rotenone-induced ROS production comparable to naïve PC12 cells. Again, both L-DOPA and $FeSO_4$ pre-treated PC12 cells show a significantly increased rotenone-induced ROS production compared to naïve PC12 cells at a concentration of 100 μM rotenone ($p < 0.05$ and $p < 0.001$ compared to naïve PC12 cells, respectively), indicative for an increased vulnerability (Figure 6 and Table 2).

Table 2. Summary of the changes in rotenone-induced vulnerability in the different chemically stressed PC12 models. 50% Inhibitory concentrations (IC_{50}s) are presented as compared to the model-specific DMSO control. Arrows indicate a relative increase (↑), decrease (↓) or no effect (=) in the presented parameter compared to naïve PC12 cells.

	Cell viability (IC_{50} in µM)	ROS production t = 1 h
Naïve	0.9	↑
5 µM DEX	9.8 ↑	↑
100 µM L-DOPA	0.09 ↓↓	↑↑
10 µM $FeSO_4$	0.6 ↓	↑↑

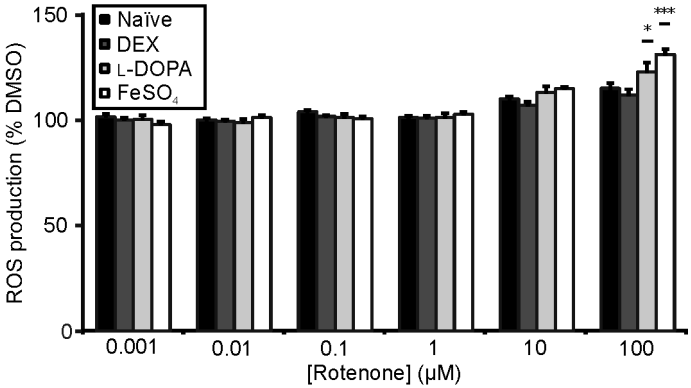

Figure 6. Bar graph illustrating the effects of 1 h rotenone (0.001–100 µM) exposure on ROS production compared to DMSO control in naïve (black bars), DEX-differentiated (dark gray bars), L-DOPA (light gray bars), and $FeSO_4$ pre-treated (white bars) PC12 cells. Data represents mean data ± SEM (n = 9, N = 3 per condition). *p < 0.05 and ***p < 0.001 compared to naïve PC12.

4. Discussion

Our data demonstrate that non-cytotoxic concentrations of dexamethasone, L-DOPA, and $FeSO_4$ can be used to chemically stress the widely used dopaminergic PC12 cell line. Both DEX-differentiation and pre-treatment with L-DOPA or $FeSO_4$ significantly increase ROS production (Figure 2). These data confirm our hypothesis that upregulation of the iron or dopamine content by chemical pre-treatment can increase the production of ROS in PC12 cells. Additionally, $FeSO_4$ pre-treated PC12 cells show increased expression of α-synuclein (Figure 3), an important marker of dopaminergic neurodegeneration (Cookson, 2009, Luk *et al.*, 2012). The calcium imaging data show that these stressed phenotypes still have functional calcium homeostasis, although there are marked changes between the different stressed PC12 models (Figure 4). These combined findings appear to be in line with previous data from Chadwick *et al.* who found alterations in cellular function and physiology in human dopaminergic SH-SH5Y cells following prolonged exposure to a chronic low level of oxidative stress induced by a tolerable H_2O_2 insult (Chadwick *et al.*, 2010).

We further hypothesized that a chemically-induced increase in ROS production would render the cells more vulnerable to the environmental pollutant rotenone. The cell viability data demonstrate a clear concentration-dependent, rotenone-induced decrease in cell viability (Figure 5). Compared to naïve PC12 cells, both $FeSO_4$ and L-DOPA pre-treated PC12 cells show increased vulnerability to rotenone, whereas DEX-differentiated PC12 cells appear less vulnerable (Table 2). Additionally, ROS production is increased compared to DMSO control upon exposure to rotenone in all PC12 models (Figure 6). L-DOPA and $FeSO_4$ pre-treated PC12 cells appear to be most vulnerable to rotenone (Figure 6), whereas DEX-differentiated PC12 cells show a rotenone-induced increase in ROS production comparable to naïve PC12 cells.

Our current findings show a significantly increased basal ROS production in DEX-differentiated PC12 cells, which is in line with previous findings

demonstrating DEX induces ROS production in PC12 cells (Woodman and Lockette, 2009) and other cell types (Almeida *et al.*, 2011, You *et al.*, 2009). Nonetheless, DEX-differentiated PC12 cells appear to be less vulnerable to rotenone in the cell viability assay. This suggests that, as both DEX and L-DOPA increase dopamine content and ROS production, increased dopamine content or ROS production do not fully explain the differences in vulnerability to rotenone and other factors might be involved.

Interestingly, growing evidence suggests a role for the pro-inflammatory response in the degeneration of dopamine-containing neurons in the SN *in vivo* by showing a protective effect of anti-inflammatory drugs, including DEX, on dopaminergic neuron damage (Castano *et al.*, 2002, Gao *et al.*, 2003, Kurkowska-Jastrzebska *et al.*, 2004). These protective properties may be caused by an inhibition of the inflammatory process involved in neuronal damage, or a direct interaction with the neurons (Kurkowska-Jastrzebska *et al.*, 2004). However, it is yet unclear if and how this plays a role in the current findings.

Despite the growing knowledge on the pathology and mechanisms underlying PD, treatment is currently still mostly symptomatic, i.e. trying to restore dopamine concentrations (Obeso *et al.*, 2010, Alberio *et al.*, 2012). Of the anti-PD drugs, L-DOPA is most prescribed (Gao *et al.*, 2003). On a cellular level, our previous studies have indeed demonstrated that L-DOPA increased the vesicular catecholamine content of PC12 cells to approximately 150% (Hondebrink *et al.*, 2009, Westerink *et al.*, 2000). However, the use of L-DOPA in PD treatment is debated because of its side effects and because it is known to generate ROS (Gao *et al.*, 2003). Our current findings lend support to this theory by demonstrating an increase in basal ROS production in L-DOPA pre-treated PC12 cells. However, this L-DOPA pre-treatment does not increase α-synuclein expression in PC12 cells. Nonetheless, our data on cell viability and ROS production demonstrate that L-DOPA pre-treatment increases the vulnerability of the PC12 cell to the environmental pollutant rotenone, suggesting a more vulnerable phenotype. L-DOPA itself may thus contribute to the pathogenesis of dopaminergic neurodegeneration via oxidative stress.

High concentrations of iron can be a source of free radical damage to neuronal cells and have been linked to neuronal cell death in different neurodegenerative diseases, including PD (Bolognin *et al.*, 2009, Double *et al.*, 2000). In the current study, pre-treating PC12 cells with iron for 24 h appears to be sufficient to increase ROS production in the cell to such an extent that it is not only significantly higher than in naïve PC12 cells, but also causes the cells to become more prone to rotenone-induced ROS production and cell death. Pre-treatment with iron thus appears to use up, at least partly, the intracellular defensive mechanisms, e.g. the anti-oxidative systems, rendering the cells more vulnerable to an additional stressor, like rotenone. Additionally, $FeSO_4$ pre-treated PC12 cells have increased α-synuclein expression, which is in line with previous studies indicating that the presence of metal ions accelerates α-synuclein fibril formation (Leong *et al.*, 2009).

This is the first study demonstrating an increase in vulnerability in PC12 cells by chemical pre-treatment with L-DOPA and $FeSO_4$. Although for some research questions primary neurons could be preferable, a stressed subtype of the PC12 cell line can be useful for *in vitro* neurotoxicity testing (e.g. of pesticides), especially as a first (high throughput) screen. PC12 cells pre-treated with $FeSO_4$ could be preferable, as these cells show the highest increase in basal ROS production and have an increased α-synuclein expression, without large impairments in Ca^{2+}-homeostasis. Additionally, $FeSO_4$ pre-treated cells show an increased vulnerability to rotenone in assays for cell viability and ROS production. Moreover, iron is biologically relevant, as neurons of the SN have a high iron content that increases with age and iron-dependent oxidative stress has been linked to neuronal cell death in dopaminergic neurodegeneration. As such, stressed PC12 subtypes may prove valuable to investigate how increased cellular stress influences neurotoxic outcome, for example in case of mixture toxicity.

Acknowledgements

We gratefully acknowledge Aart de Groot and Gina van Kleef for technical assistance and Rob Bleumink for his assistance with the immunofluorescent stainings for α-synuclein. This study was supported by the Netherlands Organization for Health Research and Development [ZonMw grant number 85300003] and the Faculty of Veterinary Medicine of Utrecht University.

CHAPTER 4

Don't judge a neuron only by its cover: neuronal function in *in vitro* developmental neurotoxicity testing

Martje W. G. D. M. de Groot, Remco H. S. Westerink, and Milou M. L. Dingemans

Neurotoxicology Research Group, Toxicology Division, Institute for Risk Assessment Sciences (IRAS), Faculty of Veterinary Medicine, Utrecht University, NL-3508 TD Utrecht, The Netherlands

Toxicological Sciences (2013). **132**(1): 1–7
DOI:10.1093/toxsci/kfs269

Abstract

Classical cases of developmental neurotoxicity (DNT) in humans and advances in risk assessment methods did not prevent the emergence of new chemicals with (suspected) DNT potential. Exposure to these chemicals may be related to the increased worldwide incidence of learning and neurodevelopmental disorders in children. DNT is often investigated in a traditional manner (*in vivo* using large numbers of experimental animals), whereas development of *in vitro* methods for DNT reduces animal use and increases insight into cellular and molecular mechanisms of DNT. Several essential neurodevelopmental processes, including proliferation, migration, differentiation, formation of axons and dendrites, synaptogenesis, and apoptosis, are already being evaluated *in vitro* using biochemical and morphological endpoints. Yet, investigation of chemical-induced effects on the development of functional neuronal networks, including network formation, inter- and intracellular signaling and neuronal network function, is underrepresented in DNT testing. This view therefore focuses on *in vitro* models and innovative experimental approaches for functional DNT testing, ranging from optical and electrophysiological measurements of intra- and intercellular signaling in neural stem/ progenitor cells to measurements of network activity in neuronal networks using multielectrode arrays. The development of functional DNT assays will strongly support the decision-making process for measures to prevent potential chemical-induced adverse effects on neurodevelopment and cognition in humans. We therefore argue that for risk assessment, biochemical and morphological approaches should be complemented with investigations of neuronal (network) functionality.

Keywords: *In vitro* methods; Neural progenitor cells; Neuronal network function; Intercellular and intracellular communication; Neurodevelopmental disorders; Risk assessment.

1. Introduction

The developing brain is a sensitive target for chemical disruption (Rice and Barone, 2000). Epidemiological studies have demonstrated that exposure of the developing nervous system to neurotoxicants, such as lead and polychlorinated biphenyls, results in adverse effects in humans. These include developmental delays or alterations in behavior, cognition, and motor functions (Winneke, 2011). However, these classical cases of developmental neurotoxicity (DNT) in humans and advances in risk assessment methods did not prevent the emergence of new (suspected) developmentally neurotoxic chemicals. Over the past three decades, the incidence of learning and neurodevelopmental disorders in children appears to be increased (Herbert, 2010). Exposure to environmental chemicals has been identified as a risk factor for these neurodevelopmental disorders (Bellinger, 2012). Despite these findings, DNT testing is not a primary objective in chemical testing programs.

DNT is often investigated in a traditional manner: *in vivo* using large numbers of experimental animals, mostly rodents (OECD, 2007). The development of *in vitro* methods for DNT can play a role in the reduction of animal use while increasing time- and cost-effectiveness. Moreover, these methods have the potential to provide insight into cellular and molecular mechanisms of DNT that are not readily identified in experimental animal studies. Many efforts are currently undertaken in the field of (developmental) neurotoxicity to improve the predictivity of *in vitro* models by increasing their sensitivity and specificity (e.g. Lein *et al.*, 2007).

During development, the brain evolves from embryonic ectodermal cells to a complex network of many specialized, highly interconnected and structured cells. Development continues after birth and developmental processes need to take place within a strictly controlled time frame and in the right order. The DNT of a chemical is therefore not only related to the dose and whether or not the chemical (or its metabolites) can reach the nervous system, but

also to the developmental phase during which the brain is exposed (Rice and Barone, 2000). The specific vulnerability of the developing brain is also related to the lower capacity of the blood-brain barrier to protect the brain from xenobiotics (Ek *et al.*, 2012). Although the regenerative capacity of the developing brain may allow for adaptation to or compensation for chemical-induced effects, exposure during key periods of brain development may also result in enhanced susceptibility at a later age (e.g. Eriksson *et al.*, 2003).

The rapid development and marketing of new chemicals constantly alters the human exposure situation. In several cases, exposure reduction measures have been necessary for a particular chemical after identification of adverse effects in children. To avoid such situations in the future, the development of screening methods for potential developmentally neurotoxic chemicals is critical. In this view, we therefore support the implementation of *in vitro* assays to identify and prioritize cellular and molecular mechanisms of DNT, and we advocate the inclusion of functional parameters. Currently, no guidelines on *in vitro* DNT models and tests exist, but several *in vitro* testing approaches have been initiated (Bal-Price *et al.*, 2010, van Thriel *et al.*, 2012, Coecke *et al.*, 2007).

For the investigation of chemical-induced effects on the (developing) brain, specific cellular processes can be investigated using *in vitro* models. These cellular processes are critical for the formation of functional neuronal networks that receive, conduct, and transmit signals via chemical or electrical synapses, and relay information between specific brain regions for information processing as well as learning and memory formation. Essential neurodevelopmental processes include proliferation, migration, differentiation, formation of axons and dendrites, synaptogenesis, myelination, and apoptosis (Lein *et al.*, 2007, Rice and Barone, 2000). Many of these parameters are already being evaluated *in vitro* using biochemical and morphological endpoints (Table 1A). However, investigation of chemical-induced effects on the development of neuronal network functionality is underrepresented in DNT testing (<20% of original research articles in a PubMed search for *in vitro* DNT

are related to neuronal function; for details see Supplemental Material). Parameters to investigate in neuronal network functionality include network formation, action potential generation, calcium homeostasis, synaptic transmission, and synaptic plasticity (Table 1B). In this view, approaches and recent innovations are reviewed with emphasis on those that allow for investigation of chemical-induced effects on the development of functional neuronal networks that form the basis for (human) cognition.

2. *In vitro* models for DNT testing

Various *in vitro* systems, including cell lines, primary cell cultures, and stem cell models, are used to model the developing nervous system. Immortalized neuronotypic cell lines provide a homogeneous cell population that is often well characterized and controlled. In many cases, they are easily cultured, divide rapidly, and can be derived from different species, including humans. Compared with primary cells, cell lines readily allow the incorporation of exogenous genes. Additionally, some of these cells can be differentiated into different neural subtypes (Costa *et al.*, 2011a). However, their genetic stability decreases with increasing number of passages, neurites do not always represent true axons or dendrites and functional synapses are often absent (Breier *et al.*, 2010). Additionally, transformed cell lines may represent only a subset of cells and may not have the same (functional) phenotype as primary cells.

Primary cells usually have the same phenotype as brain cells *in vivo* and maintain most neurodevelopmental processes. They can be isolated relatively easily from distinct brain areas and at different developmental stages (Costa *et al.*, 2011a, Breier *et al.*, 2010). However, these cultures often contain populations of postmitotic neurons, which is a disadvantage for the study of neurodevelopmental processes. Practical limitations include a relatively short life span, variability between cultures, and the limited availability of certain tissues (e.g., from human fetuses and/or surgical patients; Costa *et al.*, 2011a, Breier *et al.*, 2010).

Stem cells, which are characterized by their ability to selfrenew by proliferation, are abundantly present in the developing nervous system and give rise to the different cell types in the brain. Therefore, (cord blood-derived) embryonic stem cells (ESCs) and neural progenitor cells (NPCs) are particularly suited for the investigation of neurodevelopmental processes (Breier *et al.*, 2010, Buzanska *et al.*, 2009, Davila *et al.*, 2004). ESCs are pluripotent, and they can give rise to (almost) all cell types of the organism, whereas multipotent progenitor cells already have some characteristics from the region from which they are isolated. As a result, (neuronal) progenitor cells give rise to tissue-specific cell types (Breier *et al.*, 2010, Davila *et al.*, 2004). Therefore, NPCs may be more efficiently applied to generate a heterogeneous neural culture than pluripotent ESCs, because ESCs first need to differentiate into a neural phenotype. Also, NPC cell lines with differentiation potential have been generated (e.g. Donato *et al.*, 2007). It is not yet firmly established whether ESCs/NPCs can form functional neuronal networks, though recent findings indicate that ESCs develop functional neuronal characteristics *in vitro* (Heikkila *et al.*, 2009, Weick *et al.*, 2011, Zimmer *et al.*, 2011a). In most cases, however, ESCs require several weeks of differentiation before functional neuronal (network) characteristics develop, which is a limiting factor for the throughput capacity in a toxicological setting.

Neuronal network function depends critically on the presence of multiple neural cell types (Fellin, 2009), including neurons, oligodendrocytes, microglia, and astrocytes. The importance of the presence of multiple neural cell types for DNT testing depends on the parameter of interest. For example, acute effects on neurotransmitter release can be investigated in a homogenous cell culture, but effects on cell viability will vary between different cell types and heterogeneous cell models, for example due to variations in their antioxidant capacity (Giordano *et al.*, 2009) and receptor profile. As mentioned earlier, the DNT potential of a chemical can vary depending on the stage of brain development during which an organism is exposed. This specific characteristic is not fully represented in most *in vitro* models, but can potentially be improved in heterogeneous models and using subchronic (developmental) exposure scenarios.

Table 1. *In vitro* developmental neurotoxicity testing. Key neurodevelopmental processes in the structural **A**. and functional **B**. development of functional neuronal networks, corresponding *in vitro* endpoints and example approaches for DNT studies. For a table including references, readers are referred to the Table S1.

	Process	*In vitro* endpoint	Example approach
A. Structure	Proliferation	Cell viability	Biochemistry
		Apoptosis	Biochemistry
	Migration	Migration distance	(High content) image analysis
		Cytoskeletal proteins	Fluorescent imaging
			Gene/protein expression
	Differentiation	Neurotransmitter receptors	Immunocytochemistry
			Gene/protein expression
		Cell-specific markers	Immunocytochemistry
		Enzyme activity	Biochemistry
			Gene/protein expression
		Neurite outgrowth	(High content) image analysis
		Myelination	Gene/protein expression
	Synaptogenesis	Synaptic proteins	Immunocytochemistry
		Synaptic connections	(High content) image analysis
B. Function	Intracellular signaling	Calcium concentration	Fluorescent imaging
		Oxidative stress	Fluorescent imaging
		Kinase signaling	Biochemistry
		Ion channel function	Electrophysiology
		Membrane potential	Fluorescent imaging
			Electrophysiology
	Intercellular signaling	Neurotransmitter release	Electrophysiology
			Fluorescent imaging
		Neurotransmitter receptors	Electrophysiology
	Network function	Network activity	Electrophysiology
		Synaptic plasticity	Electrophysiology

3. Experimental approaches for DNT testing

3.1 Biochemical and morphological DNT testing

In *in vitro* DNT studies, basal neurodevelopmental processes such as proliferation, migration, and differentiation are commonly assessed (Table 1A). These parameters are being investigated in different cell models, including NPCs. These cells can be cultured in monolayers or as free-floating spheres and proliferate in the presence of the appropriate growth factors. In spheres, withdrawal of growth factors triggers cells to migrate out of the sphere onto an extracellular matrix and differentiate into different cell types expressing neuronal and glial markers (Breier *et al.*, 2010, Moors *et al.*, 2009). As such, effects of chemicals on proliferation and migration distance can be measured. Additionally, effects on the presence of different cell types in the migrated network can be determined, e.g., by investigating marker proteins such as nestin, β(III)-tubulin, and glial fibrillary acidic protein for developing and mature neurons and astrocytes, respectively (Kuegler *et al.*, 2010).

Most *in vitro* DNT studies describe effects of chemicals on cell viability in neural cell types. When based on cell viability only, the distinction between general toxicity and (developmental) neurotoxicity remains unclear. Nevertheless, dose range finding for the investigation of specific DNT parameters should, in all cases, be included to prevent confounding by effects on cell viability. Mitochondrial function (including the generation of ATP, metabolism of reactive oxygen species, and modulation of calcium homeostasis) is not only essential for neuronal viability and function (including plasticity), but also plays an important role in the structural development (e.g., by regulating apoptosis) of neuronal networks (Cheng *et al.*, 2010). Endpoints of mitochondrial function in isolated mitochondria or intact (neural) cells that may be used in *in vitro* DNT include mitochondrial respiration, ATP turnover, and proton leak (reviewed in Brand and Nicholls, 2011).

Structural aspects of functional network development include neurite outgrowth (i.e., the development of axons and dendrites) and synaptogenesis. Several studies have demonstrated the ability of *in vitro* models to detect

chemically-induced changes in neurite outgrowth, using manual or (semi) automated methods to acquire microscopic images and quantify neurite development (Radio *et al.*, 2010, Radio and Mundy, 2008).

Recently, systems have been developed for simultaneous investigation of multiple endpoints. An example is the imaging-based quantification of neurite growth in LUHMES human neuronal precursor cells. This approach allows for the simultaneous evaluation of cell viability and neurite outgrowth, thereby identifying specific neuritotoxic chemicals (Stiegler *et al.*, 2011). Moreover, high content image analysis (HCA) platforms have been developed to track phenotypic changes in individual cells using different fluorescent labels in a multiwell format. As such, HCA allows for the investigation of chemical-induced effects on multiple morphological endpoints in neuronal (network) development over time, including neuron density, neurite length, and the number of synapses (Harrill *et al.*, 2011b, Radio *et al.*, 2010).

3.2 Neuronal (network) function in DNT testing

In functional neuronal networks, intercellular communication takes place at the synaptic connections, whereas intracellular signaling cascades, such as calcium signaling, modulate neuronal signals. Besides affecting a multitude of (sub)cellular processes, calcium is the trigger of vesicular neurotransmitter release in neuronal cells through activation of the exocytotic release machinery (Neher and Sakaba, 2008). Chemical-induced changes in intracellular calcium dynamics, e.g., by effects on the influx, efflux, or compartmentalization of calcium, can alter neurotransmitter release, thereby modulating intercellular communication.

Changes in intracellular calcium levels can be investigated using fluorescent markers, preferably at high spatial (single-cell) and temporal resolution (Heusinkveld and Westerink, 2011). Changes in neurotransmitter release can be investigated using amperometry or other electrophysiological techniques (Westerink, 2004) as well as optical techniques, e.g., imaging of FM dyes (Brumback *et al.*, 2004) or fluorescent false neurotransmitter (Gubernator

et al., 2009). For intercellular communication, proper function of (mainly postsynaptic) neurotransmitter receptors is also critical. Several chemicals have been shown to modulate neurotransmitter receptor function (Atchison, 1988), potentially resulting in altered neuronal network function. Receptor function and chemical-induced effects thereon can be studied *in vitro* by electrophysiological measurements. To this aim, high-throughput patch clamp systems (e.g. Spencer *et al.*, 2012), which are at this moment mostly used in a drug development setting, could be applied in (developmental) neurotoxicity testing.

The (development of) intercellular communication in *in vitro* neuronal networks can be investigated using fluorescent dyes for monitoring membrane potential (Wolff *et al.*, 2003) or more directly using functional electrophysiological recordings, e.g., using multielectrode arrays (MEAs). MEA systems typically consist of a cell culture surface with an integrated array of microelectrodes, allowing simultaneous extracellular recording of electrical activity at different individual sites in a neuronal network. This can be used to study (the development of) spontaneous activity patterns as well as evoked activity (Johnstone *et al.*, 2010). Importantly, the latter also allows for the investigation of synaptic plasticity (activity dependent synaptic efficiency), which is critical for learning and memory formation (Citri and Malenka, 2008). *In vitro* synaptic plasticity is generally investigated in *ex vivo* brain slices, in particular hippocampal slices using standard protocols (Hernandez *et al.*, 2005). Investigation of plasticity in neural cells cultured on MEAs (e.g. Chiappalone *et al.*, 2008) could improve throughput for chemical testing, although a standard protocol for the investigation of (chemical-induced effects on) plasticity in a neurodevelopmental context remains to be developed.

Chemical-induced changes in network function measured in a MEA system may be due to changes in electrical activity as well as in the release or receival of intercellular signals. MEA systems thus provide an integrated, but not pathway specific, measure for effects on neurotransmission that can be applied for DNT screening purposes. MEA approaches have only relatively recently been

introduced in neurotoxicological research, mostly for the investigation of acute disruption of network function. Recent investigations of the interlaboratory variation in MEA recordings in rat cortical cultures have shown that neurotoxic responses can be measured reproducibly (Novellino *et al.*, 2011). Only very recently, MEA research has been initiated for the investigation of DNT, demonstrating the development of function in neuronal cultures (Hogberg *et al.*, 2011, Robinette *et al.*, 2011). To improve the throughput of MEA systems, a multiwell MEA was recently introduced and tested with a training set of chemicals for its application in neurotoxicity testing (McConnell *et al.*, 2012). This higher throughput format may further increase the potential of MEA systems in (developmental) neurotoxicity testing.

4. Discussion

Recent approaches and innovations for the *in vitro* investigation of chemical-induced effects on neurodevelopmental processes allow for investigation of functional endpoints (Table 1B). These endpoints, such as calcium homeostasis, neurotransmitter release, and intercellular communication in neuronal networks, reflect the actual function of the nervous system and are therefore a valuable addition to biochemical and morphological endpoints. Other important aspects in the development of the nervous system, e.g., myelinization, are largely unexplored in (developmental) neurotoxicity studies. It is also notable that *in vitro* neuronal cultures have low metabolic capacity. Specific impact of metabolites therefore has to be investigated separately, e.g., by directly exposing the cells to the metabolites of interest.

The maintenance of newly formed synapses depends on their activity. Functional neuronal processes that play a role in interneuronal communication (e.g. calcium signaling, neurotransmitter release, and neurotransmitter receptor function) are therefore not only the ultimate goal of functional neuronal network formation, but are also critically involved in the developmental process itself. As such, acute neurotoxicity may also affect brain development, depending

on the timing of exposure to a neurotoxic chemical. The predictivity of acute neurotoxicity for DNT potential is however not yet characterized.

Noteworthy, recommendations for the development of screening and prioritization methods for DNT as well as a draft list of model chemicals were recently provided (Crofton *et al.*, 2011). It should also be noted that most of the approaches highlighted in this view originate from the neuroscience field. Therefore, emerging techniques and innovations in neuroscience should be closely followed and assessed for their potential and applicability in (developmental) neurotoxicity studies.

For a large number of high-production chemicals, basic and more specific toxicological data are currently lacking (Lein *et al.*, 2007). Replacing animal experiments with *in vitro* models already allows for higher testing capacity. In view of the large number of chemicals to be tested, the use of medium-to-high throughput approaches is, in general, preferable for chemical screening purposes for (functional) DNT effects. Most biochemical and structural assays for *in vitro* DNT testing have the potential for medium-to-high throughput testing and there are cases where medium-to-high throughput testing was able to confirm the (developmental) neurotoxic potential of well-known DNT chemicals (e.g. Breier *et al.*, 2008, Radio *et al.*, 2008, Culbreth *et al.*, 2012, Harrill *et al.*, 2011a). However, achieving this level of throughput is often challenging for functional analysis and in-depth investigation of DNT mechanisms. Additionally, the generation of large amounts of data, either by testing many chemicals using high-throughput approaches or generating high density data (e.g., using MEAs, HCA, or optical recordings) brings forth new requirements in data storage and analysis for which the implementation of bioinformatics is necessary.

In vitro assays are useful to regulators involved in hazard and risk assessment and legislation of chemicals, as well as to chemical and pharmaceutical industries that may want to apply in-house DNT screening assays in chemical and drug development. However, due to the complexity of the developing

(central) nervous system and considerations such as exposure timing, *in vitro* models are not likely to completely replace *in vivo* DNT testing. Nevertheless, there is general agreement within the field of toxicology that the future of toxicity testing is a tiered testing strategy that focuses on pathways that are critical for adequate functioning of cells, organs, and organisms (Seiler *et al.*, 2011, Crofton *et al.*, 2011, Bal-Price *et al.*, 2010). This includes the integration of different testing strategies for exposure and toxicity with emphasis on nonanimal models, including integrated genomic and proteomic analyses of chemical-induced effects on signaling pathways (e.g. Pennings *et al.*, 2012), developmental processes, and the formation of functional neuronal networks (e.g. Slotkin and Seidler, 2010).

Apart from being adverse on an individual level, neurodevelopmental disorders have economic consequences due to reduced potential to contribute to society as well as additional costs for medical care. Low-dose exposure to chemicals has the potential to cause small but population-wide adverse effects on cognition and incidence rates of neurodevelopmental disorders in humans. The development of screening assays for DNT is critical for the decision-making process to prevent this. We therefore argue that for risk assessment of chemical-induced effects on human neurodevelopment and cognitive function, biochemical and morphological approaches should be complemented with investigations of neuronal network functionality.

Acknowledgments

We apologize to all authors of primary literature or previous reviews on (functional) *in vitro* models for DNT that we could not include due to space limitations. The authors declare they have no actual or potential competing financial interests. This work was funded by the European Union (DENAMIC; FP7-ENV-2011-282957), the Netherlands Organization for Health Research and Development (ZonMw; 85300003) and the Faculty of Veterinary Medicine of Utrecht University.

Supplemental Material

PubMed search on developmental neurotoxicity *in vitro*:

Search term "*in vitro* AND (DNT OR developmental neurotox*)" resulted in 189 hits. After removal of publications on different subjects with the abbreviation DNT (dinitrotoluene, dermonecrotic toxin, double negative thymocytes) as well as reviews, workshop summaries and letters, 82 research papers remained. Publications were considered to be not relevant for developmental neurotoxicity *in vitro* if the research included *in vivo* exposure or chemical exposure duration less than 24h. After application of these exclusion criteria, 55 research papers remained. Of these 55 research papers on developmental neurotoxicity *in vitro*, only 12 were related to parameters considered ´functional´ as described in this forum article (intracellular signaling including oxidative stress, calcium homeostasis and kinase signaling, electrophysiological recordings in MEAs).

Table S1. *In vitro* developmental neurotoxicity testing. Key neurodevelopmental processes in the structural **A**. and functional **B**. development of functional neuronal networks, corresponding *in vitro* endpoints and example approaches for DNT studies.

	Process	*In vitro* endpoint	Example approach	Example reference
A. Structure	Proliferation	Cell viability	Biochemistry	Slotkin et al., 2009
		Apoptosis	Biochemistry	Howard et al., 2003
	Migration	Migration distance	(High content) image analysis	Schreiber et al., 2010
		Cytoskeletal proteins	Fluorescent imaging	Flaskos et al., 2011
			Gene/protein expression	Mundy et al., 2008
	Differentiation	Neurotransmitter	Immunocytochemistry	Slotkin and Seidler, 2008
		receptors	Gene/protein expression	Zimmer et al., 2011b
			Immunocytochemistry	Schreiber et al., 2010
		Cell-specific markers	Biochemistry	Visan et al., 2012
		Enzyme activity	Gene/protein expression	Zurich et al., 2004
			(High content) image analysis	Slotkin and Seidler, 2008
		Neurite outgrowth	Gene/protein expression	Zimmer et al., 2011b
		Myelination		
	Synaptogenesis	Synaptic proteins	Immunocytochemistry	Harrill et al., 2011a
		Synaptic connections	(High content) image analysis	Frimat et al., 2010
B. Function	Intracellular signaling	Calcium concentration	Fluorescent imaging	Barhoumi et al., 2010
				Dingemans et al., 2010a
		Oxidative stress	Fluorescent imaging	Chen et al., 2010
		Kinase signaling	Biochemistry	VanDemark et al., 2009
		Ion channel function	Electrophysiology	Burr and Ray, 2004
				Spencer et al., 2012
		Membrane potential	Fluorescent imaging	Wolff et al., 2003
			Electrophysiology	Pancrazio et al., 2001
	Intercellular signaling	Neurotransmitter release	Electrophysiology	Westerink, 2004
			Fluorescent imaging	Gubernator et al., 2009
				Brumback et al., 2004
		Neurotransmitter receptors	Electrophysiology	Hondebrink et al., 2011b
	Network function	Network activity	Electrophysiology	Gramowski et al., 2000
				Hogberg et al., 2011
		Synaptic plasticity	Electrophysiology	Chiappalone et al. 2008
				Johnstone et al., 2010t

CHAPTER 5

Characterization of calcium responses and electrical activity in differentiating mouse neural progenitor cells *in vitro*

Martje W. G. D. M. de Groot, Milou M. L. Dingemans, Katinka H. Rus, Aart de Groot, and Remco H. S. Westerink.

Neurotoxicology Research Group, Toxicology Division, Institute for Risk Assessment Sciences (IRAS), Faculty of Veterinary Medicine, Utrecht University, PO Box 80.177, NL-3508 TD Utrecht,
The Netherlands

Toxicological Sciences (2014). **137**(2): 428–435
DOI:10.1093/toxsci/kft261

Abstract

In vitro methods for developmental neurotoxicity (DNT) testing have the potential to reduce animal use and increase insight into cellular and molecular mechanisms underlying chemical-induced alterations in the development of functional neuronal networks. Mouse neural progenitor cells (mNPCs) differentiate into nervous system-specific cell types and have proven valuable to detect DNT using biochemical and morphological techniques. We therefore investigated a number of functional neuronal parameters in primary mNPCs to explore their applicability for neurophysiological *in vitro* DNT testing. Immunocytochemistry confirmed that mNPCs express neuronal, glial, and progenitor markers at various differentiation durations (1, 7, 14, and 21 days). Because intracellular calcium ($[Ca^{2+}]_i$) plays an essential role in neuronal development and function, we measured stimulus-evoked changes in $[Ca^{2+}]_i$ at these differentiation durations using the Ca^{2+}-responsive dye Fura-2. Increases in $[Ca^{2+}]_i$ (averages ranging from 65 to 226 nM) were evoked by depolarization, ATP, L-glutamic acid, acetylcholine, and dopamine (up to 87%, 57%, 93%, 28%, and 37% responding cells, respectively) and to a lesser extent by serotonin and gamma-aminobutyric acid (both up to 10% responding cells). Notably, the changes in percentage of responsive cells and their response amplitudes over time indicate changes in the expression and functionality of the respective neurotransmitter receptors and related calcium signaling pathways during *in vitro* differentiation. The development of functional intercellular signaling pathways was confirmed using multielectrode arrays, demonstrating that mNPCs develop electrical activity within 1–2 weeks of differentiation (55% active wells at 14 days of differentiation; mean spike rate of 1.16 spikes/s/electrode). The combined data demonstrate that mNPCs develop functional neuronal characteristics *in vitro*, making it a promising model to study chemical-induced effects on the development of neuronal function.

Keywords: Differentiating mouse neural progenitor cells; Functional endpoints for *in vitro* neurotoxicity testing; Fura-2 single-cell fluorescent microscopy; Multielectrode array; Calcium homeostasis; Electrical activity.

1. Introduction

The awareness and concern about the potential developmental neurotoxicity (DNT) of low-level exposure to environmental chemicals has prompted considerable efforts to develop *in vitro* models and methods to study chemical-induced alterations in neuronal development. Many essential neurodevelopmental processes are evaluated *in vitro* using biochemical and morphological endpoints, and recent innovations allow for the inclusion of functional neuronal parameters (reviewed in de Groot *et al.*, 2013). Neuronal function is defined by inter- and intracellular signaling processes. In particular, calcium signaling plays a critical role in neuronal development and function. Disturbances in the basal intracellular calcium concentration ($[Ca^{2+}]_i$) may affect many cellular processes, including neurodevelopment (Lohmann, 2009). Moreover, calcium is essential for neurotransmission and plasticity, as a tightly regulated stimulus-evoked increase in $[Ca^{2+}]_i$ triggers vesicular neurotransmitter release via activation of the exocytotic release machinery (Neher and Sakaba, 2008). Changes in calcium homeostasis, e.g. by a chemical insult, can thus also disturb neurotransmitter release and subsequently modulate intercellular communication.

DNT is studied in a wide array of *in vitro* models, ranging from immortalized neuronotypic cell lines to brain slices (reviewed in de Groot *et al.*, 2013). Different cell types are present in the brain, and this heterogeneity of neural cells types supports neuronal network functionality (Araque and Navarrete, 2010). Cultures of neural progenitor cells (NPCs) have previously been shown to contain multiple cell types, i.e. neuronal and glial cells, comparable with the *in vivo* situation (Breier *et al.*, 2010). Moreover, basic processes of brain development, including proliferation, differentiation, and migration have already been evaluated in mouse NPCs (mNPCs; Gassmann *et al.*, 2012). However, the functional neuronal aspects of mNPCs are still largely unexplored despite the importance of these processes for neuronal development and function. In the present study, we therefore characterized several neurophysiological processes in *in vitro* differentiating mNPCs to

explore their applicability for functional DNT testing. The expression of neuronal, glial, and progenitor markers in primary mNPCs was confirmed using immunocytochemistry. Changes in $[Ca^{2+}]_i$ evoked by a set of stimuli, including membrane depolarization and common neurotransmitters, were investigated in mNPCs at various differentiation durations using the Ca^{2+}-responsive dye Fura-2. Additionally, mNPCs were cultured on multiwell multielectrode arrays (MEAs) to investigate the development of electrical activity *in vitro*.

2. Materials and methods

2.1 Chemicals

Dulbecco's Modified Eagle's Medium (DMEM), Ham's F12 nutrient mixture, N2 supplement, B27 supplement (without vitamin A), murine fibroblast growth factor (mFGF), murine epidermal growth factor (mEGF), penicillin-streptomycin (5000 U/mL–5000 µg/mL), 0.05% trypsin-EDTA, and Fura-2 AM were obtained from Life Technologies (Bleiswijk, The Netherlands); all other chemicals were obtained from Sigma-Aldrich (Zwijndrecht, The Netherlands). External saline solution for Ca^{2+}-imaging experiments, containing (in mM) 125 NaCl, 5.5 KCl, 2 $CaCl_2$, 0.8 $MgCl_2$, 10 HEPES, 24 glucose, and 36.5 sucrose (pH set at 7.3), and high-potassium saline solution, containing (in mM) 5.5 NaCl, 100 KCl, 2 $CaCl_2$, 0.8 $MgCl_2$, 10 HEPES, 24 glucose, and 36.5 sucrose (pH set at 7.3), were prepared with deionized water (Milli-Q®; resistivity > 10 MΩ·cm). Stock solutions of 2 mM ionomycin were prepared in dimethylsulfoxide (DMSO) and kept at −20°C. Solutions containing gamma-aminobutyric acid (GABA; 100 µM), 5-hydroxytryptamine hydrochloride (serotonin; 100 µM), acetylcholine chloride (ACh; 100 µM), disodium ATP (100 µM), or sodium L-glutamic acid (100 µM) were prepared in saline and separate aliquots for every experimental day were kept at −20°C. Solutions containing dopamine hydrochloride (100 µM) were prepared immediately before use.

2.2 NPC isolation and culture

2.2.1 Ethics statement and animal care

Timed-pregnant (embryonic day 14; E14) C57bl/6NHsd mice were obtained from Harlan Laboratories B.V. (Horst, The Netherlands). Animals were treated humanely and with regard for alleviation of suffering. All experimental procedures were performed according to Dutch law and approved by the Ethical Committee for Animal Experimentation of Utrecht University.

2.2.2 mNPC isolation and cell culture

mNPCs were isolated from embryonic mouse brains (E14; protocol adapted from Gassmann *et al.*, 2012 and Azari *et al.*, 2011). Briefly, timed-pregnant C57bl/6NHsd mouse dams were euthanized by decapitation after inhalation anesthesia with isoflurane. Uteri were rapidly dissected and the embryos removed and decapitated. The age of the embryos was determined according to the staging criteria of Theiler, in which E14 corresponds to Theiler stage 22 (Bard *et al.*, 1998). Whole embryonic brains were collected by dissection on ice and mechanically dissociated to a single-cell suspension. Tissues were kept in DMEM on ice during the entire isolation procedure. Living cells were seeded at a density of 5×10^5 cells/mL in T75 culture flasks (Greiner Bio-one, Solingen, Germany) in 20 mL cell culture medium (DMEM/Ham's F12 nutrient mixture [DMEM:Hams F12 ratio 3:1], supplemented with 2% B27 supplement [without vitamin A], 20 ng/mL mFGF, 20 ng/mL mEGF, 50 U/mL penicillin, and 50 µg/mL streptomycin) at 37 °C in a 5% CO_2 atmosphere. Cells were cultured in suspended sphere form and culture medium was replaced weekly. Spheres were triturated (bi) weekly and seeded at a density of 5×10^4 cells/mL to form secondary spheres.

2.2.3 Subculture and differentiation of mNPCs for experiments

To initiate differentiation prior to experiments, mNPCs were seeded on poly-L-lysine (PLL)–coated culture material in DMEM:Hams F12 (3:1) medium, supplemented with 1% N2 supplement, 50 U/mL penicillin, and 50 µg/mL streptomycin (N2 medium) for up to 21 days at 37 °C in a 5% CO_2 atmosphere. For light microscopic imaging, mNPC spheres were seeded in

35 mm culture dishes (ThermoScientific, Waltham, Massachusetts). For immunocytochemistry, mNPC spheres were subcultured on 12 mm German glass coverslips (no. 1; Rofa-Mavi, Beverwijk, The Netherlands) in 24-well plates. For single-cell fluorescent Ca^{2+}-imaging experiments, mNPC spheres were seeded in 35 mm glass bottom dishes (MatTek, Ashland, Oregon). For MEA experiments, mNPCs were subcultured as single cells in 48-well MEA plates (Axion Biosystems Inc., Atlanta, Georgia). mNPCs were seeded as a 100 µL droplet of cell suspension (5×10^6 cells/mL) on the electrode field in each well. The droplet of cells was allowed to adhere to the electrode field for approximately 4 h, after which 400 µL of N2 medium was added to each well. The wells in the MEA plates and the glass coverslips were covered with medium for 0.5–1 h just prior to seeding the cells. For all types of experiments, medium was replaced every 7 days.

2.3 Immunocytochemistry

At various differentiation durations (1, 7, 14, and 21 days), cells were fixed with 4% paraformaldehyde (PFA) in 0.1 M phosphate buffer (pH 7.4) for 20 min at room temperature (rt). Subsequently, coverslips were quenched for PFA, permeabilized, and incubated with blocking buffer (2% bovine serum albumin and 0.1% saponin in PBS) containing 20 mM NH_4Cl for 20 min at rt. Each of the subsequent wash and incubation steps was performed in blocking buffer. Next, a subset of coverslips was incubated with goat anti-glial fibrillary acidic protein (GFAP; ab53554, Abcam, Cambridge, United Kingdom) and rabbit anti-β(III)-tubulin (ab76288, Abcam, Cambridge, United Kingdom) antibodies, both at a final dilution of 1:100 for 70 min at rt. The other subset of coverslips was incubated with rat anti-nestin antibodies (ab81462, Abcam, Cambridge, United Kingdom) at a dilution of 1:100 for 70 min at rt. Subsequently, coverslips were washed 3 times and incubated with fluorochrome-conjugated secondary antibodies; donkey anti-goat DyLight 568 (Jackson ImmunoResearch Laboratories Inc., West Grove, Pennsylvania) and donkey anti-rabbit Alexa 488 (Life Technologies, Bleiswijk, The Netherlands) for the double stain or goat anti-rat Alexa 488 (Life Technologies, Bleiswijk, The Netherlands) for the single stain, at a final dilution of

1:100 for 30 min at rt in the dark. Nuclear staining was performed by incubating the coverslips with 4',6-diamidino-2-phenylindole (DAPI; Life Technologies, Bleiswijk, The Netherlands) at a concentration of 200 nM for 3 min at rt in the dark. The washing procedure was repeated and the coverslips were sealed with FluorSave (Calbiochem, San Diego, California). Immunostained coverslips were visualized using a Leica SPEII Confocal microscope (Leica DMI4000 equipped with TCS SPE-II) using a ×20 oil immersion objective (N.A. 1.4–0.7) and images were captured using Leica Application Suite Advanced Fluorescence software (LAS AF version 2.6.0; Leica Microsystems GmbH, Wetzlar, Germany).

2.4 Intracellular calcium imaging

Stimulation-evoked changes in $[Ca^{2+}]_i$ were measured in mNPCs at various differentiation durations (1 [1–2], 7 [7–8], or 14 [13–15] days) using the Ca^{2+}-sensitive fluorescent ratio dye Fura-2 AM as described previously (Hendriks *et al.*, 2012). Following a 5 min baseline measurement, cells were stimulated with high-K^+ saline (100 mM K^+), 100 µM ATP, 100 µM GABA, 100 µM dopamine, 100 µM serotonin, 100 µM ACh, or 100 µM L-glutamic acid (effective concentrations were based on pilot studies) for 30 s using an automated continuous superfusion system (AutoMate Scientific Inc., Berkeley, California). As a control for experimental setup and to calculate calcium concentrations from the F_{340}/F_{380} ratios (see 2.6 Data analysis and statistics), maximum and minimum ratios (R_{max} and R_{min}) were determined at the end of the experiment by addition of the ionophore ionomycin (final concentration 5 µM) and the calcium chelator EDTA (final concentration 17 mM), respectively.

2.5 MEA recordings

Electrical activity of the mNPCs was measured using PLL-coated 48-well MEA plates. Each well contains 16 nanotextured gold microelectrodes (~40–50 µm diameter; 350 µm center-to-center spacing) with 4 integrated ground electrodes, yielding a total of 768 channels (Axion Biosystems Inc.). Spontaneous electrical activity in mNPCs was recorded at various

differentiation durations (1, 7, 14, and 21 days). Signals were recorded using a Maestro 768-channel amplifier with integrated heating system and temperature controller and a data acquisition interface (Axion Biosystems Inc.). Axion's Integrated Studio (AxIS 1.7.8) was used to manage data acquisition (Figure 1). Prior to the 30min recording of spontaneous activity, MEA plates were allowed to equilibrate in the Maestro for 5–10 min. At the end of the experiments, 48-well plates were cleaned for reuse by rinsing with Milli-Q® and overnight incubation with 0.05% trypsin-EDTA. Subsequently, plates were washed with Milli-Q®, filled and incubated with ethanol overnight, washed with ethanol, and placed upside down (lid on) at 55°C overnight. To obtain raw data files, channels were sampled simultaneously at a constant temperature of 37°C with a gain of 1200 × and a sampling frequency of 12.5 kHz/channel using a band-pass filter (200–5000 Hz). Afterward, raw data files were rerecorded to obtain Alpha Map files for further data analysis in NeuroExplorer (see 2.6 Data Analysis and Statistics section). During the rerecording, spikes were detected using the AxIS spike detector (Adaptive threshold crossing, Ada BandFlt v2) with a variable threshold spike detector set at 7 times SD of the internal noise level (rms) on each electrode.

2.6 Data analysis and statistics

Changes in the ratio of fluorescence evoked by 340 and 380nm excitation wavelengths (F_{340}/F_{380} ratio; R), reflecting changes in $[Ca^{2+}]_i$, were analyzed using custom-made MS-Excel macros. Free cytosolic $[Ca^{2+}]_i$ was calculated using a modified Grynkiewicz's equation (Grynkiewicz *et al.*, 1985): $[Ca^{2+}]_i = K_{d*} \times (R - R_{min})/(R_{max} - R)$, where K_{d*} is the dissociation constant of Fura-2 AM determined in the experimental setup. Cells with basal $[Ca^{2+}]_i$ > mean ± 2 × SD were considered outliers and were removed from the data set (~5%). Responding cells were defined as those with a stimulus-evoked net increase in $[Ca^{2+}]_i$ > 50 nM (2 × SD of basal $[Ca^{2+}]_i$). The amplitudes of stimulus-evoked net increases in $[Ca^{2+}]_i$ were determined from these responding cells and outliers with stimulus-evoked net increases in $[Ca^{2+}]_i$ > average ± 2 × SD were removed (~5%).

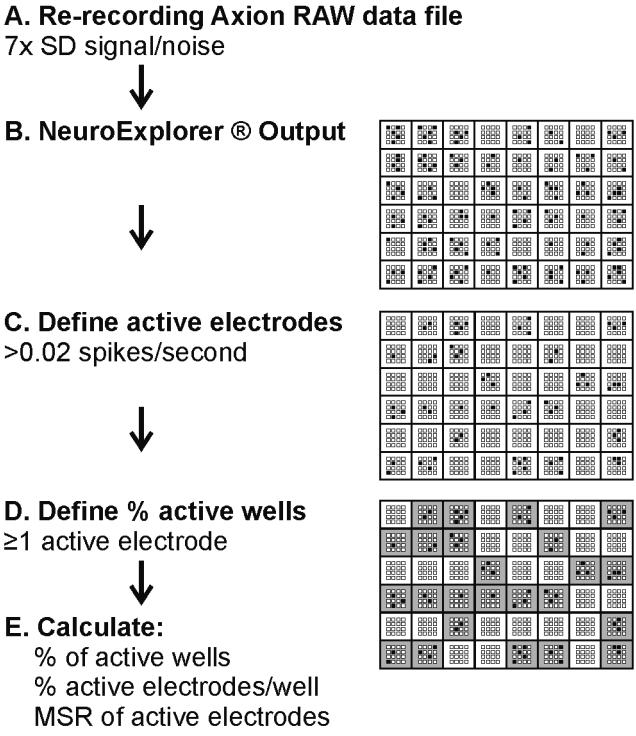

Figure 1. Schematic illustration of the collection and analysis of the MEA data. Multiwell MEA plates (48-well) are represented schematically. Closed and open small squares indicate electrodes where spikes are detected or absent, respectively. Spontaneous neuronal activity is recorded for 30 min from mNPC cultures at the various differentiation durations using hardware and software from Axion Biosystems. Axis recordings were rerecorded **A**. to generate spike count files, using a spike detection threshold of 7× SD of the internal noise level (rms), that were further analyzed using NeuroExplorer software **B**. Active electrodes and wells were defined **C**. and **D**. and percentage of active wells (grey) and percentage of active electrodes (per active well) were calculated **E**., as well as the MSR of the active electrodes (in spikes/s/electrode). Abbreviation: rms, root mean square.

Spike count files generated from MEA recordings were loaded into NeuroExplorer 4.0 software (Nex Technologies, Madison, Wisconsin) for further analysis of the percentage of active wells (defined as ≥ 1 active electrode), the percentage of active electrodes (defined as > 0.02 spikes/s) per well, and the average mean spike rate (MSR) per active electrode (spikes/s/electrode; Figure 1). Only data from active wells were used for further analysis. Malfunctioning electrodes were removed *post hoc* (<0.1%). Electrodes were considered outliers if their MSR > average MSR ± 2 × SD and were removed after data analysis (~5%).

All statistical analyses were performed using SPSS 20 (SPSS, Chicago, Illinois). One-way ANOVA was performed to investigate changes on all parametric data with differentiation duration. Chi-square analysis was used for non-parametric data in contingency tables.

3. Results

3.1 Light microscopic and immunocytochemical characterization of mNPC differentiation

mNPCs proliferate as suspended spheres in culture medium with B27, mEGF, and mFGF (Figure 2A1). Upon differentiation (switch from B27 to N2 supplement and removal of growth factors), the spheres adhere to PLL-coated surfaces and mNPCs migrate out of the spheres in a radial pattern (Figure 2A2). Over time, these mNPCs form a network that increases in complexity with more irregular connections between the migrated cells and spheres (Figure 2A3–5).

At 1, 7, 14, and 21 days of differentiation, mNPC cultures were labeled with fluorescent antibodies for GFAP and β(III)-tubulin or nestin (Figure 2B and 2C). Immunocytochemical analyses revealed the presence of β(III)-tubulin and GFAP positive cells already after 1 day of differentiation. β(III)-tubulin and GFAP expression increases over time of differentiation (Figure 2B1–4). Nestin expression is observed at all differentiation durations investigated (Figure 2C1–4).

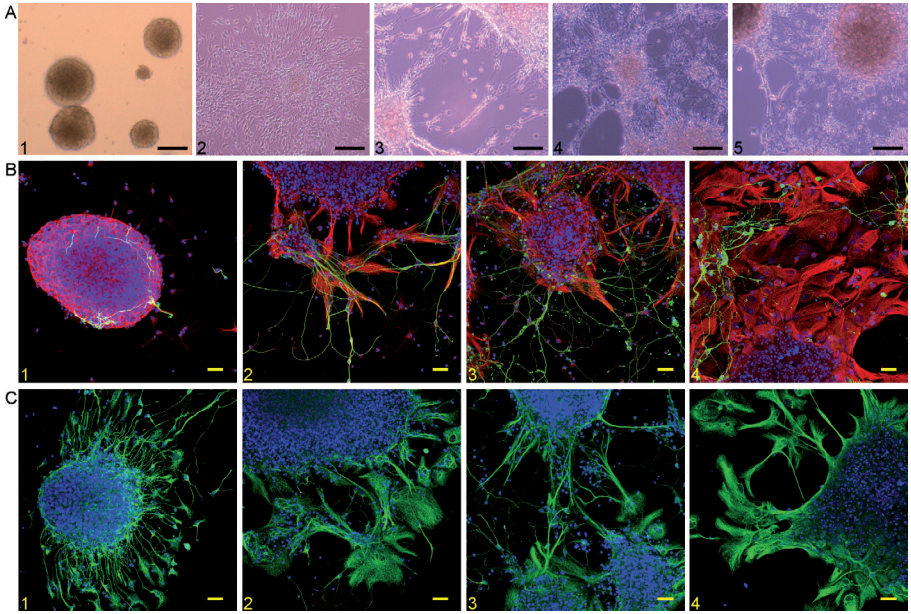

Figure 2. Expression of markers in mNPCs changes with differentiation duration. Light microscopic (A) and immunofluorescent (B and C) images of primary mNPCs at various differentiation durations. **A.** mNPCs proliferate as suspended spheres (A1) and, upon differentiation, adhere to the cell culture surface and migrate out of the spheres (A2–5; 1, 7, 14, and 21 days of differentiation). Scale bar 100 μm; magnification ×10. **B.** Immunocytochemical staining of mNPCs for GFAP (red) and β(III)-tubulin (green) (from left to right, B1–4; 1, 7, 14, and 21 days of differentiation). Nuclei are stained with DAPI (blue). Scale bar 25 μm; magnification ×20 oil immersion. **C.** Immunocytochemical staining of mNPCs for nestin (green) (from left to right, C1–4; 1, 7, 14, and 21 days of differentiation). Nuclei are stained with DAPI (blue). Scale bar 25 μm; magnification ×20 oil immersion.

3.2 Characterization of stimulus-evoked Ca^{2+} responses in differentiating mNPCs

Basal $[Ca^{2+}]_i$ in mNPCs differentiated for 1 or 7 days amounted to 97 ± 1 nM (n = 2126) and 94 ± 1 nM (n = 2294), respectively. At 14 days of differentiation, basal $[Ca^{2+}]_i$ was slightly increased, amounting to 114 ± 1nM (n = 1700; ANOVA $p < 0.001$).

At all investigated differentiation durations, it was possible to induce an increase in $[Ca^{2+}]_i$ using different types of stimulation. As shown in Figure 3 and Figure S1, depolarization (100 mM K^+) of mNPCs differentiated for 1, 7, or 14 days resulted in increases in $[Ca^{2+}]_i$. The percentage of responding mNPCs increased with differentiation duration ($p < 0.001$), and depolarization-evoked increases in $[Ca^{2+}]_i$ were observed in 35% (1 day differentiation), 87% (7 days differentiation), and 74% (14 days differentiation) of cells. The depolarization-evoked net increase in $[Ca^{2+}]_i$ at 1, 7, and 14 days of differentiation amounted to 150 ± 7 nM (n = 141), 226 ± 7 nM (n = 470), and 166 ± 6 nM (n = 300), respectively (ANOVA $p < 0.001$).

Similarly, stimulation with excitatory neurotransmitters resulted in increases in $[Ca^{2+}]_i$ at all tested differentiation durations (Figure 3 and Figure S1). Stimulation with ATP (100 µM) resulted in net increases in $[Ca^{2+}]_i$ in approximately half of the cells (57%, 44%, and 50% at 1, 7, and 14 days of differentiation, respectively; $p = 0.018$). The ATP-evoked net increases in $[Ca^{2+}]_i$ amounted to 208 ± 8 nM (n = 172), 195 ± 14 nM (n = 73), and 147 ± 8 nM (n = 97; ANOVA $p < 0.001$). Stimulation of mNPCs with L-glutamic acid (100 µM) resulted in a clear differentiation duration-dependent increase in the percentage of responding cells ($p < 0.001$). The percentage of responding cells increased from 33% (1 day differentiation) to 55% (7 days differentiation) and 93% (14 days differentiation). The net increases in $[Ca^{2+}]_i$ were comparable at the various differentiation durations, amounting to 223 ± 16 nM (n = 79), 208 ± 15 nM (n = 141), and 192 ± 7 nM (n = 250) at 1, 7, and 14 days of differentiation, respectively (ANOVA

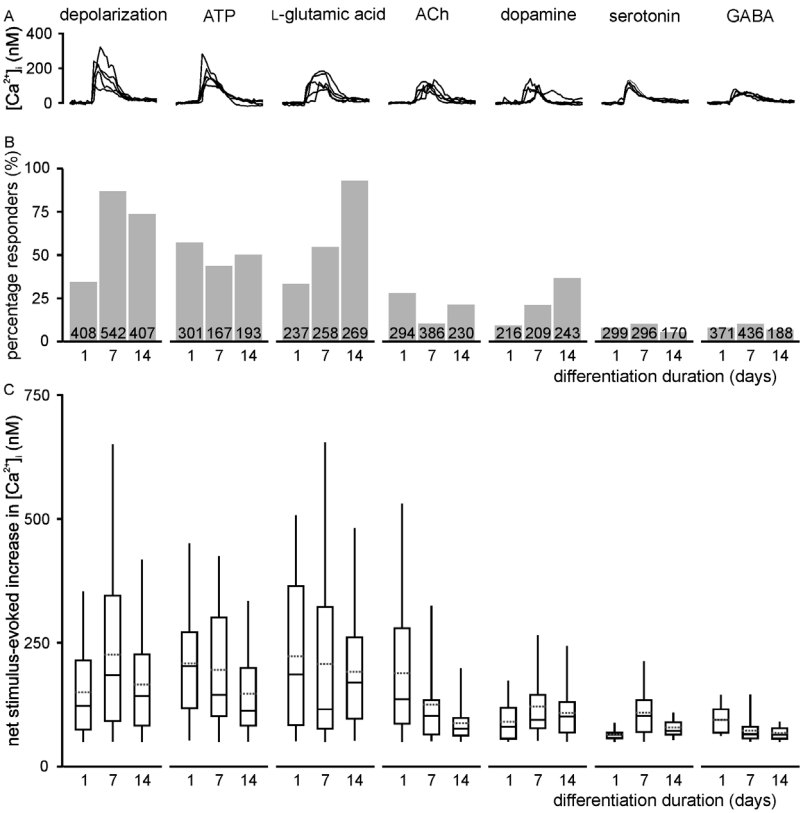

Figure 3. Changes in stimulation-evoked $[Ca^{2+}]_i$ responses with differentiation duration in mNPCs. **A**. Representative 2 min $[Ca^{2+}]_i$ traces illustrating stimulation-evoked net $[Ca^{2+}]_i$ increases ($[Ca^{2+}]_i$) at 7 days of differentiation during 30 s superfusion with the different stimuli (indicated above the traces) following a 30 s baseline recording. Percentage of cells responding to the different stimuli **B**. and net amplitudes of the increase in $[Ca^{2+}]_i$ **C**. (calculated from the responding cells only) at 1, 7, or 14 days of differentiation. Total numbers of cells per stimulus and differentiation duration are indicated in the bars. Boxes represent the 25th–75th percentile range of evoked $[Ca^{2+}]_i$ increases and whiskers indicate minimum and maximum values. Median and mean values are indicated with closed and grey dotted lines within the boxes, respectively.

p = 0.187). Superfusing mNPCs with ACh (100 µM) evoked increases in $[Ca^{2+}]_i$ in 28% (1 day differentiation), 10% (7 days differentiation), and 21% (14 days differentiation) of cells (p < 0.001). The net increases in $[Ca^{2+}]_i$ slightly decrease with differentiation duration, amounting to 189 ± 14 nM (n = 82), 125 ± 12 nM (n = 40), and 88 ± 5 nM (n = 48), respectively (ANOVA p < 0.001).

Increases in $[Ca^{2+}]_i$ in mNPCs could also be evoked by dopamine (100 µM). The percentage of mNPCs responding to dopamine increased with differentiation duration from 9% (1 day differentiation) to 21% (7 days differentiation) and 37% (14 days differentiation; p < 0.001). The net increases in $[Ca^{2+}]_i$ were comparable at the various differentiation durations and amounted to 91 ± 8 nM (n = 20), 121 ± 9 nM (n = 44), and 109 ± 5 nM (n = 89) at 1, 7, and 14 days of differentiation, respectively (ANOVA p = 0.084).

Relatively small net increases in $[Ca^{2+}]_i$ could be evoked in 8%, 10%, and 5% of mNPCs (1, 7, and 14 days differentiated, respectively; p = 0.185) with serotonin (100 µM). The serotonin-evoked net increases amounted to 65 ± 2 nM (n = 24), 109 ± 9 nM (n = 30), and 79 ± 6 nM (n = 9) in mNPCs differentiated for 1, 7, and 14 days, respectively (ANOVA p < 0.001).

Superfusion with GABA (100 µM) resulted in small increases in $[Ca^{2+}]_i$ in 8%, 10%, and 7% of the cells (1, 7, and 14 days of differentiation, respectively; p = 0.371). The evoked net increases in $[Ca^{2+}]_i$ decreased with differentiation duration, from 95 ± 5 nM (n = 30; 1 day differentiated), 73 ± 4 nM (n = 44; 7 days differentiated) to 68 ± 4 nM (n = 13; 14 days differentiated; ANOVA p < 0.001).

3.3 Characterization of electrical activity in differentiating mNPCs

Electrical activity of mNPCs was investigated in 48-well MEA plates at various differentiation durations (1, 7, 14, and 21 days) using 6 mNPC cultures (12–24 wells/culture) obtained from 3 preparations. Development of electrical

activity over time in a representative mNPC culture is depicted in a spike raster plot (Figure 4). Only a few spikes on a few active electrodes are observed after 7 days of differentiation (Figure 4A), but the electrical activity in mNPCs increases at 14 and 21 days of differentiation (Figure 4B and 4C). At 7 days of differentiation, electrical activity could be detected in 20% of the wells (n = 17 out of 84; Figure 5A). With increasing differentiation duration, the percentage of active wells increases up to 55% (n = 46 out of 84; 14 days of differentiation) and 48% (n = 40 out of 84; 21 days of differentiation; $p < 0.001$). On the other hand, the percentage of active electrodes within active wells is rather constant over time from day 7 onward, amounting to 15% ± 3% (n = 42 in 17 active wells), 16% ± 2% (n = 115 in 46 active wells), and 13% ± 1% (n = 84 in 40 active wells) at 7, 14, and 21 days of differentiation, respectively (ANOVA p = 0.44; Figure 5B).

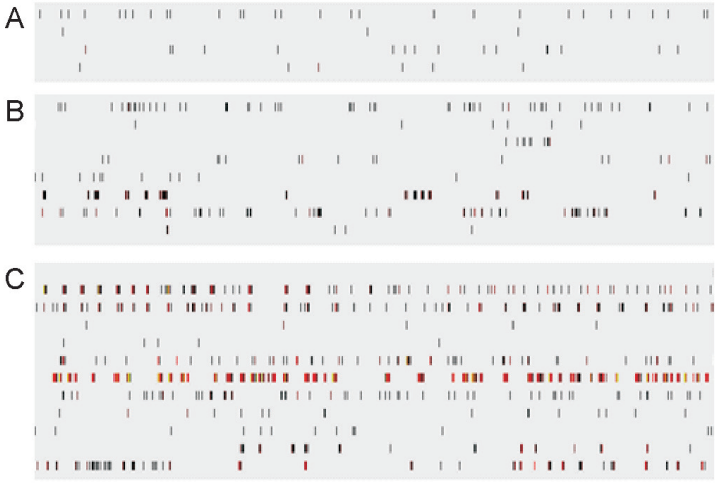

Figure 4. Representative spike raster plot illustrating the development of neuronal activity in a mNPC culture during 21 days of differentiation. Each panel contains spikes generated by a mNPC culture in a 100 s interval on different days during differentiation (**A–C**. depict day 7, 14, and 21, respectively). Each row represents one active electrode and every mark depicts one spike.

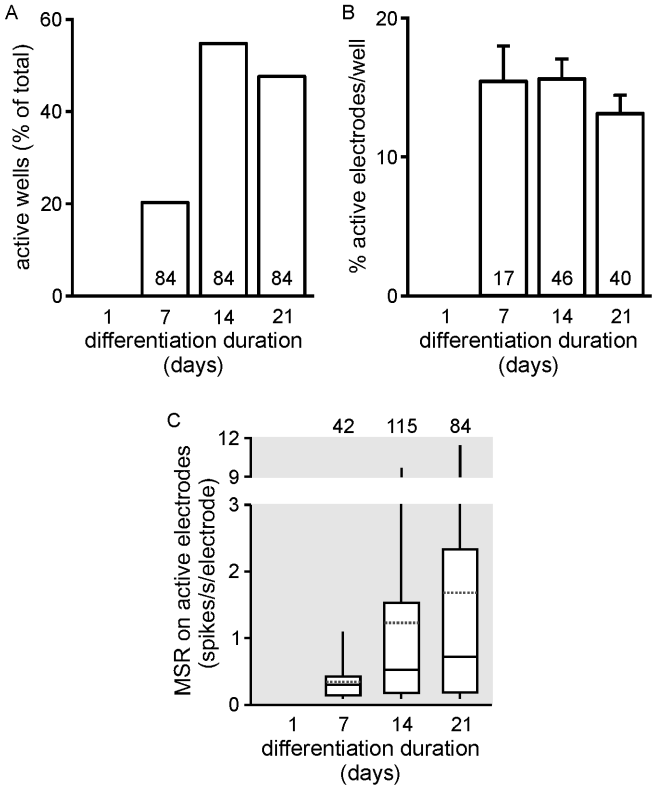

Figure 5. Changes in electrical activity with differentiation duration in mNPCs cultured on multiwell MEA plates. **A.** Percentage of active wells during differentiation (derived from a total of 84 wells). **B.** Average percentage of active electrodes per well at various differentiation durations (derived from active wells only, with a total of 16 electrodes/well). Data are presented as mean ± SEM of 17–46 active wells from 5 to 6 mNPC cultures. Total number of wells (A) and total number of active wells (B) are indicated in the bars. **C.** Average MSR at various differentiation durations. MSR (spikes/s) is averaged over all active electrodes (numbers indicated above the boxes) from active wells. Note the change in scale. Boxes represent the 25th–75th percentile range and whiskers indicate minimum and maximum values. Median and mean values are indicated with solid and grey dotted lines within the boxes, respectively.

To further assess electrical activity, the MSR was calculated for all the active electrodes in the cultures (Figure 5C). The MSR is low at 7 days of differentiation (0.27 ± 0.04 spikes/s; *n* = 42 active electrodes) but increases significantly with increasing differentiation duration. At 14 days of differentiation, MSR amounts to 1.16 ± 0.15 spikes/s (*n* = 115 active electrodes) and increases further to 1.60 ± 0.25 spikes/s (*n* = 84 active electrodes) at day 21 of differentiation (ANOVA $p = 0.001$).

4. Discussion

Many efforts are currently being undertaken to include *in vitro* models in (developmental) neurotoxicity testing. A recent interest lies with progenitor/stem cell models, as these cells have the potential to proliferate and differentiate *in vitro*. These properties can be used to model brain development in a heterogeneous model *in vitro*. The aim of the present characterization study was to explore the applicability of mNPCs for the future evaluation of chemical-induced alterations in (the development of) neuronal function.

mNPCs have stem-like properties and thus proliferate *in vitro* (a clear advantage over postmitotic primary neurons) and differentiate into neural cell types upon withdrawal of growth factors (Moors *et al.*, 2009, Breier *et al.*, 2010). Our light microscopical and immunocytochemical data confirm that primary mNPCs develop into a heterogeneous network of neuronal cells that becomes more complex over time (Figure 2). Neuronal, glial, and progenitor markers are present in this network as early as 1 day after differentiation and their expression patterns change during differentiation (Figure 2B and 2C). The increased expression of β(III)-tubulin and GFAP with differentiation duration indicates the *in vitro* development of a neuronal phenotype. These findings confirm the presence of multiple cells types and are comparable with previous findings with both rodent and human NPCs (Moors *et al.*, 2009, Breier *et al.*, 2010, Gassmann *et al.*, 2012).

Considering the critical role of calcium signaling in neuronal function (Neher and Sakaba, 2008), we investigated the change in basal and stimulation-evoked $[Ca^{2+}]_i$ in mNPCs at various differentiation durations. Basal $[Ca^{2+}]_i$ amounted to approximately 100 nM at 1 and 7 days of differentiation and was only mildly increased after 14 days of differentiation. This thus allows for the investigation of possible effects of acute or (sub)chronic chemical exposure on basal $[Ca^{2+}]_i$, which could result in alterations of Ca^{2+}-dependent developmental processes (Lohmann, 2009).

Calcium responses to depolarization, ATP, L-glutamic acid, ACh, dopamine, serotonin, and GABA are already present after 1 day of differentiation (Figure 3 and Figure S1). These calcium responses indicate the expression and functionality of voltage- and ligand-gated ion channels, although the identification of the specific neurotransmitter receptors involved would require additional studies. Moreover, the percentages of responding cells for the different stimuli indicate that each mNPC can express multiple receptor types. Changes in percentages of responsive cells and/or their response amplitudes are observed during differentiation, indicative of developmental changes in the expression and functionality of the related neurotransmitter receptors and calcium signaling pathways. As such, our $[Ca^{2+}]_i$ data indicate that (co)exposure studies with chemicals during *in vitro* development can be used to study chemical-induced alterations in expression and functionality of ion channels and allow a mechanistic basis for the interpretation of neurotoxic effects in mNPCs. Additionally, mNPCs can also be used for acute neurotoxicity studies with interest in targets related to in particular depolarization, ATP, glutamate, and ACh in a heterogeneous cell system. For specific research questions, other cellular models such as cell lines with increased ion channel expression levels and thus more robust evoked $[Ca^{2+}]_i$ responses may be more practical. Also, considering the small percentage of mNPCs responding to dopamine, serotonin, and GABA, other *in vitro* models may be more efficient to study these targets.

Neuronal activity requires the proper function of numerous receptors, ion channels, and signaling pathways. Within 1–2 weeks of differentiation, mNPCs cultured on MEAs develop spontaneous electrical activity *in vitro* (Figure 4 and 5). The spontaneous electrical activity increases with differentiation duration, demonstrating the development of functional intercellular signaling pathways that can all be a possible target for chemical-induced effects. As such, mNPCs can be used for the investigation of chemical-induced alterations in the development of neuronal functionality, though additional experiments may be required to establish the exact cellular or molecular target(s) of the chemical(s) of interest.

At present, rat neonatal cortical cultures are commonly used for neurotoxicity studies on (the development of) neuronal functionality (Hogberg *et al.*, 2011, Robinette *et al.*, 2011). A chemical training set study and an interlaboratory study have confirmed the potential of cortical cultures on MEAs to screen chemicals for neurotoxicity. In these studies, cortical cultures grown on MEAs were shown to be a sensitive (87% identification of 23 positive compounds with a variety of mechanisms of action) and specific (100% identification of 7 negative compounds) tool to screen compounds for potential neurotoxic effects (McConnell *et al.*, 2012). Moreover, six independent laboratories in Europe and the United States used primary cortical cultures grown on MEAs to evaluate the effects of fluoxetine, muscimol, and verapamil on MSR demonstrating good reproducibility, both intra- and interlaboratory, of the effects of these chemicals on neuronal activity (Novellino *et al.*, 2011). The predictivity of studies with neuronal functionality of mNPCs on MEAs for DNT in animals and humans remains to be determined. Of particular interest for the field of DNT testing would be to determine the value of mNPC neurophysiology as a complementary parameter to the established morphological and biochemical methods (reviewed in de Groot *et al.*, 2013).

Multiwell MEA systems allow for evaluation of (developmental or chemically-induced) changes in intercellular communication by simultaneous and noninvasive (thus allowing for repeated measurements at multiple

differentiation and exposure durations) extracellular recordings of electrical activity at different locations in an *in vitro* culture with improved throughput compared with classical electrophysiological approaches. This increased throughput appears critical for the use of mNPCs in DNT testing considering the variation within the data (as apparent from the large response range in Figure 3 and 5). Notwithstanding this variation, the average electrical activity (MSR) in mNPCs (~1.2 spikes/s/electrode at 14 days of differentiation) is comparable with previously reported activity in primary cortical cultures on MEAs (McConnell *et al.*, 2012). Moreover, the use of a heterogeneous cellular model on MEAs allows for the evaluation of external influences on intercellular communication in an integrated manner. This is of importance as a possible downstream effect on neurotransmission via chemical-induced effects on neurotransmitter receptors, ion channels, or signaling pathways can be detected in a screening approach (followed by targeted mechanistic studies), thus increasing throughput. In such a tiered approach, the toxic mechanism of a particular chemical that affects neuronal activity in mNPCs on MEAs can be further investigated using, eg, $[Ca^{2+}]_i$ imaging. Notably, this integrated system may also be useful for the toxicity screening of mixtures, as the prediction of downstream effects on cellular function is challenging in case of different and unknown targets of the individual chemicals.

In the present study, we used NPCs derived from embryonic mouse brains. Human NPCs are (commercially) available and are already being used as a model for *in vitro* neurodevelopment. Although the use of human cell models evades the need for interspecies translation, the use of animal-derived cells, including mNPCs, has advantages, such as the ease of deriving cells from different developmental stages or brain structures, lower costs, greater availability of fetal tissue, and more consistency between cells from different cultures, eg, because of genetic stability (Breier *et al.*, 2010). Moreover, a particular disadvantage of human NPCs could be the uncertainties in exposure history of the donor, which is of extra importance in a developmental context. To summarize, the data presented here demonstrate that mNPCs develop into a complex heterogeneous cellular network that displays increases in $[Ca^{2+}]_i$

responses to a variety of stimuli and develops spontaneous electrical activity within 1–2 weeks of differentiation. This indicates that mNPCs develop functional neuronal characteristics *in vitro*, making mNPCs a promising model for the investigation of possible effects of (suspected) developmental neurotoxicants on the development of functional neuronal characteristics, such as inter- and intracellular signaling in response to neurotransmitters or (spontaneous) neuronal activity. A possible approach for DNT testing could be a tiered approach, in which mNPCs on MEAs are used to detect chemical-induced effects on neuronal function, whereas (co)exposure studies on stimulation-evoked $[Ca^{2+}]_i$ responses are used to clarify the involved mechanisms.

Acknowledgments

The authors gratefully acknowledge Gina van Kleef and Rob Bleumink for their excellent technical assistance with cell culture and immunocytochemistry, respectively. Dr. Marianne Bol is gratefully acknowledged for helpful discussions. The authors declare they have no actual or potential competing financial or personal interests. This work was funded by the European Union (DENAMIC project: FP7-ENV-2011-282957), The Netherlands Organization for Health Research and Development (ZonMw: 85300003) and the Faculty of Veterinary Medicine of Utrecht University.

Supplemental material

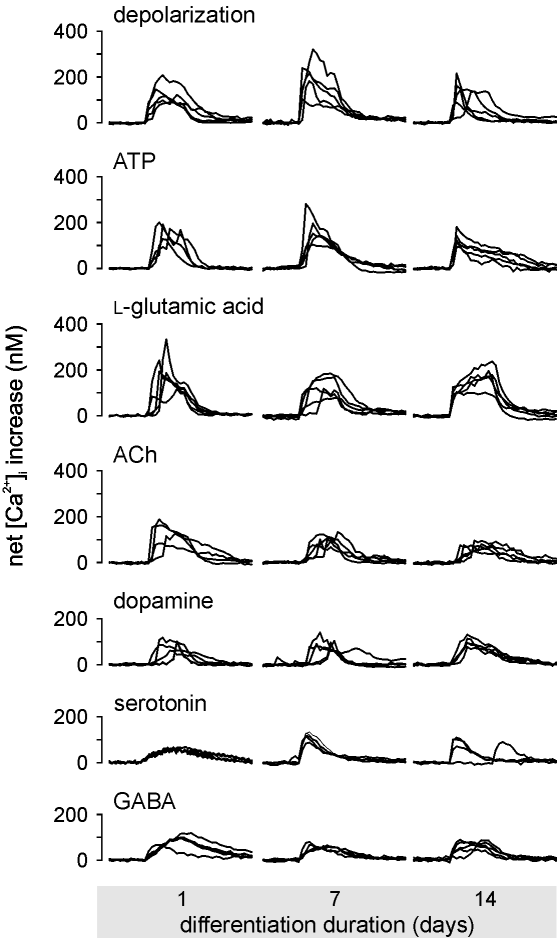

Figure S1. Representative $[Ca^{2+}]_i$ traces evoked by different stimuli. Duration of the traces is 2 min (except for serotonin at a differentiation duration of 1 day; 5 min), and illustrate the stimulation-evoked $[Ca^{2+}]_i$ responses at 1, 7 and 14 days of differentiation during 30 s superfusion with the different stimuli (as indicated above the traces) following a 30 s baseline recording.

PART II:
NEUROTOXIC EFFECTS OF ELF-EMF IN VITRO

CHAPTER 6

Assessment of the neurotoxic potential of exposure to 50 Hz extremely low frequency electromagnetic fields (ELF-EMF) in naïve and chemically stressed PC12 cells

Martje W.G.D.M. de Groot, Marjolijn D.M. Kock, and Remco H.S. Westerink.

Neurotoxicology Research Group, Toxicology Division, Institute for Risk Assessment Sciences (IRAS), Faculty of Veterinary Medicine, Utrecht University, P.O. Box 80.177, NL 3508 TD Utrecht, The Netherlands

Neurotoxicology (2014). **44**: 358–364
DOI:10.1016/j.neuro.2014.07.009

Abstract

Increasing exposure to extremely low frequency electromagnetic fields (ELF-EMF), generated by power lines and electric appliances, raises concern about potential adverse health effects of ELF-EMF. The central nervous system is expected to be particularly vulnerable to ELF-EMF as its function strongly depends on electrical excitability. We therefore investigated effects of acute (30 min) and sub-chronic (48 h) exposure to 50 Hz ELF-EMF on naïve and chemically stressed pheochromocytoma (PC12) cells. The latter have higher levels of iron and/or reactive oxygen species (ROS) and display increased vulnerability to environmental insults. Effects of ELF-EMF on Ca^{2+}-homeostasis, ROS production and membrane integrity were assessed using Fura-2 single-cell fluorescence microscopy, H_2-DCFDA and CFDA assays, respectively. Our data demonstrate that acute exposure of naïve PC12 cells to 50 Hz ELF-EMF up to 1000 μT fails to affect basal or depolarization-evoked $[Ca^{2+}]_i$. Moreover, sub-chronic ELF-EMF exposure up to 1000 μT has no consistent effects on Ca^{2+}-homeostasis in naïve PC12 cells and does not affect ROS production and membrane integrity. Notably, in chemically stressed PC12 cells both acute and sub-chronic ELF-EMF exposure also failed to exert consistent effects on Ca^{2+}-homeostasis, ROS production and membrane integrity. Our combined findings thus indicate that exposure to 50 Hz ELF-EMF up to 1000 μT, i.e. 10,000 times above background exposure, does not induce neurotoxic effects *in vitro*, neither in naïve nor in chemically stressed PC12 cells. Though our data require confirmation, e.g. in developing neuronal cells *in vitro* or (developing) animals, it appears that the neurotoxic risk of ELF-EMF exposure is limited.

Keywords: Extremely low frequency electromagnetic fields (ELF-EMF); Single-cell fluorescence calcium-imaging; Intracellular $[Ca^{2+}]_i$; *In vitro* neurotoxicity; Oxidative stress; Chemically stressed PC12 cells.

1. Introduction

Exposure to extremely low frequency electromagnetic fields (ELF-EMF) has dramatically increased during the last decennia. The growing electrical demand, advancing technologies and changes in lifestyle have created more and more artificial sources of ELF-EMF. Electric and magnetic fields in the ELF range (3–300 Hz) are mostly associated with manmade sources, including electric power systems and electronic appliances for consumer and industrial use that mostly operate at a frequency of 50–60 Hz (IARC Working Group, 2002, World Health Organization, 2007a). Great public and scientific concern was raised when early epidemiological studies indicated a correlation between ELF-EMF exposure and the development of childhood leukemia (Wertheimer and Leeper, 1979, Li *et al.*, 1998), which has been confirmed in several studies (Ahlbom *et al.*, 2000, Greenland *et al.*, 2000, Hardell and Sage, 2008, Kheifets *et al.*, 2010b, Li *et al.*, 2009, but also see Bunch *et al.*, 2014).

Unlike higher frequency EMF, ELF-EMF are non-ionizing with low-energy photons. Consequently, ELF-EMF are not likely to induce thermal effects in humans (Pall, 2013). However, their low frequency does enable them to penetrate deep into tissues. ELF-EMF reportedly have effects on a range of endpoints, including adverse effects on female breast cancer, fertility, and genotoxicity (Bernabo *et al.*, 2010, Chen *et al.*, 2013, Ivancsits *et al.*, 2005) as well as beneficial effects on wound and bone fracture repair (Costin *et al.*, 2012, Zhong *et al.*, 2012). Effects of ELF-EMF have been investigated in different research areas, including immunology, endocrinology, and neurology (World Health Organization, 2007a, Feychting *et al.*, 2005). However, there is little knowledge regarding the molecular and cellular mechanisms underlying the presumed effects of ELF-EMF.

Of the many suspected target organs of ELF-EMF, the central nervous system (CNS) could be particularly vulnerable since neuronal function and signaling is highly voltage-dependent. Recently, ELF-EMF was reported to affect synaptic plasticity in the hippocampus of adult rats after chronic exposure

(50 Hz, 100 µT, 2 h/day for 90 days; Komaki *et al.*, 2014) and in brain hippocampal slices from rats exposed during gestation or as newborns (50 Hz, 0.5 [fetal] or 3 [newborn] mT for 7 days; Balassa *et al.*, 2013), suggesting ELF-EMF effects on neuronal function. On the other hand, there are also studies showing "negative" results, i.e. no effects of ELF-EMF exposure, e.g. on the expression of neuronal nicotinic acetylcholine receptor (involved in e.g. neuronal signaling as well as learning and memory) in SH-SY5Y neuroblastoma cells after exposure to 50 Hz ELF-EMF with various field strength and exposure times (Antonini *et al.*, 2006).

Neuronal function and signaling critically depend on proper calcium homeostasis and it has been previously hypothesized that the common pathway in the different presumed biological effects of ELF-EMF involves alterations in intracellular calcium levels ($[Ca^{2+}]_i$; Kavet *et al.*, 2001, Saunders and Jefferys, 2007). Indeed, several *in vitro* studies have shown that ELF-EMF exposure can result in a rapid increase in basal $[Ca^{2+}]_i$ in different (neuronal) cell types (Barbier *et al.*, 1996, Hojevik *et al.*, 1995, Liburdy *et al.*, 1993, Lisi *et al.*, 2006), which may be due to direct stimulation of voltage-gated calcium channels (VGCCs) in the plasma membrane (Pall, 2013). In line with this notion, (selective) inhibition of different VGCC subtypes (L-, N-, P/Q, and T-type) has been shown to lower or block a diversity of responses to ELF-EMF (reviewed in Pall, 2013). Additionally, ELF-EMF exposure was reported to increase basal $[Ca^{2+}]_i$ and to increase expression of proteins involved in Ca^{2+}-regulation (e.g. ferritin and Peroxiredoxins 3) in bone marrow-derived mesenchymal stem cells differentiated into neurons following 12 days of ELF-EMF exposure (50 Hz, 1000 µT; Kim *et al.*, 2013). Increased basal $[Ca^{2+}]_i$ was also observed in nerve growth factor (NGF)-differentiated pheochromocytoma (PC12) cells following 7 days of ELF-EMF exposure (50 Hz, 1000 µT; Morabito *et al.*, 2010). On the other hand, data from bovine adrenal chromaffin cells indicate that basal $[Ca^{2+}]_i$ is unaltered by acute (10 min) ELF-EMF exposure (60 Hz, 0.1–2 mT; Craviso *et al.*, 2002).

Although many studies point toward effects of ELF-EMF on the CNS, findings are often inconsistent and hard to compare between studies due to the use of different cell types, exposure systems, exposure durations and/or field strengths. There is thus a clear need to further examine the potential effects of ELF-EMF exposure. This holds in particular for effects on Ca^{2+}-homeostasis in neuronal cells. $[Ca^{2+}]_i$ is carefully controlled by calcium efflux, buffering and intracellular storage and, in particular, influx through e.g. VGCCs (Westerink, 2006). We therefore investigated effects of ELF-EMF exposure on basal and depolarization-evoked increases in $[Ca^{2+}]_i$, ROS production and membrane integrity in pheochromocytoma (PC12) cells. ELF-EMF exposure has been reported to alter the cellular anti-oxidant capacity in several *in vitro* and *ex vivo* neuronal models (Ciejka *et al.*, 2011, Di Loreto *et al.*, 2009, Falone *et al.*, 2008, Falone *et al.*, 2007, Morabito *et al.*, 2010, Pall, 2013) and adverse effects are more likely to show up in stressed neuronal cells with higher levels of iron and reactive oxygen species (ROS; Lesuisse and Martin, 2002, Snyder and Connor, 2009, Yankner *et al.*, 2008). Therefore, we also investigated effects of ELF-EMF exposure in chemically stressed PC12 cells that differ from naïve PC12 cells in their VGCC density, dopamine levels, ROS production and expression of α-synuclein compared to naïve PC12 cells (as described previously; de Groot and Westerink, 2014).

Since ELF-EMF exposure in our daily life is extremely variable in intensity and duration, we investigated the effects of acute (30 min) and sub-chronic (48 h) exposure to ELF-EMF. The field intensities used in this study ranged from 1 to 1000 μT, i.e. up to two orders of magnitude below and one order of magnitude above the safe exposure levels for the general public currently recommended by the European Council and the International Commission on Non-Ionizing Radiation Protection (IARC; IARC Working Group, 2002, Council of the European Union, 1999).

2. Materials and methods

2.1 Chemicals

RPMI 1640, penicillin-streptomycin, PBS, Fura-2 AM and 2',7'-dichlorodihydrofluorescein diacetate (H_2-DCFDA), and 5,6-carboxyfluorescein diacetate succinimidyl ester (CFDA) were obtained from Life Technologies (Bleiswijk, The Netherlands); all other chemicals were obtained from Sigma-Aldrich (Zwijndrecht, the Netherlands), unless described otherwise. Saline solutions for Ca^{2+}-imaging experiments, containing (in mM) 125 NaCl, 5.5 KCl, 2 $CaCl_2$, 0.8 $MgCl_2$, 10 HEPES, 24 glucose, and 36.5 sucrose (pH set at 7.3), were prepared with deionized water (Milli-Q®; resistivity > 10 MΩ·cm). Stock solutions of 2 mM ionomycin were prepared in DMSO and kept at –20°C. $FeSO_4$ stock solution (10 mM) was prepared from $FeSO_4 \cdot 7\ H_2O$ in Milli-Q® containing 0.5% H_2SO_4 and kept at 4°C. Dexamethasone (DEX) stock solution (10 mM) was prepared in ethanol and stored at –20°C. L-DOPA stock solutions (10 mM) were freshly prepared prior to each experiment in cold colorless RPMI 1640 without supplementation. Stock solutions of all compounds were diluted in RPMI 1640 culture medium without supplementation to obtain the desired concentrations just prior to the experiments.

2.2 Cell culture

Naïve rat pheochromocytoma (PC12) cells (Greene and Tischler, 1976) clone CRL-1721 (passage 18) obtained from ATCC (American Type Culture Collection, Manassas, VA, USA), were grown for a maximum of 10 passages in RPMI 1640 containing L-glutamine supplemented with 5% fetal calf serum and 10% horse serum (ICN Biomedicals, Zoetermeer, the Netherlands), 100 IU/mL penicillin, and 100 mg/mL streptomycin at 37°C in a 5% CO_2 atmosphere as described previously (de Groot and Westerink, 2014). Culture medium was refreshed every 2–3 days. All cell culture flasks, plates, and dishes were coated with poly-L-lysine (50 µg/mL).

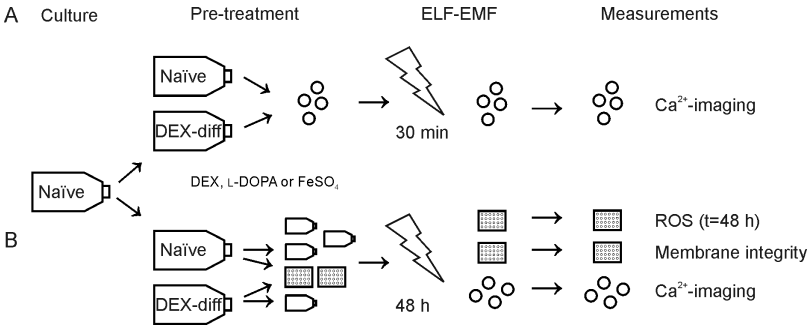

Figure 1. Schematic illustration of the culture and pre-treatment conditions of the different PC12 models during acute **A**. and sub-chronic **B**. ELF-EMF exposure experiments, including an overview of the investigated parameters.

2.3 Chemically stressed PC12 cells

Prior to ELF-EMF exposure experiments, naïve PC12 cells were pre-treated with 5 µM DEX for 3–5 days or with non-cytotoxic concentrations of L-DOPA (100 µM) or $FeSO_4$ (10 µM) for 24 h to obtain different chemically stressed PC12 phenotypes (Figure 1; de Groot and Westerink, 2014).

2.4 ELF-EMF exposure

Exposure devices: block-pulsed ELF-EMF with a main frequency of 50 Hz (<10% harmonics) and different magnetic field intensities (1–1000 µT rms) were generated using two custom-made devices (Immunent BV, Velthoven, The Netherlands, also see de Kleijn *et al.*, 2011, Bouwens *et al.*, 2012 and Figure S1): a copper coil fitted to the stage of the fluorescence microscope for acute exposure during Ca^{2+}-imaging (see section 2.5 Acute ELF-EMF exposure experiments) and a copper coil fitted into an incubator for sub-chronic exposure (see section 2.6 Chronic ELF-EMF exposure experiments). Both exposure devices consist of double copper wired solenoid coils connected to a signal generator with preprogrammed exposure protocols. The copper coils consist of one continuous copper conductor, ensuring equal current in

different coil components. Both systems generate both AC and DC vertical field components with field strengths (B_{AC} and B_{DC}) in the range from 1 to 1000 µT. Field strengths were calibrated and monitored by an EMDEX II Tesla meter (Enertech Consultants, Campbell, California, USA) and the coil current was regularly monitored by a Tenma 72–7226 clamp meter (Tenma Test Equipment, Springboro, OH, USA).

Sham-exposure: for acute (30 min) exposure experiments, a subset of cells was placed in the switched-off microscope-fitted coil for sham-exposure (approximately 0.2 µT, i.e. background ELF-EMF from the fluorescence microscope set-up). For sub-chronic (48 h) exposure experiments, a subset of cells was placed in a second incubator and received 48 h sham-exposure (approximately 0.4 µT, i.e. incubator-generated background ELF-EMF), while cells in the incubator-fitted coils in the exposure-incubator received sub-chronic (48 h) exposure to ELF-EMF.

2.5 Acute ELF-EMF exposure experiments

Naïve and DEX-differentiated PC12 cells were subcultured in 35 mm glass bottom dishes (MatTek, Ashland, MA, USA) at a density of 4.5×10^5 cells/dish and a subset of the naïve PC12 cells was chemically stressed with 100 µM L-DOPA or 10 mM $FeSO_4$ in the dishes for 24 h prior to the start of the imaging experiments (Figure 1A). For acute exposure experiments, the different PC12 phenotypes were (sham-) exposed to a block-pulsed ELF-EMF with different intensities (0–1000 µT) for 30 min during fluorescence $[Ca^{2+}]_i$ imaging experiments using the microscope-fitted coils.

Changes in $[Ca^{2+}]_i$ were measured using the Ca^{2+}-sensitive fluorescent ratio dye Fura-2 AM as described previously (de Groot and Westerink, 2014). In short, culture dishes containing the different PC12 phenotypes were placed into the microscope-fitted solenoid coil at room temperature under continues superfusion with saline. After a 5 min baseline recording, $[Ca^{2+}]_i$ was increased by depolarization of the cells by switching the superfusion solution to high K^+-containing saline (100 mM) for 18 s (K1). Next, cells were allowed to

recover for 10 min before the start of the (sham-) ELF-EMF exposure. At the end of the 30 min (sham-) ELF-EMF exposure, cells were again depolarized with high K^+-containing saline (K2) to obtain a treatment ratio (TR, see data-analysis) and to investigate possible effects of acute ELF-EMF exposure on the depolarization-evoked increase of $[Ca^{2+}]_i$ (Figure 2A for example recording).

Maximum and minimum ratios (R_{max} and R_{min}) were determined at the end of each recording by addition of ionomycin (final concentration 5 µM) and ethylenediamine tetraacetic acid (EDTA; final concentration 17 mM). Changes in F_{340}/F_{380} ratio, reflecting changes in $[Ca^{2+}]_i$, were further analyzed using custom-made MS-Excel macros. Free cytosolic $[Ca^{2+}]_i$ was calculated from the F_{340}/ F_{380} ratios using Grynkiewicz's equation (Grynkiewicz *et al.*, 1985): $[Ca^{2+}]_i = K_{d*} \times (R - R_{min})/(R_{max} - R)$, where K_{d*} is the dissociation constant of Fura-2 AM determined in the experimental set-up.

2.6 Chronic ELF-EMF exposure experiments

To assess whether sub-chronic (48 h) ELF-EMF exposure affects cell viability, we assessed membrane integrity and ROS production after sub-chronic ELF-EMF exposure. For both assays, naïve and DEX-differentiated PC12 cells were seeded in 75 cm^2 flasks at a density of 22.5×10^6 cells/flask and subcultured in transparent 24-well plates at a density of 6×10^5 cells/well in colorless RPMI 1640 medium without supplementation (Greiner Bio-one, Solingen, Germany). After a 2 h attachment period, a subset of naïve PC12 cells was pre-treated for 24 h with L-DOPA or $FeSO_4$ (de Groot and Westerink, 2014 and Figure 1B).

Membrane integrity was assessed using a CFDA-AM assay, which is based on nonspecific cytoplasmic-esterase activity (protocol adapted from Heusinkveld *et al.*, 2013). Briefly, the PC12 phenotypes were exposed to different intensities block-pulsed ELF-EMF using the incubator-fitted copper coils (see section 2.4 ELF-EMF exposure) or sham-exposed in an incubator without coils. After a 48 h exposure, cells were incubated with 4 µM CFDA-AM for 30 min at 37 °C and 5% CO_2, after which hydrolyzed CFDA was measured spectrophotometrically at

493/541 nm (excitation/emission, Infinite M200 microplate; Tecan Trading AG, Männedorf, Switzerland) as a measure of cell viability.

Cumulative ROS production was assessed using the fluorescent dye H_2-DCFDA (protocol adapted from Heusinkveld *et al.*, 2010). Briefly, the different PC12 phenotypes were incubated with 1.5 µM H_2-DCFDA for 30 min at 37°C and 5% CO_2. After measurement of basal ROS production (t = 0 h), cells were exposed to ELF-EMF for 48 h using the incubator-fitted coils (see section 2.4 ELF-EMF exposure) or sham-exposed in an incubator without coils, after which cumulative ROS production was measured (t = 48 h). At both time points, fluorescence was determined spectrophotometrically at 480/ 530 nm (excitation/emission) on an Infinite M200 microplate reader equipped with a Xenon Flash light source (10 W; Tecan Trading AG, Männedorf, Switzerland) controlled by iControl software (version 7.1) as a measure of ROS production.

To measure effects of sub-chronic (48 h) ELF-EMF exposure on calcium homeostasis, DEX-differentiated and naïve PC12 cells were seeded in 25 cm^2 flasks at a density of 7.5 × 10^6 cells/flask, after which a subset of naïve cells were pre-treated with 100 µM L-DOPA or 10 µM $FeSO_4$ for 24 h. After pre-treatment, naïve, L-DOPA and $FeSO_4$ pre-treated PC12 cells were subcultured in 35 mm glass bottom dishes (MatTek, Ashland, MA, USA) at a density of 6 × 10^5 cells/dish in fresh RPMI 1640 (Figure 1B). To compensate for the slower cell division and to prevent de-differentiation over 48 h, DEX-differentiated PC12 cells were subcultured at a density of 9 × 10^5 cells/dish in DEX-containing RPMI 1640. Culture dishes were then exposed to block-pulsed ELF-EMF with different intensities (0–1000 µT) for 48 h in the incubator-fitted copper coils (see section 2.4 ELF-EMF exposure). After 48 h, changes in $[Ca^{2+}]_i$ were measured in the ELF-EMF (sham-) exposed PC12 phenotypes using the Ca^{2+}-sensitive fluorescent ratio dye Fura-2 AM as described in Section 2.5 (Figure 3A for example recording).

2.7 Data analysis and statistics

All data are presented as mean ± SEM from the number of wells or cells (*n*) indicated, derived from *N* independent experiments. For acute ELF-EMF experiments, basal $[Ca^{2+}]_i$ is expressed as a basal ratio: $[Ca^{2+}]_i$ during ELF-EMF exposure (min 15–38; Figure 2A) compared to $[Ca^{2+}]_i$ during baseline (Figure 2A). Additionally, depolarization-evoked $[Ca^{2+}]_i$ is expressed as a treatment ratio (TR; K2/K1): the amplitude of the second K^+-evoked increase in $[Ca^{2+}]_i$ in the presence of ELF-EMF (K2, in µM) expressed as a percentage of the first depolarization- evoked increase in $[Ca^{2+}]_i$ (K1, in µM) in the absence of ELF-EMF.

For sub-chronic (48 h) ELF-EMF experiments, basal $[Ca^{2+}]_i$ (a 2.5 min interval prior to K1) is expressed as a percentage of basal $[Ca^{2+}]_i$ in sham-exposed controls. Depolarization-evoked changes in $[Ca^{2+}]_i$ are expressed as changes in K1 as a percentage of K1 in sham-exposed controls, and as a depolarization ratio (DR; K2/K1), comparable to the TR for acute experiments (Figure 3A).

Background-corrected data from cell viability assays are expressed as percentage of sham-exposed controls within each different PC12 cell model. ROS data are expressed as a percentage compared to the basal ROS production (t = 0 h) and compared to time-matched sham-exposed controls within each different PC12 cell model.

Cells or wells that showed effects two times SD above or below average are considered outliers (<5% for cell viability assays and <10% for Ca^{2+}-experiments) and were excluded from further analysis. All statistical analyses were performed using SPSS 20 (SPSS, Chicago, IL, USA). One-way analyses of variance (ANOVA) for field strength, followed by Bonferroni post hoc analyses (for data with equal variances) or Games Howell post hoc analyses (for data with unequal variances) were performed to investigate changes in cell viability and calcium homeostasis (basal [ratio], TR and DR) in the different cell models after sub-chronic (48 h) or acute (30 min) ELF-EMF exposure. p-values < 0.05 were considered statistically significant. To estimate biological relevance, a minimal effect size was calculated for the

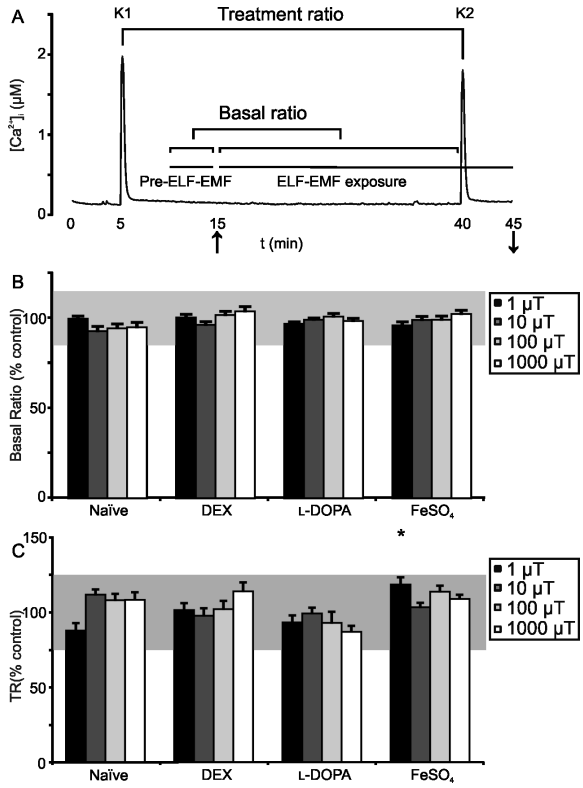

Figure 2. Effects of acute ELF-EMF exposure on Ca^{2+}-homeostasis in naïve and chemically stressed PC12 cells. **A.** Representative example trace of intracellular $[Ca^{2+}]_i$ in naïve sham-exposed PC12 cells showing the treatment (TR; K2/K1) and basal ratio (exposure/pre-ELF-EMF). Arrows indicate the start and end of the 30 min ELF-EMF exposure. **B.** Basal ratio (normalized to sham-exposed cells) during acute ELF-EMF exposure in the different PC12 models. **C.** TR (normalized to sham-exposed cells) during acute ELF-EMF exposure in the different PC12 models. For each model, data represent mean ± SEM compared to sham-exposed controls from 29–93 cells from 3–8 separate experiments. Gray-shaded areas (in B and C) indicate minimal relevant effect size derived from the average standard deviation from sham-exposed cells. *$p < 0.05$ compared to sham-exposed controls. Effects have to be larger than the minimal effect size (gray-shaded area, derived from the average standard deviation from sham-exposed cells) and statistically significant to be considered biologically relevant.

different parameters in each assay. This minimal effect size is an average of the standard deviations of the sham-exposed data in each chemically stressed PC12 model and is indicated in the bar graphs as a gray-shaded area. Data are considered biologically relevant if the effect > minimal effect size and $p < 0.05$.

3. Results

3.1. Acute ELF-EMF exposure does not affect basal or depolarization-evoked $[Ca^{2+}]_i$ in naïve and chemically stressed PC12 cells

In naïve, sham-exposed PC12 cells basal $[Ca^{2+}]_i$ (Figure 2A, 0–5 min) is stable and low (99 ± 2 nM, $n = 85$). Upon depolarization with high potassium-containing saline (Figure 2A, K1), $[Ca^{2+}]_i$ increases up to 2.0 ± 0.1 μM, after which $[Ca^{2+}]_i$ returns to basal levels (Figure 2A, 5–15 min). The ratio between $[Ca^{2+}]_i$ during sham-ELF-EMF exposure and $[Ca^{2+}]_i$ in the pre-ELF-EMF interval (basal ratio; Figure 2A) amounts to 92 ± 1% in sham-exposed, naïve PC12 cells (data not shown). Cells are depolarized with high-K^+ saline (Figure 2A, K2) for a second time at the end of the 30 min ELF-EMF (sham) exposure, and $[Ca^{2+}]_i$ increases up to 1.6 ± 0.1 μM (data not shown). The TR (Figure 2A) in naïve, sham-exposed PC12 cells amounts to 74 ± 2% (data not shown).

Following normalization of the basal and treatment ratio of naïve, sham-exposed PC12 cells, effects of acute (30 min) ELF-EMF exposure were investigated. As apparent from Figure 2B, acute exposure to block-pulsed ELF-EMF up to 1000 μT does not affect the basal ratio in naïve PC12 cells. Moreover, the TR is not affected by ELF-EMF up to 1000 μT in naïve PC12 (Figure 2C).

As described previously, the different chemically stressed PC12 phenotypes have functional, but distinct Ca^{2+}-characteristics (de Groot and Westerink, 2014). We also calculated normalized basal ratios and TRs for the sham-exposed, chemically stressed PC12 phenotypes so these could be used

as controls for the specific phenotypes (summarized in Figure 2B and 2C). From these sham-ELF-EMF exposed controls, the minimal effect size (see section 2.7 Data analysis and statistics) was calculated from the average standard deviations of sham-exposed cells and amounts to 15% for basal ratio and 25% for TR (gray-shaded area in Figure 2B and 2C). As illustrated in Figure 2B, acute exposure to block-pulsed ELF-EMF up to 1000 µT does not affect the basal ratio in any of the chemically stressed PC12 models. Similarly, acute exposure to block-pulsed ELF-EMF up to 1000 µT has no major effects on TR in any of the chemically stressed PC12 models (Figure 2C). In $FeSO_4$ pre-treated cells, the TR is slightly increased at 1 µT (119 ± 5%; $p < 0.05$), but remains below the minimal effect size.

3.2. Sub-chronic ELF-EMF exposure has no consistent effects on Ca^{2+}-homeostasis in naïve or chemically stressed PC12 cells

To further investigate possible effects of ELF-EMF exposure, we assessed effects of sub-chronic (48 h) ELF-EMF exposure on Ca^{2+}-homeostasis in naïve and chemically stressed PC12 cells. First, we investigated membrane integrity and ROS production after chronic ELF-EMF exposure to exclude possible effects on cell viability. In naïve and chemically stressed PC12 cells, membrane integrity was not affected by a 48 h ELF-EMF exposure up to 1000 µT (Figure S2A). As ROS production is a more subtle measure of cellular stress and a precursor for cellular dysfunction, cumulative ROS production was measured after a 48 h ELF-EMF exposure. ROS production was not increased by ELF-EMF exposure up to 1000 µT in any of the PC12 models compared to their respective sham-exposed controls (Figure S2B).

After a 48 h sham-exposure, basal $[Ca^{2+}]_i$ prior to K1 (Figure 3A) is ~100 nM (107 ± 3 nM; 98 ± 3 nM; 94 ± 3 nM; 107 ± 3 nM in respectively naïve, DEX-differentiated, L-DOPA and $FeSO_4$ pre-treated PC12 cells (see Figure S3 for average Ca^{2+}-traces). The minimal effect size calculated on basal $[Ca^{2+}]_i$ in the sub-chronic $[Ca^{2+}]_i$ experiments is 30% (gray-shaded area in Figure 3B). Basal $[Ca^{2+}]_i$ was not affected to a relevant degree in naïve and DEX-differentiated

PC12 cells after sub-chronic ELF-EMF exposure up to 1000 µT (Figure 3B). Basal $[Ca^{2+}]_i$ was slightly increased in L-DOPA pre-treated PC12 cells after sub-chronic ELF-EMF exposure to 10 µT (125 ± 5%; $p < 0.05$) and slightly decreased in $FeSO_4$ pre-treated PC12 cells after sub-chronic ELF-EMF exposure to 1 and 10 µT (83 ± 4% and 83 ± 4%, respectively, $p < 0.05$).

Effects of ELF-EMF exposure on depolarization-evoked increases in $[Ca^{2+}]_i$ are summarized in Figure 3C and D. As the PC12 models are exposed to ELF-EMF prior to the start of the measurements in the sub-chronic experiments, K1 is analyzed to investigate if exposure resulted in altered depolarization-evoked $[Ca^{2+}]_i$. The minimal effect size calculated on K1 in sub-chronic experiments is 35% (gray-shaded area in Figure 3C). $[Ca^{2+}]_i$ increases up to 1.9 ± 0.1 µM in naïve sham-exposed PC12 cells upon depolarization, which is not affected by ELF-EMF exposure up to 1000 µT (Figure 3C). In DEX-differentiated PC12 cells, K1 is 2.0 ± 0.1 µM in sham-exposed cells and is significantly increased after exposure to 10, 100 and 1000 µT ELF-EMF (to 123 ± 7%; 124 ± 4%; and 128 ± 8%, respectively, $p < 0.05$). In sham-exposed L-DOPA pre-treated PC12 cells, K1 is 1.9 ± 0.1 µM, which increases up to 134 ± 8% after exposure to 100 µT ELF-EMF ($p < 0.05$). In sham-exposed $FeSO_4$ pre-treated PC12 cells, K1 is 2.3 ± 0.1 µM and is significantly decreased at 1 and 100 µT (82 ± 4%; and 81 ± 4%, respectively, $p < 0.05$). Although some changes are statistically significant, none of the changes in K1 exceed the minimal effect size and these changes are therefore not considered to be biologically relevant.

Next, we calculated the DR for all PC12 models to investigate whether there are any consistent effects on depolarization-evoked $[Ca^{2+}]_i$ (Figure 3D). The minimal effect size calculated on DR is 25% (gray-shaded area in Figure 3D). In naïve PC12 cells, the DR is not affected by ELF-EMF exposure up to 1000 µT (Figure 3D). In DEX-differentiated PC12 cells, the DR is increased at 1 µT compared to sham-exposed controls (112 ± 2%; $p < 0.05$), but not at higher intensities. In L-DOPA pre-treated PC12 cells, the DR is increased to 119 ± 5% and 116 ± 5% at 100 and 1000 µT, respectively ($p < 0.05$). Similarly, in $FeSO_4$ pre-treated PC12 cells, the DR is increased at 1, 100 and 1000 µT

(111 ± 2%, 114 ± 3% and 128 ± 5%, respectively; $p < 0.05$). However, of these changes in DR, only the increase at 1000 µT in $FeSO_4$ pre-treated PC12 cells exceeds the minimal effect size.

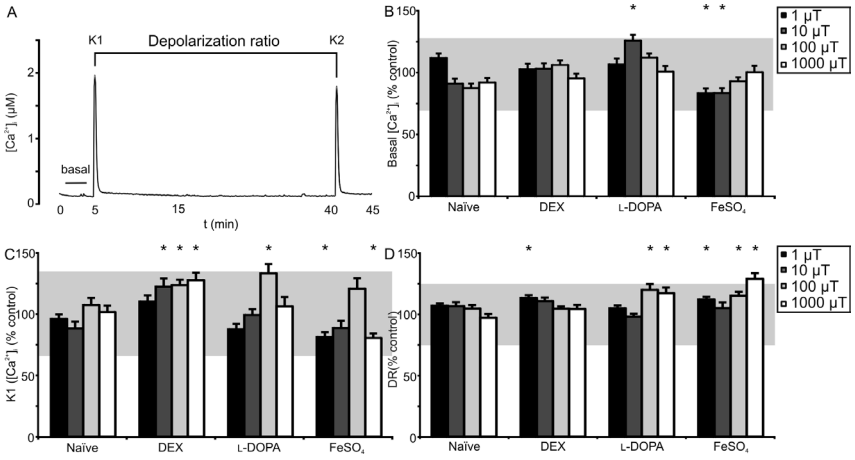

Figure 3. Effects of sub-chronic (48 h) ELF-EMF exposure on Ca^{2+}-homeostasis in the different PC12 models. **A.** Representative example trace of intracellular $[Ca^{2+}]_i$ in naïve sham-exposed PC12 cells illustrating basal $[Ca^{2+}]_i$ (1.5–4 min), depolarization-evoked $[Ca^{2+}]_i$ (K1 and K2) and the depolarization ratio (DR; K2/K1). **B.** Basal $[Ca^{2+}]_i$ (normalized to sham-exposed cells) after a 48 h ELF-EMF exposure in the different PC12 models. **C.** K1 (normalized to sham-exposed cells) after 48 h ELF-EMF exposure in the different PC12 models. **D.** DR (normalized to sham-exposed cells) after a 48 h ELF-EMF exposure in the different PC12 models. Data represent mean ± SEM compared to sham-exposed controls from 32–132 cells from 3–9 separate experiments. *$p < 0.05$ compared to sham-exposed controls. Note that effects have to be larger than the minimal effect size (gray-shaded area, derived from the average standard deviation from sham-exposed cells) and statistically significant to be considered biologically relevant.

4. Discussion

Proper calcium homeostasis is essential for the regulation of a variety of cellular responses, including neuronal communication (Neher and Sakaba, 2008, Westerink, 2006) and neurodevelopment (Pravettoni *et al.*, 2000). Our data clearly demonstrate that acute (30 min) exposure to 50 Hz ELF-EMF does not affect calcium homeostasis in naïve or chemically stressed PC12 cells (Figure 2). In an earlier study, acute ELF-EMF exposure (50 Hz; 50 μT; 30 min) was found to increase basal $[Ca^{2+}]_i$ in primary rat pituitary cells (Barbier *et al.*, 1996). However, in line with our findings, Morabito *et al.* also found no effects on basal or depolarization-evoked $[Ca^{2+}]_i$ in naïve PC12 cells following acute ELF-EMF exposure (50 Hz; 0.1 and 1000 μT; 30 min), although they reported a decrease in the number of spontaneously active cells (Morabito *et al.*, 2010). Similarly, in primary bovine chromaffin cells, both basal and depolarization-evoked $[Ca^{2+}]_i$ were unaffected by acute ELF-EMF exposure (60 Hz; 0.01–2 μT; 10 min; Craviso *et al.*, 2002).

Although acute peak exposures occur, especially in occupational settings, most of the real life exposure to ELF-EMF is chronic and low-level. We therefore also investigated effects of sub-chronic (48 h) ELF-EMF exposure on Ca^{2+}-homeostasis. In the present study, both basal and depolarization-evoked $[Ca^{2+}]_i$ were not consistently or dose-dependently affected by a 48 h ELF-EMF exposure up to 1000 μT (Figure 3). Sub-chronic ELF-EMF exposure up to 1000 μT also did not affect membrane integrity (Figure S2A), in line with previous studies on cell viability in naïve PC12 cells (50 Hz; 100 and 1000 μT; 7 days; Morabito *et al.*, 2010). Finally, our results indicate that sub-chronic ELF-EMF exposure up to 1000 μT does not increase ROS production (Figure S2B), as also shown in e.g. human SH-SY5Y neuroblastoma cells after sub-chronic ELF-EMF exposure (50 Hz; 1000 μT up to 48 h; Falone *et al.*, 2007).

It was recently suggested that it is essential to investigate multiple but related endpoints in a single study, study effects in multiple well-characterized model systems, and/or use multiple techniques to assess common endpoints

to increase reproducibility in (neuro-) toxicology (Westerink, 2013, Miller, 2014). In the present study, we therefore investigated effects of both acute (30 min) and sub-chronic (48 h) ELF-EMF exposure for a range of field strengths on three different, though related endpoints. Moreover, we not only used well-characterized naïve PC12 cells, but also used chemically stressed PC12 models that have previously been shown to have a more stressed phenotype compared to naïve PC12 cells. These models were hypothesized to be more sensitive to EMF due to their altered phenotypes; DEX-differentiated PC12 cells have increased VGCC density and elevated intracellular dopamine levels (Elhamdani *et al.*, 2000, Westerink and Ewing, 2008), L-DOPA pre-treated PC12 cells have strongly elevated intracellular dopamine levels (Hondebrink *et al.*, 2009, Westerink *et al.*, 2000) and $FeSO_4$ pre-treated PC12 cells have increased α-synuclein expression and increased intracellular ROS levels (de Groot and Westerink, 2014). These chemically stressed cells show increased basal ROS production while maintaining functional but distinct calcium homeostasis. Additionally, the vulnerability to the environmental pollutant rotenone is increased in both ROS and viability assays in $FeSO_4$ and L-DOPA pre-treated PC12 cells, confirming their increased sensitivity compared to naïve PC12 cells (de Groot and Westerink, 2014).

In the chemically stressed PC12 cells there are some small, but statistically significant changes in depolarization-evoked $[Ca^{2+}]_i$ after sub-chronic ELF-EMF exposure to various field strengths (Figure 3C and D). However, these changes appear to be independent of field strength and even the direction of the changes (increase or decrease) is inconsistent between and within the different PC12 models. When taking into consideration the biological variation on the different Ca^{2+}-parameters (± 25–30%) to derive minimal effect sizes, most of the observed changes do not exceed the minimal effect size. It can therefore be debated whether these changes have biological relevance. So, since none of the investigated models or endpoints showed consistent effects of acute or sub-chronic exposure to ELF-EMF up to 1000 μT, the neurotoxic effects associated with these exposures may be limited. Since PC12 cells express L-, N-, and P/ Q-type VGCCs (Heusinkveld *et al.*, 2010),

EMF-ELF exposure may also be without effect in other excitable cell types that express these VGCCs.

Humans are exposed to EMF from different sources, both daily and incidental. For ELF-EMF, these include household appliances and power lines. Environmental background levels of ELF fields are very low. Typical exposure levels for the general population are around 0.01–0.2 μT for magnetic fields (IARC Working Group, 2002). For people living in close proximity to power lines, long-term exposure to ELF magnetic field can exceed several tenths of μT. However, considerably higher exposures may occur (often for shorter durations), especially in occupational settings. Current exposure limits are set at 1000 μT for occupational exposure and 200 μT for residential exposure (International Commission on Non-Ionizing Radiation Protection, 2010). It should be emphasized that these guidelines are based on evidence regarding acute effects, as the International Commission on Non-Ionizing Radiation Protection (ICNIRP) concluded that there is no evidence to support chronic conditions related to ELF-EMF exposure (International Commission on Non-Ionizing Radiation Protection, 2010). It is apparent that the currently assessed field strengths up to 1000 μT are well above normal everyday exposure levels (International Commission on Non-Ionizing Radiation Protection, 2010) and the current residential and occupational reference levels lie well within the exposure range used in these studies. We therefore conclude from our combined data, derived from different cell models, that exposure to 50 Hz ELF-EMF up to 1000 μT does not induce neurotoxic effects *in vitro*. Consequently, the neurotoxic risk of ELF-EMF exposure appears to be limited, though this notion requires confirmation *in vitro* (e.g. in developing neuronal cells) and *in vivo*.

Acknowledgements

We gratefully acknowledge Aart de Groot, Gina van Kleef and Jan Cuppen, for technical assistance. This work was funded by the Netherlands Organization for Health Research and Development [ZonMw grant number 85300003] and the Faculty of Veterinary Medicine of Utrecht University.

Supplemental material

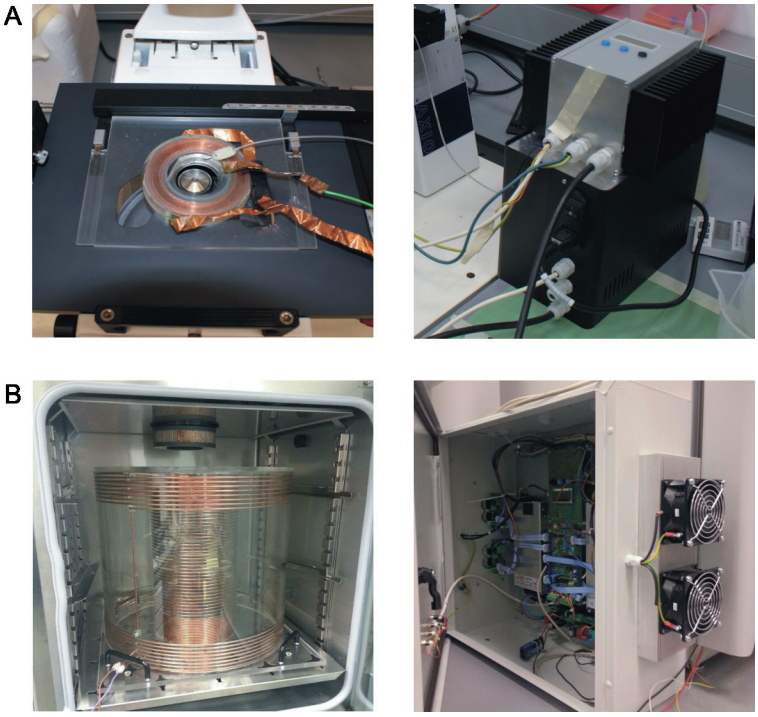

Figure S1. ELF-EMF exposure devices. **A.** Microscope-fitted copper coils (left) for ELF-EMF exposure during acute (30 min) experiments and connected signal generator (right) with preprogrammed 30 min signals. **B.** Incubator-fitted copper coils for sub-chronic (48 h) exposure experiments and connected signal generator (right) with preprogrammed 48 h signals.

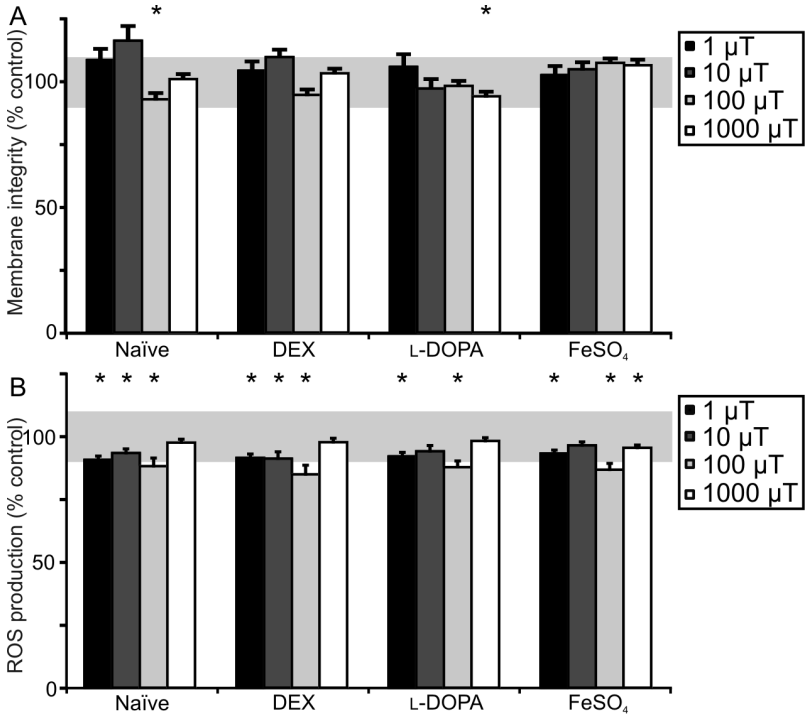

Figure S2. Effects of sub-chronic block-pulsed ELF-EMF exposure on viability markers in the different PC12 models. **A.** Bar graph illustrating effects of an 48 h block-pulsed ELF-EMF exposure (1–1000 µT) on membrane integrity (normalized to sham-exposed cells) in naïve (black bars), DEX-differentiated (dark grey bars), L-DOPA (light grey bars), and $FeSO_4$ pre-treated (white bars) PC12 cells in the CFDA assay. **B.** Bar graph illustrating effects of an 48 h block-pulsed ELF-EMF (1–1000 µT) exposure on cumulative ROS production (normalized to sham-exposed cells) in naïve (black bars), DEX-differentiated (dark grey bars), L-DOPA (light grey bars), and $FeSO_4$ pre-treated (white bars) PC12 cells in the H_2DCFDA assay. Data represent mean ± SEM (*n* at least 22, *N* at least 6 per condition). * $p < 0.05$ as compared to sham-exposed controls. Grey-shaded areas indicate minimal relevant effect size derived from the average standard deviation from sham-exposed cells.

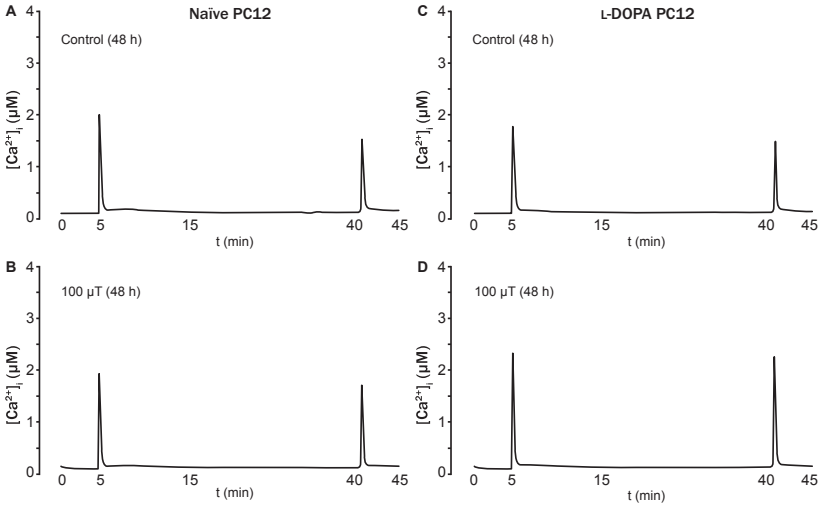

Figure S3. Example traces illustrating the effects of (sub-) chronic block-pulsed ELF-EMF exposure on Ca^{2+}-homeostasis in naïve and L-DOPA pre-treated PC12 cells. **A.** Average Ca^{2+}-trace of naïve PC12 cells after an 48 h chronic sham-exposure. **B.** Average Ca^{2+}-trace of naïve PC12 cells after an 48 h chronic exposure to 100 µT 50 Hz ELF-EMF. **C.** Average Ca^{2+}-trace of L-DOPA pre-treated PC12 cells after an 48 h chronic sham-exposure. **D.** Average Ca^{2+}-trace of of L-DOPA pre-treated PC12 cells after an 48 h chronic exposure to 100 µT 50Hz ELF-EMF.

CHAPTER 7

In vitro developmental neurotoxicity following chronic exposure to 50 Hz extremely low frequency electromagnetic fields (ELF-EMF) in primary rat cortical cultures

Martje W.G.D.M. de Groot, Regina G.D.M. van Kleef, Aart de Groot and Remco H.S. Westerink

Neurotoxicology Research Group, Toxicology Division, Institute for Risk Assessment Sciences (IRAS), Faculty of Veterinary Medicine, Utrecht University, P.O. Box 80.177, NL 3508 TD Utrecht, The Netherlands.

Toxicological Sciences (2015). **Advance online access**
DOI: 10.1093/toxsci/kfv242

Abstract

Exposure to 50–60 Hz extremely low frequency electromagnetic fields (ELF-EMF) has increased considerably over the last decades. Several epidemiological studies suggested that ELF-EMF exposure is associated with adverse health effects, including neurotoxicity. However, these studies are debated as results are often contradictory and the possible underlying mechanisms are unknown. Since the developing nervous system is particularly vulnerable to insults, we investigate effects of chronic, developmental ELF-EMF exposure *in vitro*. Primary rat cortical neurons received 7 days developmental exposure to 50 Hz block-pulsed ELF-EMF (0–1000 μT) to assess effects on cell viability (Alamar Blue/CFDA assay), calcium homeostasis (single-cell fluorescence microscopy), neurite outgrowth (β(III)-tubulin immunofluorescent staining) and spontaneous neuronal activity (multielectrode arrays [MEAs]). Our data demonstrate that cell viability is not affected by developmental ELF-EMF (0–1000 μT) exposure. Depolarization- and glutamate-evoked increases in intracellular calcium concentration ($[Ca^{2+}]_i$) are slightly increased at 1 μT, whereas both basal and stimulation-evoked $[Ca^{2+}]_i$ show a modest inhibition at 1000 μT. Subsequent morphological analysis indicated that neurite length is unaffected up to 100 μT, but increased at 1000 μT. However, neuronal activity appeared largely unaltered following chronic ELF-EMF exposure up to 1000 μT. The effects of ELF-EMF exposure were small and largely restricted to the highest field strength (1000 μT), i.e. 10,000 times above background exposure and well above current residential exposure limits. Our combined data therefore indicate that chronic ELF-EMF exposure has only limited (developmental) neurotoxic potential *in vitro*.

Keywords: Primary rat cortical cultures; *In vitro* developmental neurotoxicity (DNT); Extremely low frequency electromagnetic fields (ELF-EMF); Single-cell fluorescent microscopy; Neurite outgrowth; Multielectrode arrays (MEA).

1. Introduction

Electromagnetic fields (EMF) are an integral part of everyday life. They exist both naturally (e.g. the earths geometric field) and from man-made sources, both in home and in the work environment. Extremely low frequency (ELF)-EMF are defined as EMF with frequencies between 3 and 300 Hz (IARC Working Group, 2002, World Health Organization, 2007a). As most electrical appliances operate at a frequency of 50 or 60 Hz (Europe and US, respectively), we are exposed to ELF-EMF on a daily basis. Man-made sources of ELF-EMF include high-tension power lines, electric power systems and electronic appliances for consumer and industrial use (IARC Working Group, 2002, World Health Organization, 2007a). Average daily exposure intensities in the ELF range are typically very low (<0.1 μT), but can reach up to tenths of μT's in close proximity to power lines (IARC Working Group, 2002, World Health Organization, 2007a). Exposure resulting from these man-made ELF-EMF is several orders of magnitude larger than those from natural sources. Because of their low frequency, 50 Hz EMF are non-ionizing and unable to break bonds between molecules (Otto and von Muhlendahl, 2007). Moreover, they are not likely to induce thermal effects in humans (Pall, 2013, World Health Organization, 2007a), although their low frequency does enable the magnetic field to penetrate deep into tissues (e.g. muscle, heart or brain).

Since the late 1970s, researchers have investigated the possible effects of ELF-EMF on the risk of (chronic) disease, such as multiple types of cancer, cardiovascular- and neurodegenerative diseases (reviewed in Ahlbom *et al.*, 2001, Feychting *et al.*, 2005, World Health Organization, 2007a). Of the many endpoints investigated in epidemiological studies of EMF, childhood leukemia is the endpoint for which there is most evidence of an association (Ahlbom *et al.*, 2001, Greenland *et al.*, 2000, Kheifets *et al.*, 2010, but also see Bunch *et al.*, 2014). These epidemiological findings suggest that children may be more vulnerable to ELF-EMF exposure. Moreover, children could be particular prone to effects of ELF-EMF as the developing central nervous system (CNS) is very sensitive to external influences, e.g. exposure to chemicals (Rice and

Barone, 2000). Also, CNS function and development critically depend on many voltage-dependent processes (Butz *et al.*, 2009, van Ooyen, 1994), e.g. opening of ion-channels and generation of action potentials, that may be influenced by EMF exposure.

There is some evidence supporting potential ELF-EMF effects on neuronal cells, although studies often differ in their experimental setup (e.g. the cell type used or the frequency, intensity and duration of the exposure) and outcomes are therefore often inconsistent, hard to interpret, or even difficult to reproduce. Acute (30 min) and chronic (7 day) exposure to 50 Hz ELF-EMF (100–1000 μT) has previously been shown to increase the production of reactive oxygen species (ROS) and affect calcium homeostasis in undifferentiated pheochromocytoma (PC12) cells (Morabito *et al.*, 2010). However, our more recent *in vitro* study demonstrated that acute and sub-chronic (48 h) exposure to 50 Hz ELF-EMF did not evoke consistent effects on ROS production and intracellular Ca^{2+}-concentrations ($[Ca^{2+}]_i$) in naïve or in chemically stressed PC12 cells (de Groot *et al.*, 2014b).

Considering such inconsistencies and the lack of scientific data on possible long-term effects of developmental exposure to ELF, we investigated the effects of chronic ELF-EMF exposure during neuronal development using primary rat cortical neurons. Primary cortical cultures have been investigated for several decades and are widely used in the field of (developmental) neurotoxicology (e.g. Briz *et al.*, 2010, Robinette *et al.*, 2011, Hogberg *et al.*, 2011, McConnell *et al.*, 2012, Valdivia *et al.*, 2014, Wallace *et al.*, 2015). As such, cortical cultures have proven to be a valuable tool to study neuronal function and developmental neurotoxicity, especially when investigating functional endpoints. Moreover, they are the current standard for studying neuronal signaling using the multielectrode array (MEA; Hogberg *et al.*, 2011).

During neurodevelopment, proper regulation of intracellular calcium (Ca^{2+}) levels is of critical importance. Changes in the intracellular Ca^{2+}-concentrations ($[Ca^{2+}]_i$) affect many (sub-) cellular processes, including proliferation,

excitability, motility, plasticity, apoptosis, and gene transcription (Berridge *et al.*, 1999, Clapham, 2007). Moreover, in neuronal cells, the influx of Ca^{2+} through voltage-gated channels is the classical trigger that activates the exocytotic release machinery and initiates vesicular neurotransmitter release (Barclay *et al.*, 2005, Westerink, 2006, Neher and Sakaba, 2008). $[Ca^{2+}]_i$ is thus essential for the regulation of neuronal communication, but it is also involved in neuronal differentiation, neurite outgrowth and axonal pathfinding (Rusanescu *et al.*, 1995, Neher and Sakaba, 2008, Arie *et al.*, 2009, Leclerc *et al.*, 2011). Consequently, chemical-induced changes in $[Ca^{2+}]_i$ have been previously investigated in (amongst others) cortical cultures and proven to be a sensitive endpoint for assessing neurotoxicity (Briz *et al.*, 2010, Hausherr *et al.*, 2014, Meijer *et al.*, 2015). Neurotransmission, which is the main function of the nervous system, not only depends on proper calcium signaling, but also on cell viability and the correct development and maintenance of neuronal network structure (e.g. neurite outgrowth). We therefore not only assessed effects of developmental ELF-EMF exposure on neuronal activity (as measure for proper neurotransmission), but also on cell viability, calcium homeostasis and neurite outgrowth to evaluate the developmental neurotoxicity of 50 Hz ELF-EMF exposure in primary rat cortical neurons *in vitro*.

2. Materials and methods

2.1 Chemicals

Neurobasal®-A Medium, L-glutamine, fetal bovine serum (FBS), B27 supplement (without vitamin A), penicillin-streptomycin (5000 U/mL–5000 µg/mL), and Fura-2 AM were obtained from Life Technologies (Bleiswijk, The Netherlands); all other chemicals were obtained from Sigma-Aldrich (Zwijndrecht, The Netherlands) unless described otherwise. External saline solution for Ca^{2+}-imaging experiments, containing (in mM) 125 NaCl, 5.5 KCl, 2 $CaCl_2$, 0.8 $MgCl_2$, 10 HEPES, 24 glucose, and 36.5 sucrose (pH set at 7.3), and high-potassium saline solution, containing (in mM) 5.5 NaCl, 100 KCl, 2 $CaCl_2$, 0.8 $MgCl_2$, 10 HEPES, 24 glucose, and 36.5 sucrose (pH set at 7.3), were prepared with deionized water (Milli-Q®; resistivity > 10 MΩ·cm). Stock

solutions of 2 mM ionomycin were prepared in dimethylsulfoxide (DMSO) and kept at −20°C. Solutions containing sodium L-glutamic acid (100 µM) were prepared in saline and stored at −20°C in separate aliquots for every experimental day.

2.2 Cell culture

Timed-pregnant (E18) Wistar (HsdCpb:WU) rats were obtained from Harlan Laboratories B.V. (Horst, The Netherlands). Animals were treated humanely and with regard for alleviation of suffering. All experimental procedures were performed according to Dutch law and approved by the Ethical Committee for Animal Experimentation of Utrecht University.

Cortical cultures were isolated from PND 1 fetal Wistar rat brains (corresponding to the last trimester of pregnancy in humans, see Clancy *et al.*, 2007) as described previously (Nicolas *et al.*, 2014, Meijer *et al.*, 2015 and Supplemental Material p.1). Briefly, PND 1 rat pups were decapitated and cortices were rapidly dissected on ice. Tissues were kept in dissection medium (Neurobasal®-A supplemented with sucrose [25 g/L], L-glutamine [450 µM], glutamate [30 µM], penicillin-streptomycin [1%] and FBS [10%], pH 7.4) and on ice during the entire isolation procedure. Cells were seeded in dissection medium on poly-L-lysine (50 µg/mL) coated culture materials.

Cortical cells were kept at 37°C in a 5% CO_2 atmosphere. After one day *in vitro* (DIV1), 90% of the culture medium was replaced by glutamate medium (Neurobasal®-A supplemented with sucrose [25 g/L], L-glutamine [450 µM], glutamate [30 µM], penicillin-streptomycin [1%] and B-27 supplement [2%], pH 7.4). At DIV4 and 11, 90% of the glutamate medium was replaced with FBS culture medium (Neurobasal®-A supplemented with sucrose [25 g/L], L-glutamine [450 µM], penicillin-streptomycin [1%] and FBS [10%], pH 7.4).

2.3 ELF-EMF exposure

Cortical cultures were chronically exposed to ELF-EMF for 7 days during development (DIV8–15, Figure 1). Block-pulsed ELF-EMF with a main

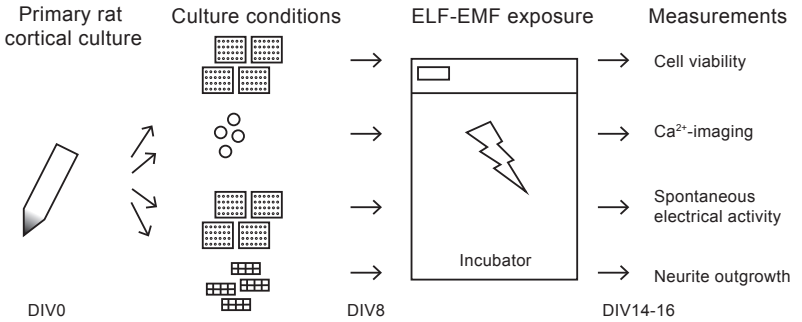

Figure 1. Schematic representation of the experimental set-up and investigated parameters of the chronic developmental ELF-EMF exposure (0–1000 µT) experiments in primary rat cortical cultures. Abbreviation: DIV, days *in vitro*.

frequency of 50 Hz (<10% harmonics) and different magnetic field intensities (1–1000 µT rms) were generated using a custom-made device (Immunent BV, Velthoven, The Netherlands, also see de Groot *et al.*, 2014b, Supplemental Material p.2 and Figure S1) consisting of double copper wired solenoid coils fitted into an incubator and connected to a signal generator with preprogrammed exposure protocols. A subset of cells was placed in a second incubator fitted with the same double copper wired solenoid coils connected to a signal generator and received 7 day sham-exposure (approximately 0.4 µT, i.e. incubator-generated background ELF-EMF).

2.4 Cell viability measurements

Cell viability was assessed with a combined Alamar Blue (AB) and CFDA assay as described earlier (Heusinkveld *et al.*, 2013). Briefly, after a 7 day ELF-EMF (sham-) exposure, cortical cultures were incubated with 12 µM AB solution (resazurin in PBS) and 4 µM CFDA-AM for 30 min at 37 °C and 5% CO_2, after which resorufin and hydrolyzed CFDA were measured spectrophotometrically at respectively 530/590 and 493/541 nm (excitation/emission, Infinite M200 microplate; Tecan Trading AG, Männedorf, Switzerland) as a measure of cell viability.

2.5 Intracellular calcium imaging

To measure effects of chronic ELF-EMF exposure on calcium homeostasis, changes in $[Ca^{2+}]_i$ were measured using the Ca^{2+}-sensitive fluorescent ratio dye Fura-2 AM as described previously (de Groot *et al.*, 2014b) after a 7 day ELF-EMF exposure [DIV14–16] (Figure 4A for example recording). In short, Fura-2 loaded cortical cells were placed under the microscope at room temperature under continuous superfusion with saline. After a 5 min baseline recording, $[Ca^{2+}]_i$ was increased by switching the superfusion solution to either 100 µM glutamate or 100 mM potassium-containing saline for 18 s (Stim). Next, the superfusion solution was switched back to saline and cells were allowed to recover for 10 min.

Changes in F_{340}/F_{380} ratio, reflecting changes in $[Ca^{2+}]_i$, were further analyzed using custom-made MS-Excel macros that semi-automatically calculate free cytosolic $[Ca^{2+}]_i$ from F_{340}/F_{380} (R) using Grynkiewicz's equation (Grynkiewicz *et al.*, 1985): $[Ca^{2+}]_i = K_{d*}(R - R_{min})/(R_{max} - R)$, where K_{d*} is the dissociation constant of Fura-2 AM determined in the experimental set-up and maximum and minimum ratios (R_{max} and R_{min}) were determined at the end of each recording by addition of ionomycin (final concentration 5 µM) and ethylenediamine tetraacetic acid (EDTA; final concentration 17 mM).

2.6 Immunocytochemistry

After a 7 day EMF exposure cortical cultures were fixed on DIV15 with 4% paraformaldehyde (PFA) in 0.1 M phosphate buffer (pH 7.4) for 30 min at room temperature (rt). Subsequently, coverslips were quenched for PFA, permeabilized, and incubated with blocking buffer (2% bovine serum albumin and 0.1% saponin in PBS) containing 20 mM NH4Cl for 20 min at rt. Each of the subsequent wash and incubation steps was performed in blocking buffer. Next, coverslips were incubated with rabbit anti-β(III)-tubulin (ab18207, Abcam, Cambridge, United Kingdom) at a final dilution of 1:500 overnight at 4°C. Subsequently, coverslips were washed 3 times with blocking buffer and incubated with donkey anti-rabbit Alexa 488 (Life Technologies, Bleiswijk, The Netherlands) at a final dilution of 1:100 for 30 min at rt in the dark.

Nuclear staining was performed by incubating the coverslips with 4',6-diamidino-2-phenylindole (DAPI; Life Technologies, Bleiswijk, The Netherlands) at a concentration of 200 nM for 2–3 min at rt in the dark. The washing procedure was repeated and coverslips were sealed with FluorSave (Calbiochem, San Diego, California). Using the abovementioned protocol, a subset of coverslips was co-stained for glial fibrillary acidic protein (GFAP; see Figure S2) to demonstrate the presence of both neurons and astrocytes in these cortical cultures. Immunostained coverslips were visualized using a Leica SPEII Confocal microscope (Leica DMI4000 equipped with TCS SPE-II) using a ×20 oil immersion objective (N.A. 1.4-0.7) and images were captured as *.tif files using Leica Application Suite Advanced Fluorescence software (LAS AF version 2.6.0; Leica Microsystems GmbH, Wetzlar, Germany).

2.7 MEA measurements

Electrical activity of the cortical cells cultured on 48-well MEA plates was measured as described previously (see Figure S3 and de Groot *et al.*, 2014a). Briefly, spontaneous electrical activity in cortical cultures was recorded at various culture durations (DIV8, 11 and 15). Signals were recorded using a Maestro 768-channel amplifier with integrated heating system and temperature controller and a data acquisition interface (Axion Biosystems Inc.). Axion's Integrated Studio (AxIS 2.0.2.11) was used to manage data acquisition. Prior to the 30 min recording of spontaneous activity, MEA plates were allowed to equilibrate in the Maestro for ~5 min. To obtain raw data files, channels were sampled simultaneously at a constant temperature of 37 °C with a gain of 1200× and a sampling frequency of 12.5 kHz/channel using a band-pass filter (200–5000 Hz). Afterwards, raw data files were re-recorded to obtain Alpha Map files for further data analysis in NeuroExplorer (see 2.8 Data analysis and statistics). During the re-recording, spikes were detected using the AxIS spike detector (Adaptive threshold crossing, Ada BandFlt v2) with a variable threshold spike detector set at 7 times standard deviation (SD) of the internal noise level (rms) on each electrode.

2.8 Data analysis and statistics

All data are presented as mean ± SEM from *n* wells (cell viability and spontaneous electrical activity), or cells (calcium imaging), derived from *N* independent experiments or images (neurite outgrowth). For every endpoint, *n* and *N* are indicated in the result section and figure legends. All data presented were obtained from at least three separate cortical cultures.

Background-corrected data from cell viability assays are normalized to sham-exposed controls.

For $[Ca^{2+}]_i$-imaging experiments, basal $[Ca^{2+}]_i$ (a 2 min interval prior to stimulation) is expressed as a percentage of basal $[Ca^{2+}]_i$ in sham-exposed controls. Stimulation-evoked changes in $[Ca^{2+}]_i$ are corrected for basal $[Ca^{2+}]_i$ (Net Stim) and expressed as a percentage of Net Stim in sham-exposed controls. Additionally, the percentage of responders per group was calculated. A response to stimulation was defined as a net increase in $[Ca^{2+}]_i$ > 50 nM. For investigation of EMF-effects on evoked-$[Ca^{2+}]_i$, non-responding cells were removed from further analysis.

For analysis of neurite outgrowth, images captured using LAS AF software were loaded into HCA vision (version 2.1.6, CSIRO Computational Informatics, North Ryde, Australia) for automated neurite analysis (Vallotton *et al.*, 2007, Wang *et al.*, 2010). Detection of cell bodies and neurites and subsequent analysis of neurite length were optimized using the HCA vision wizard, according to manufacturer's instructions. After automated batch-analysis, all images were analyzed in a double-blind fashion by another researcher (see Figure S4). The total neurite length of each sample was divided by the number of cells in the sample to correct for differences in cell number between samples and to obtain average neurite length/cell, which was normalized to sham-exposed controls.

For MEA experiments, spike count files were loaded into NeuroExplorer 5.007 software (Nex Technologies, Madison, Wisconsin) for further analysis (see

Figure S3) of the average mean spike rate (MSR; spikes/s), average median interspike interval (mISI) and average percentage of spikes within a burst (per active well). Only data from active electrodes (≥ 0.01 spikes/s at DIV8) and wells (≥ 1 active electrode) were used for further analysis.

Cells or wells that showed effects two times SD above or below average are considered outliers (<5% for cell viability assays and ~10% for Ca^{2+}-imaging, MEA recordings and neurite length) and were excluded from further analysis. All statistical analyses were performed using SPSS 22 (SPSS, Chicago, IL, USA).

One-way analyses of variance (ANOVA) for field strength, followed by Bonferroni post-hoc analyses (for data with equal variances) or Games Howell post-hoc analyses (for data with unequal variances) were performed to investigate changes in cell viability, calcium homeostasis (basal and Net Stim), spontaneous electrical activity and neurite length after ELF-EMF exposure. *p*-values < 0.05 were considered statistically significant.

3. Results

3.1 ELF-EMF exposure does not affect cell viability

To exclude that the data on neuronal morphology and function are due to direct cytotoxicity resulting from chronic ELF-EMF exposure, effects of a 7 day ELF-EMF exposure (50 Hz, 0–1000 µT) on cell viability were investigated using a combined AB/CFDA assay. In these assays respectively mitochondrial activity and membrane integrity were assessed. ELF-EMF exposure up to 1000 µT for 7 days did not affect mitochondrial activity (Figure 2A). A minor increase in membrane integrity was observed in the CFDA assay at 10 µT (110.6 ± 2%, n=11, N=3, $p < 0.05$), but this effect could not be detected at any of the other intensities (Figure 2B).

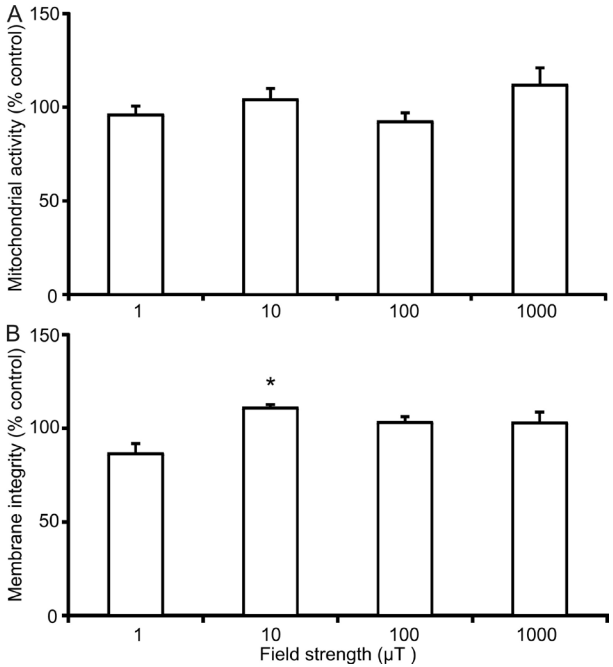

Figure 2. Effects of chronic, developmental ELF-EMF exposure on cell viability in primary rat cortical cultures. Bar graph illustrating effects of a 7 day block-pulsed 50 Hz ELF-EMF exposure (1–1000 µT) on mitochondrial activity **A**., membrane integrity **B**. (normalized to sham-exposed controls) in rat cortical cultures in the AB and CFDA assay, respectively. Data represent mean ± SEM (n=10–12 wells, N=3 per condition). *$p < 0.05$ compared to sham-exposed controls.

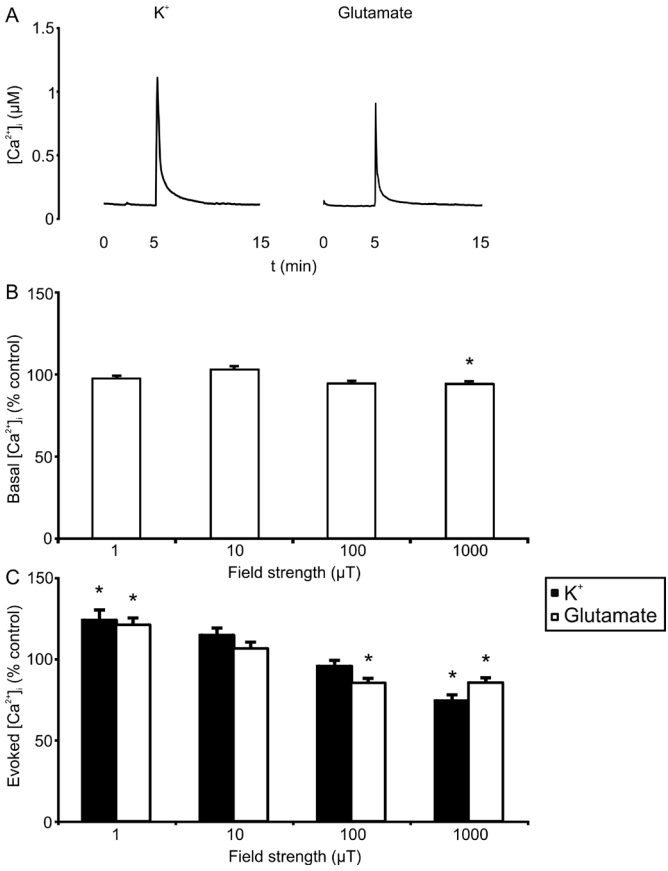

Figure 3. Effects of chronic, developmental ELF-EMF exposure on Ca^{2+}-homeostasis in primary rat cortical cultures. **A.** Representative example traces of intracellular $[Ca^{2+}]$ in non-ELF-EMF exposed rat cortical cultures illustrating low and stable basal $[Ca^{2+}]_i$ (1.5–4 min) and a rapid and transient increase in $[Ca^{2+}]_i$ upon depolarization with high potassium (K^+) [left] or glutamate [right]. **B.** Basal $[Ca^{2+}]_i$ after a 7 day 50 Hz ELF-EMF exposure in developing rat cortical cultures (normalized to sham-exposed cultures). **C.** Potassium- (black bars) and glutamate-evoked (white bars) increases in $[Ca^{2+}]_i$ after a 7 day 50 Hz ELF-EMF exposure in developing rat cortical cultures (normalized to sham-exposed cultures). Data represent mean ± SEM compared to sham-exposed controls (n=198–288 cells, N= 8–10 per condition). *$p < 0.05$ compared to sham-exposed controls.

3.2 High intensity ELF-EMF exposure affects evoked $[Ca^{2+}]_i$

In rat cortical cultures, basal $[Ca^{2+}]_i$ (Figure 3A, 2.5–4.5 min) is stable and low (115 ± 2 nM, *n*=421, *N*=18). Following normalization of the basal $[Ca^{2+}]_i$ to sham-exposed controls, effects of chronic ELF-EMF exposure were investigated (Figure 3B). Basal $[Ca^{2+}]_i$ was not affected by chronic block-pulsed ELF-EMF up to 100 µT. Only at 1000 µT, basal $[Ca^{2+}]_i$ is slightly decreased to 94 ± 1% (*n*=521, *N*=19, $p < 0.05$).

Upon stimulation with high potassium, $[Ca^{2+}]_i$ increases up to 1.1 ± 0.05 µM (*n*=198, *N*=8; Figure 3A, left panel, *t*=5 min). After this increase, $[Ca^{2+}]_i$ rapidly returns to basal (Figure 3A, left panel, 5–15 min). Effects of ELF-EMF exposure on depolarization-evoked increases in $[Ca^{2+}]_i$ (≥ 97% responding cells for all groups) were normalized to sham-exposed controls (Figure 2C, black bars). K^+-evoked $[Ca^{2+}]_i$ is slightly increased to 123 ± 6% (*n*=198, *N*=9, $p < 0.05$) at 1 µT, whereas it is decreased at 1000 µT (73 ± 4%, *n*=229, *N*=9, $p < 0.05$).

When stimulated with glutamate, $[Ca^{2+}]_i$ increases up to 0.9 ± 0.04 µM (*n*=207, *N*=10; Figure 4A, right panel, *t*=5 min) in sham-exposed controls. After this increase, $[Ca^{2+}]_i$ rapidly returns to basal (Figure 4A, right panel, 5–15 min). Effects of ELF-EMF exposure on glutamate-evoked increases in $[Ca^{2+}]_i$ (≥ 98% responding cells for all groups) were normalized to sham-exposed controls (Figure 2C, white bars). Glutamate-evoked $[Ca^{2+}]_i$ is increased to 120 ± 4% (*n*=204, *N*=9, $p < 0.05$) after exposure to 1 µT block-pulsed ELF-EMF, whereas it is decreased to 84 ± 3% (*n*=234, *N*=9, $p < 0.05$) and 84 ± 3% (*n*=270, *N*=10, $p < 0.05$) at 100 and 1000 µT, respectively.

3.3. High intensity ELF-EMF exposure increases neurite length

Proper calcium signaling is essential for the regulation of a variety of processes, including neuronal differentiation and communication. To determine whether the effects of ELF-EMF exposure on $[Ca^{2+}]_i$ affect the development of rat

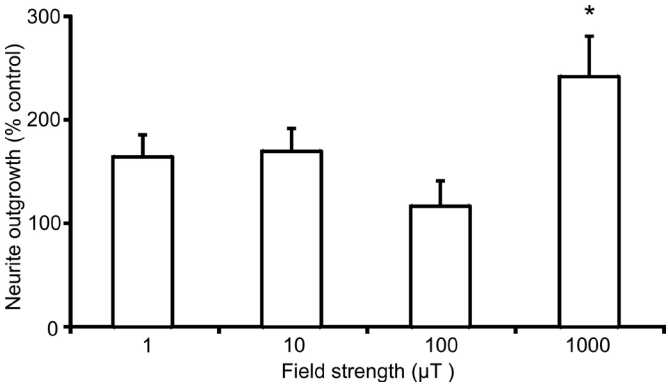

Figure 4. Effects of chronic, developmental ELF-EMF exposure on neurite outgrowth in primary rat cortical cultures. Bar graph illustrating effects of a 7 day block-pulsed 50 Hz ELF-EMF exposure (1–1000 μT) on average neurite length (normalized to sham-exposed cells) in primary rat cortical cultures. Data represent mean ± SEM compared to sham-exposed controls (n=7–11 images, containing 120–488 cells/condition, N=2–3 separate isolations per condition.) *$p < 0.05$ compared to sham-exposed controls.

cortical cultures, neurite outgrowth was assessed after developmental (sham-) exposure. Neurite outgrowth is unaffected by a 7 day developmental ELF-EMF exposure up to 100 μT, whereas average neurite length is increased to 239 ± 39% (n=7, $p < 0.05$) at 1000 μT, compared to sham-exposed control (Figure 4).

3.4 ELF-EMF exposure does not affect spontaneous electrical activity

Spontaneous electrical activity depends on proper calcium homeostasis as well as neuronal network structure. To determine whether the effects induced by exposure to ELF-EMF on $[Ca^{2+}]_i$ and neurite outgrowth affect the development of electrical activity, rat cortical cultures were grown on 48-well MEA plates and spontaneous electrical activity in the cultures was measured during development *in vitro*. Rat cortical cultures become spontaneous electrically

active during development *in vitro* (Figure 5A). After 8 days *in vitro*, the average mean spike rate (MSR) in the cultures is 0.36 ± 0.02 spikes/s (*n*=78, *N*=15 Figure 5A), which increases up to 0.47 ± 0.09 spikes/s (*n*=14, *N*=3) at DIV11 and then starts to decrease to 0.30 ± 0.07 spikes/s (*n*=14, *N*=3) at DIV15.

Since MSR has previously been shown to be a very robust parameter to assess effects on neuronal function (Nicolas *et al.*, 2014, McConnell *et al.*, 2012, Valdivia *et al.*, 2014, Hogberg *et al.*, 2011, Lefew *et al.*, 2013) we measured MSR of cortical cultures grown on MEAs that were exposed to block-pulsed ELF-EMF up to 1000 µT from DIV8 to DIV15 to investigate effects of chronic ELF-EMF exposure on the development of spontaneous electrical activity. MSR on DIV15 from exposed cultures was normalized to time-matched sham-exposed controls (Figure 5B). Although MSR appears to decrease at 1000 µT, none of the exposures resulted in a significant change in MSR. While MSR is a robust parameter to detect effects on neuronal activity, a transition from regular firing to burst-like behavior (or vice versa) could in theory remain undetected. However, our additional analysis demonstrated that ELF-EMF exposure also did not affect the median 'interspike interval' (mISI) and the percentage of spikes within a burst (data not shown).

4. Discussion

In this study we investigated the *in vitro* effects of chronic ELF-EMF exposure during neuronal development in primary rat cortical cultures. The combined results demonstrate that a 7 day developmental ELF-EMF exposure up to 1000 µT does not affect basal $[Ca^{2+}]_i$, whereas depolarization and glutamate-evoked increases in $[Ca^{2+}]_i$ were significantly inhibited at 1000 µT (Figure 4), without affecting cell viability (Figure 3). These findings are in line with previous findings by Luo *et al.*, who investigated the effects of a 24 h intermittent 50 Hz ELF-EMF exposure (1000 and 3000 µT) on calcium dynamics in primary entorhinal cortical neurons and found a dose-dependent decrease in depolarization-evoked increases in $[Ca^{2+}]_i$ after exposure to 1000 and

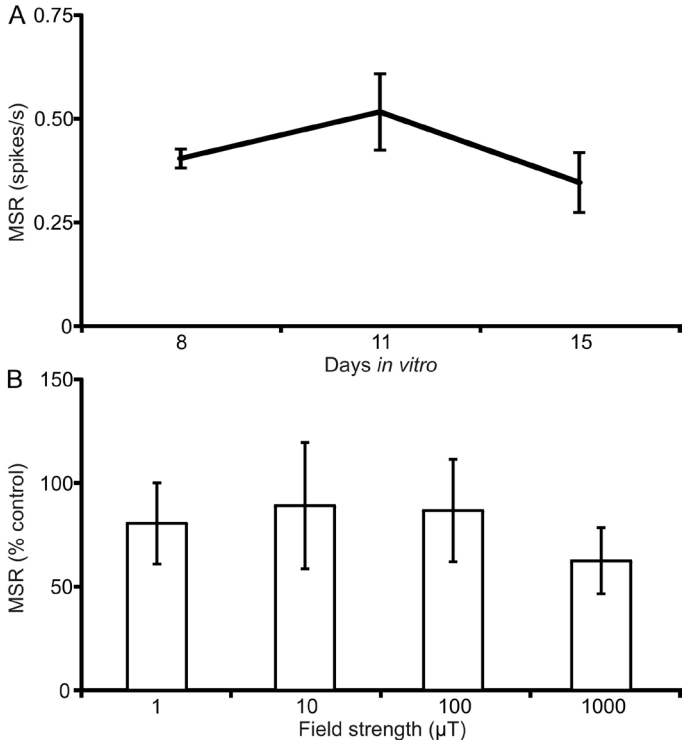

Figure 5. Effects of chronic, developmental ELF-EMF exposure on the development of spontaneous activity in developing rat cortical cultures. **A.** Curve showing the development of spontaneous electrical activity (mean spike rate [MSR] in spikes/s) in sham-exposed primary rat cortical cultures on 48-well MEA plates from DIV 8–15. **B.** Bar graph illustrating effects of a 7 day block-pulsed 50 Hz ELF-EMF exposure (1–1000 µT) on MSR (normalized to time-matched sham-exposed cells) in primary rat cortical cultures on 48-well MEA plates. Data represent mean ± SEM compared to sham-exposed controls (n=14–16 wells, N=3 per condition).

3000 µT, without effects on basal $[Ca^{2+}]_i$ (Luo *et al.*, 2014). In contrast; a 6 day developmental exposure to 1000 µT ELF-EMF increased K^+-evoked increases in $[Ca^{2+}]_i$ in neural stem cells (NSC) isolated from PND 0 mice cortices as well as a the percentage of responsive neurons (Piacentini *et al.*, 2008).

Ca^{2+} has been shown to be an important regulator of neurite outgrowth (Rusanescu *et al.*, 1995, Arie *et al.*, 2009). Axon outgrowth occurs within optimal levels of intracellular calcium (Tang *et al.*, 2003). Especially in terminal growth cones of extending axons and developing dendrites, Ca^{2+} fluctuations are linked to changes in neuron morphology and motility. Treatments that alter $[Ca^{2+}]_i$ have been shown to affect motility and in several types of neurons, axonal outgrowth is accelerated by reducing or blocking Ca^{2+} influx (Mattson and Kater, 1987, Tang *et al.*, 2003, Gomez and Zheng, 2006). This suggests that the observed decrease in evoked $[Ca^{2+}]_i$ at 1000 µT (Figure 3) may be related to the increased neurite length following 7 day exposure at this field strength (Figure 4). In agreement with our findings, ELF-EMF exposure was shown to stimulate neurite outgrowth in PC12 cells under differentiating conditions (McFarlane *et al.*, 2000, Blackman *et al.*, 1993, Zhang *et al.*, 2005), although effects were highly dependent upon culture conditions, and the field (strength) to which the cells were exposed (McFarlane *et al.*, 2000, Zhang *et al.*, 2005).

Multiwell MEA recordings have been successfully used to study and identify chemical-induced (developmental) neurotoxicity (Hogberg *et al.*, 2011, Wallace *et al.*, 2015, Robinette *et al.*, 2011, Defranchi *et al.*, 2011, Nicolas *et al.*, 2014, McConnell *et al.*, 2012). We therefore used this state of the art technique to determine if (sham-) ELF-EMF exposure affects the development of spontaneous neuronal activity of cortical cultures. While neuronal communication strongly depends on proper calcium signaling and neuronal network structure, our MEA experiments show that developmental ELF-EMF exposure *in vitro* did not affect spontaneous electrical activity, although MSR tends to (insignificantly) decrease at 1000 µT (Figure 5B).

To increase reproducibility in (neuro-) toxicology, is was recently suggested to investigate multiple but related endpoints in a single study, investigate effects in multiple well characterized model systems, and/or use multiple techniques to assess common endpoints (Miller, 2014, Westerink, 2013). Moreover, when studying effects of (potential) developmentally neurotoxic (DNT) exposures, it is recommended to use heterogeneous models and (sub) chronic (developmental) exposure scenarios (de Groot *et al.*, 2013). Primary cultures are considered to be a relevant *in vitro* model to study developmentally neurotoxic effects (Bal-Price *et al.*, 2010, Hogberg *et al.*, 2011, de Groot *et al.*, 2013). Primary cortical cultures have been successfully used to study the (developmentally) neurotoxic effects of exposures on a variety of endpoints, including cell viability and calcium homeostasis (Briz *et al.*, 2010, Meijer *et al.*, 2015) as well as electrical activity (Nicolas *et al.*, 2014, Johnstone *et al.*, 2010, Robinette *et al.*, 2011, Hogberg *et al.*, 2011, Mack *et al.*, 2014, Croom *et al.*, 2014, Wallace *et al.*, 2015). Moreover, these cultures have even been used in EPA's ToxCast studies (McConnell *et al.*, 2012, Lefew *et al.*, 2013, Valdivia *et al.*, 2014), demonstrating their capability and suitability to detect (D)NT effects. These cultures allow investigation of effects starting from very early stages of development until full morphological and functional maturation, depending on the exposure scenario and experimental setup (Hogberg *et al.*, 2011). Moreover, the presence of multiple neuronal cell types in a heterogeneous cell model (like the primary cortical cultures, also see Figure S2) is important when studying neurotoxicity, as astrocytes, microglia and oligodendrocytes are essential to maintain neuronal homeostasis and function (Kraft, 2015, Fellin, 2009). On the other hand, the heterogeneity of such primary cultures also results in large biological variation, in particular when studying highly integrated endpoints such as calcium homeostasis and neuronal activity. It is therefore possible that small ELF-EMF-induced effects remained undetected in the present study.

The different endpoints in this study (cell viability, calcium homeostasis, neurite outgrowth, and spontaneous neuronal activity) are interrelated to a considerable degree. Yet, there is little consistency between the effects

observed at different endpoints or field strengths and effect sizes are often limited. As such, these EMF-findings do not appear to obey the criteria for causality, mainly with respect to dose-response relationship and consistency (and as such also plausibility and coherence). Only exposure to 1000 μT affects multiple of the assessed endpoints, indicating a causal effect. Notably, our previous results obtained with cell lines also did not reveal consistent effects of EMF exposure (de Groot *et al.*, 2014b). Combined with the present study, our data thus provide a strong indication that the neurotoxic risk of *in vitro* EMF exposure is limited to the highest field strength (i.e. 1000 μT).

Although ELF-EMF exposure has increased over the last decades, ELF-EMF exposure levels are typically still low, i.e. average residential exposures range between 0.025-0.07 and 0.055-0.11 μT in Europa and the USA, respectively (IARC Working Group, 2002, World Health Organization, 2007a). It is apparent that the currently assessed field strengths (up to 1000 μT) are well above normal everyday exposure levels. Nevertheless, they are in the same order of magnitude as the current exposure limits for 50 Hz EMF: 1000 μT for occupational exposure and 200 μT for residential exposure (International Commission on Non-Ionizing Radiation Protection, 2010). Though our current data do not indicate a need to re-evaluate the exposure guidelines, it should be noted that current guidelines are based on evidence regarding acute effects. It therefore remains important to regularly re-evaluate the evidence regarding chronic and developmental ELF-EMF exposure and to include these exposure scenarios in the guidelines if supported by evidence.

From our current data we conclude that exposure to high intensity 50 Hz ELF-EMF affects stimulation-evoked increases in $[Ca^{2+}]_i$ and neurite outgrowth *in vitro*, but that these changes are insufficient to affect the development of electrical activity. Combined with our previous (more mechanistic) data that indicated that acute and chronic ELF-EMF exposure in (chemically stressed) neuronal cells does not induce neurotoxicity (de Groot *et al.*, 2014b) and the typical low ELF-EMF exposure levels, we conclude that the neurotoxic risk of ELF-EMF exposure appears to be limited.

Acknowledgements

We gratefully acknowledge Fiona Wijnolts, Rob Bleumink and Jan Cuppen for technical assistance. This work was supported by The Netherlands Organization for Health Research and Development (ZonMw) [grant number 85300003] and the Faculty of Veterinary Medicine of Utrecht University.

Supplemental material

Preparation and culture protocol rat cortical cultures

Cortical cultures were isolated from fetal Wistar rat brains as described previously (Nicolas *et al.*, 2014). PND 1 rat pups were decapitated and cortices were rapidly dissected on ice. Tissues were kept in dissection medium (Neurobasal®-A supplemented with sucrose [25 g/L], L-glutamine [450 µM], glutamate [30 µM], penicillin-streptomycin [1%] and FBS [10%], pH 7.4) and on ice during the entire isolation procedure. Cortices were separated from the midbrains, mechanically dissociated, filtered through a 100 µm cell strainer (Greiner Bio-one BV, Alphen a/d Rijn, The Netherlands) and triturated to a single-cell suspension. The cell suspension was centrifuged for 5 min at 800 rpm, after which the cell pellet was resuspended in a small volume of dissection medium. Cells were counted using a Trypan Blue staining and the cell suspension was diluted to contain 2×10^6 cells/mL.

For immunocytochemistry, cells were seeded on tissue culture treated, sterile 8-chamber coverslips (Ibidi GmbH, Planegg, Germany) at a density of 1×10^5 cells/chamber. Cortical cells were seeded in 48-well plates (Greiner Bio-one BV, Alphen a/d Rijn, The Netherlands) at a density of 2×10^5 cells/well for cytotoxicity experiments. For MEA experiments, cortical cultures were seeded in 48-well MEA plates (Axion Biosystems Inc., Atlanta, Georgia) as a 50 µL droplet of cell suspension (2×10^6 cells/mL) on the electrode field in each well. For single-cell fluorescent Ca^{2+}-imaging experiments, cortical cultures were seeded as 400 µL droplets (1×10^6 cells/mL) on 35mm glass bottom culture dishes (MatTek, Ashland, Oregon). The droplets of cells on 48-well MEA plates and glass bottom dishes were allowed to adhere for approximately 3 h, after which 450 µL (48-well MEA plate) or 2 mL (glass bottom dish) of dissection medium was added to the cells. All culture materials were coated with poly-L-lysine (50 µg/mL).

Cortical cells were kept at 37°C in a 5% CO_2 atmosphere. After one day *in vitro* (DIV1), 90% of the culture medium was replaced by glutamate medium (Neurobasal®-A supplemented with sucrose [25 g/L], L-glutamine [450 µM],

glutamate [30 µM], penicillin-streptomycin [1%] and B-27 supplement [2%], pH 7.4). At DIV4 and 11, 90% of the glutamate medium was replaced with FBS culture medium (Neurobasal®-A supplemented with sucrose [25 g/L], L-glutamine [450 µM], penicillin-streptomycin [1%] and FBS [10%], pH 7.4).

Extremely low frequency (ELF)-EMF exposure system

Primary cortical cultures were exposed to 50 Hz ELF-EMF using a custom-made exposure apparatus (Immunent BV, Velthoven, The Netherlands). For chronic developmental exposure experiments, ELF-EMF were generated using a copper coil fitted into an incubator (Figure S1).

The exposure system consists of double copper wired solenoid coils connected to a signal generator with preprogrammed exposure protocols. The copper coils consist of one continuous copper conductor, ensuring equal current in different coil components. The system generates AC and DC vertical field components with field strengths (B_{AC} and B_{DC}) in the range from 1 to 1000 µT. Field strengths were calibrated and monitored using an EMDEX II Tesla meter (Enertech Consultants, Campbell, California, USA) and the coil current was regularly monitored by a Tenma 72-7226 clamp meter (Tenma Test Equipment, Springboro, OH, USA).

To ensure similar treatment between exposed and control groups, cultures in the control groups were sham-exposed by placing them in a switched-off incubator-fitted coil (approximately 0.4 µT, i.e. background ELF-EMF generated by the incubator).

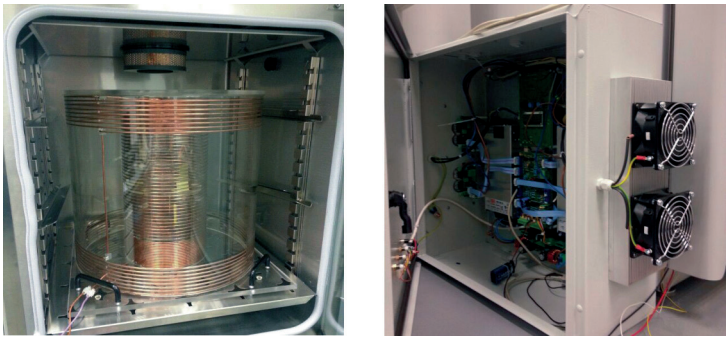

Figure S1. ELF-EMF exposure system. Incubator-fitted copper coils (left) for chronic developmental exposure experiments and connected signal generator (right) with preprogrammed signals.

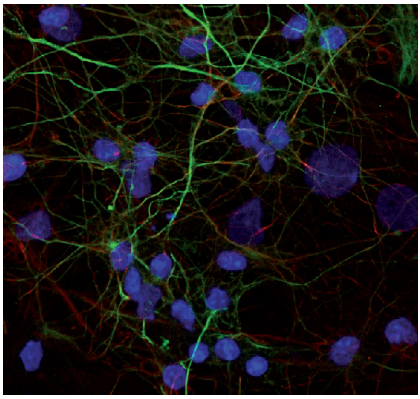

Figure S2.
Demonstration of the presence of neurons (green) and astrocytes (red) in cortical cultures. Primary rat cortical cultures grown on coverslips were fixed, quenched for PFA, permeabilized and incubated with rabbit anti-β-(III) tubulin (ab18207, Abcam, Cambridge, United Kingdom) to identify neurons, and goat anti-glial fibrillary acidic protein (GFAP; red ab53554, Abcam, Cambridge, United Kingdom) to identify astrocytes at a final dilution of 1:500 and 1:100 respectively at 4°C overnight. Subsequently, coverslips were washed and incubated with donkey anti-rabbit Alexa 488 (Life Technologies, Bleiswijk, The Netherlands) and donkey anti-inster; DyLight (goat DyLight 549) (Life Technologies, Bleiswijk, The Netherlands) both at a final dilution of 1:100 for 30 min at rt in the dark. Nuclear staining was performed by incubating the coverslips with DAPI (blue). Immunostained coverslips were visualized using a Leica SPEII Confocal microscope (×40 oil immersion objective).

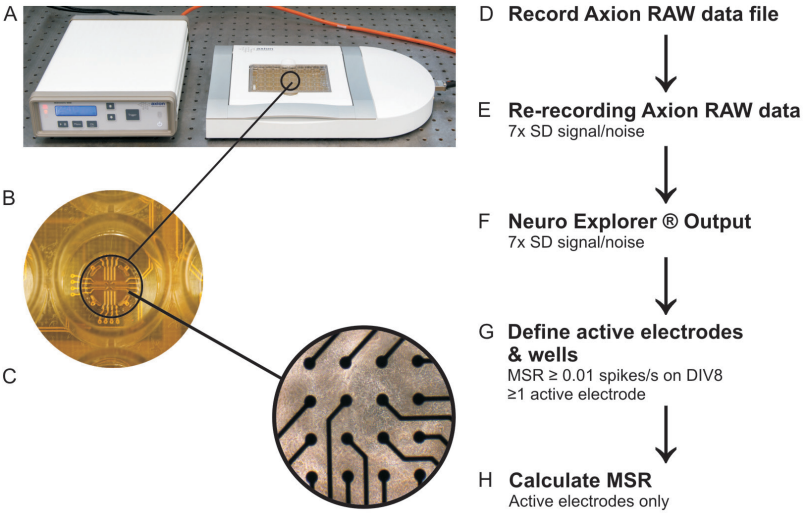

Figure S3. Schematic illustration of the collection and analysis of the MEA data. Using hardware **A** and **B**. and software from Axion Biosystems, spontaneous neuronal activity from primary rat cortical cultures grown on 48-well MEA plates **C**. was recorded for 30 min **D**. at the various days *in vitro* (DIV). Axis recordings were re-recorded **E**. to generate spike count files, using a spike detection threshold of 7 × standard deviation (SD) of the internal noise level (root mean square [rms]), that were further analyzed using NeuroExplorer software **F**. Active electrodes and wells were defined **G**. from which the mean spike rate ([MSR] in spikes/s) was calculated **H**.

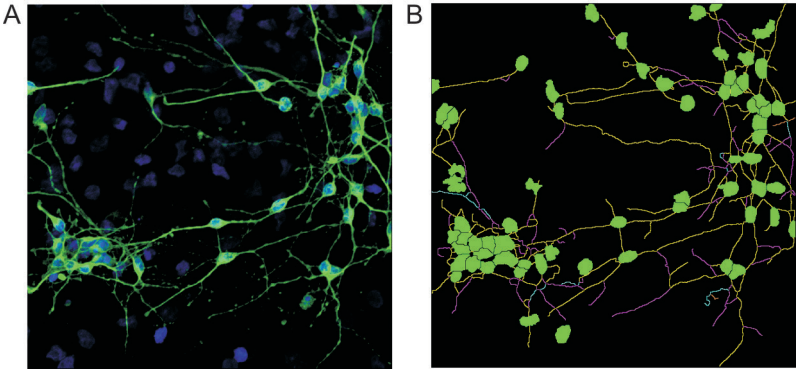

Figure S4. Representative example of the analysis of the neurite outgrowth data. Primary cortical cultures were (sham-) exposed to ELF-EMF (50 Hz; 1–1000 μT) during development from days *in vitro* (DIV) 8 to DIV15. Afterwards, cells were fixed and stained with anti-β(III)-tubulin on DIV15 **A**. and images were subsequently analyzed using HCA vision (version 2.1.6, CSIRO Computational Informatics, North Ryde, Australia) for automated neurite analysis **B**.

CHAPTER 8

Summary, general discussion and conclusions

8.1. Models in *in vitro* neurotoxicity testing

Regulatory toxicity testing, including (developmental) neurotoxicity, is currently investigated in a traditional manner: *in vivo*, using experimental animals (OECD, 1997, OECD, 2007). Consequently, current regulatory toxicity studies are often costly, time- and labor-intensive. Moreover, they are ethically debated as a large number of test animals, mostly rodents, is required (National Research Council, 2007). The clear need for alternative methods, including *in vitro* model systems, has been frequently proposed as they can reduce animal use, while at the same time increase time- and cost-effectiveness (National Research Council, 2007, Costa, 1998, Walsh *et al.*, 2005). Moreover, in the near future the traditional *in vivo* testing strategies are bound to fall short, as international regulations on chemicals, such as REACH (registration, evaluation, and authorization of chemicals), require extensive (neuro-) toxicity testing (Westerink, 2013). *In vitro* systems have the potential to improve our understanding of basic physiological processes of neuronal cells and can be used to study the neurotoxic effects of both chemical and physical exposures and elucidate the underlying mechanisms (Westerink, 2013). Over the last decades, much effort has been put into the characterization and validation of different *in vitro* approaches to study the nervous system (also see Costa *et al.*, 2011b and Walsh *et al.*, 2005). However, their suitability as a model largely depends on the research question at hand (de Groot *et al.*, 2013).

In Chapter 3, we chemically pre-treated PC12 cells to elevate their production of reactive oxygen species (ROS). The well-characterized immortalized PC12 cell line is often used in neurotoxicological research as a model for mature (dopaminergic) neurons (Westerink and Ewing, 2008, Shafer and Atchison, 1991). Neuronal cells, and especially dopaminergic neurons, are very sensitive to external influences. They have a high energy demand, while limited anti-oxidant systems make the cells vulnerable to oxidative stress. The latter has been causally linked to neurodegeneration (Gilgun-Sherki *et al.*, 2001, Uttara *et al.*, 2009, Ceccatelli *et al.*, 2007). We demonstrated that non-cytotoxic concentrations of dexamethasone, L-DOPA or $FeSO_4$ significantly increased the production of ROS in PC12 cells (Chapter 3, Table 1). Furthermore, both $FeSO_4$

and L-DOPA pre-treated PC12 cells demonstrated increased vulnerability to an environmental insult (rotenone exposure). Despite their limitations such as genetic instability with increasing passage or the lack of some of the characteristics of primary cells *in vitro* (Breier *et al.*, 2010), immortalized cell lines, like the PC12 cell line, are extensively used to investigate the neurotoxic potential of chemicals. They offer the advantage of a homogeneous population of cells and can be used to investigate specific molecular mechanisms underlying toxicity. A chemically stressed and more sensitive subtype of the PC12 cell line can be used to study the molecular mechanisms underlying neurodegenerative processes and can be useful for *in vitro* neurotoxicity testing, especially as a first tier screen.

In Chapter 4, we describe the currently most used cell models and parameters to study (exposure-induced changes in) neuronal development, ranging from cell lines to primary cultures and stem- or progenitor cells. When investigating developmental neurotoxicity (DNT), it is important to realize that during neuronal development, the nervous system evolves into a complex network of many specialized, highly connected and structured cells. As a result, the presence of multiple neuronal cell types is important when studying developmental neurotoxicity. In this respect, astrocytes, microglia and oligodendrocytes are essential to maintain neuronal homeostasis and function (Fellin, 2009, Kraft, 2015). Moreover, all of the processes underlying neural development need to take place in the right order and within a controlled time frame (Andersen, 2003, Rice and Barone, 2000). Therefore, the developmental neurotoxic potential of a certain exposure is not only related to the presence of the chemical or physical insult, its dose, or whether or not the insult can reach the nervous system, but also to the developmental phase during which the nervous system is exposed (Rice and Barone, 2000). The latter aspect is usually not fully represented in most *in vitro* systems, but this may be improved by using heterogeneous *in vitro* cell systems and subchronic (developmental) exposure scenarios[1]. The endpoints investigated in DNT studies usually focus on the structural formation of neuronal networks (Chapter 4, Table 1A), but endpoints that investigate neuronal (network)

functionality are currently largely underrepresented. Promising strategies to investigate neuronal (network) function include the investigation of changes in intracellular calcium levels and/or neurotransmitter release or (the development of) neuronal network activity (Chapter 4, Table 1B).

In Chapter 5, we characterized *in vitro* neuronal (network) activity in differentiating mouse neural progenitor cells (mNPCs) and confirmed the heterogeneous and developing nature of this cell model (Chapter 5, Figure 2). Additionally, we demonstrated that differentiating mNPCs exhibit functional calcium homeostasis and are responsive to a variety of chemical and physiological stimuli (Chapter 5, Figure 3). Moreover, the development of functional intercellular signaling pathways was confirmed using multielectrode arrays, demonstrating that mNPCs develop electrical activity (Chapter 5, Figure 5). Thus, mNPCs have the potential to become a promising model to study exposure-induced effects on (the development of) neuronal function. Recently, others have used mNPCs to detect DNT using biochemical and morphological techniques (Fritsche *et al.*, 2011, Moors *et al.*, 2009). These methods can be complementary to the investigation of functional aspects described above. Nevertheless, further (functional) characterization of mNPCs is necessary, including elucidation of differentiation pathways (Breier *et al.*, 2010) and standardization of culture protocols. Moreover, to evaluate the full potential of stem- or progenitor cell based assays, these assays need to be validated using larger sets of (developmentally) neurotoxic and non-toxic reference chemicals to determine their sensitivity and specificity (Breier *et al.*, 2010). Additionally, their shortcomings need to be identified and addressed before mNPCs can be properly used for studying DNT. For example, throughput issues need to be addressed, e.g. by the development of tools for automated sorting and plating of mNPCs (Gassmann *et al.*, 2012) and high-throughput assays using mNPCs for screening chemical-induced apoptosis (Druwe *et al.*, 2015).

Footnote: [1] In the research presented in this thesis, exposure scenarios are defined as follows: acute (30 min), sub-chronic (48 h) and chronic (7 days) developmental (e.g. during *in vitro* development). Not to be confused with acute, sub-chronic or chronic *in vivo* exposure paradigms.

The research presented in this thesis has been performed in cell systems originating from mouse or rat. The origin of nervous systems *in vitro* lies in cultures of non-human tissues and cells (for review see Walsh *et al.*, 2005). Nowadays, these non-human mammalian cultures are still widely used because of for their resemblance to human neuronal cells. However, the use of animal-derived tissues is nowadays not free from ethical considerations, although their use remains widely accepted (Robinette *et al.*, 2011). It goes without saying that the often complex neurotoxicity of chemicals is best studied in human-derived cells. Moreover, the use of human cell models evades the need for interspecies translation (Walsh *et al.*, 2005, de Groot *et al.*, 2014a). As a result, the use of *in vitro* models from preferably human origin is advocated for toxicological research in the 21st century (National Research Council, 2007). In recent years, others have investigated the use of human stem cells as model systems (Heikkila *et al.*, 2009, Jurga *et al.*, 2009, Yla-Outinen *et al.*, 2010). A disadvantage of these cultures, however, is that they often require several weeks of differentiation before they become functionally active. This in contrast to the rapid development of spontaneous electrical activity in rat cortical cultures, see Chapter 7 and (Robinette *et al.*, 2011). For reasons of time and cost effectiveness and a greater chance of infection, (human) stem cells are currently less suitable for efficient and timely screening of exposures. In addition, there are ethical concerns for using human embryonic stem cell-derived neurons and their use has been legally restricted in many countries (Robinette *et al.*, 2011). Thus, the use of animal-derived cells has clear advantages, including the ease of collecting cells from different developmental stages or brain structures, lower costs, easy availability of fetal tissue, and more consistency between cells from different cultures, because of genetic stability within a strain of a laboratory species (Breier *et al.*, 2010). Another advantage is the ease of comparison between results from *in vitro* cultures and *in vivo* (neurotoxicity) data, as the majority of (neuro)toxicological knowledge is still obtained via rodent studies (Robinette *et al.*, 2011).

In Chapters 2–5, different *in vitro* models and endpoints were evaluated that are relevant for (developmental) neurotoxicity. When using the chemically

stressed PC12 cells (Chapter 3), we make advantage of a well-characterized, easily cultured cell line that is already sensitized to chemical insult to investigate molecular mechanisms underlying toxicity. To study developmental neurotoxicity, the use of a heterogeneous, developmental cell model is more appropriate (e.g. primary rat cortical cultures or mNPCs in Chapter 5), as it better resembles the complexity of the developing nervous system. Based on the abovementioned considerations, it was decided that the latter *in vitro* system is more appropriate to study the potential neurodevelopmental toxicity of 50 Hz extremely low frequency electromagnetic fields. The results of these studies are presented in Chapter 6 and 7.

8.2. Neurotoxic effects of ELF-EMF exposure

From Chapter 1, it becomes apparent that ELF-EMF exposure has been associated with a number of health effects, including effects on the nervous system. A substantial part of the epidemiological research on EMF is from occupational settings with exposures being generally higher than in the background population. Obviously, this difference has largely facilitated the detection of effects by EMF in humans (Kheifets *et al.*, 2009), but the relevance for the general population remains difficult to assess. Over the last decades, epidemiological studies have focused on the association between ELF-EMF exposure and brain cancer (World Health Organization, 2007b, Kheifets *et al.*, 2009), but also on neurodegenerative diseases like Alzheimer's disease (AD; World Health Organization, 2007b, Kheifets *et al.*, 2009, Hug *et al.*, 2006, Garcia *et al.*, 2008), amyotrophic lateral sclerosis (ALS; World Health Organization, 2007b, Kheifets *et al.*, 2009, Johansen, 2004) and to a lesser extent Parkinson's Disease (PD; World Health Organization, 2007b, Kheifets *et al.*, 2009). Some of these epidemiological studies have pointed towards an increased risk of AD and ALS, the latter especially in electrical occupations and welding, whereas there is little support for increased risk of PD (Hug *et al.*, 2006, Garcia *et al.*, 2008, Vergara *et al.*, 2013, Ahlbom, 2001). Although neurodegenerative diseases are clearly of interest in relation to EMF exposure, the evidence for a causal association is inconsistent (Johansen, 2004, Schuz *et al.*, 2009, Mattsson and Simko, 2012). Based on the results of epidemiological

studies, a number of hypotheses regarding potential adverse health effects of ELF-EMF exposure have been brought forward. However, these studies often have a number of limitations, which makes it difficult to draw a general conclusion for adverse health effects of EMF. Some of these limitations are e.g. the ubiquitous and multiple sources of EMF, while the field strength may vary considerably over time and space, making it difficult to quantitatively determine EMF exposure in the general population. Interpretation of these studies is further hampered by possible confounding factors like socioeconomic status, viral infection, ionizing radiation, electrical shock and tobacco smoke or disease misclassification (Vergara *et al.*, 2013, Otto and von Muhlendahl, 2007, Kheifets and Shimkhada, 2005, Hug *et al.*, 2006). Importantly, often the nature of the observed associations between ELF-EMF exposure and health effects is not clear due to the lack of a dose-response relationship and plausible biological mechanism(s) (Schuz *et al.*, 2009, Johansen, 2004).

In vivo experiments have been performed to investigate possible health effects of ELF-EMF, as they allow for more controlled exposure scenarios and exposures to field intensities well above those occurring in the environment. However, only few studies have focused on (degeneration of) the nervous system by ELF-EMF exposure *in vivo* (reviewed in Mattsson and Simko, 2012, Santini *et al.*, 2009). Results from *in vivo* studies depend on the exposure scenarios, which are often high (up to several mT) *in vivo* and vary between short- (days) to long-term (weeks-months) periods. For example, long term 50 Hz ELF-EMF exposure has been shown to improve cognitive and pathological symptoms in AD rats (Liu *et al.*, 2008), whereas short-term 50 Hz ELF-EMF exposure did not produce either of these findings (Zhang *et al.*, 2015). Taken together, *in vivo* studies regarding neurodegenerative effects of EMF suggest increased oxidative stress and a potential reduction in anti-oxidant systems, especially after long-term *in vivo* ELF-EMF exposure (Falone *et al.*, 2008, Ciejka *et al.*, 2011). Effects on neurotransmitter systems are however less clear, as positive, negative and no effects on neurotransmitter turnover and/or -receptor function have been found after ELF-EMF exposure (Janac *et al.*, 2009, Sieron *et al.*, 2004, Sieron *et al.*, 2001).

In vitro experiments can overcome some of these challenges and help elucidate a biological plausible mechanism underlying some of the observed outcomes. Neurodegenerative effects of ELF-EMF exposure have been investigated in different cell models under controlled culture conditions with well-characterized exposure scenarios (reviewed in Mattsson and Simko, 2012). Many of these *in vitro* studies investigating potential neurotoxic or neurodegenerative ELF-EMF effects focused on morphology, radical production, cell viability parameters, calcium homeostasis or a combination of these endpoints (Reale *et al.*, 2014, Morabito *et al.*, 2010, Di Loreto *et al.*, 2009, Falone *et al.*, 2007, Tonini *et al.*, 2001).

Calcium homeostasis plays a pivotal role in the regulation of various cellular responses (e.g. cell viability, neurite outgrowth and electrical activity) and it depends on voltage-sensitive processes (e.g. voltage-gated channels; reviewed in Berridge *et al.*, 1999, Clapham, 2007, Arie *et al.*, 2009, Rusanescu *et al.*, 1995). Calcium homeostasis has consequently been investigated as a common mechanism underlying a variety of ELF-EMF induced effects (Walleczek, 1992, Pall, 2013). Similarly, effects of ELF-EMF on radical production have commonly been assessed, because the high energy demand and limited anti-oxidant systems make the nervous system sensitive to oxidative stress and external influences that negatively affect their oxidative status (Reale *et al.*, 2014). From a clinical point of view, oxidative stress has also been linked to neuronal cell death in several neurodegenerative diseases (Ruszkiewicz and Albrecht, 2015, Halliwell, 2006).

Therefore, in Chapter 6, the effects of 50 Hz EMF exposure on cell viability, ROS production and calcium signaling were assessed in naïve and the previously characterized chemically stressed PC12 cells (Chapter 3). It was demonstrated that (sub-) chronic 50 Hz EMF exposure did not affect cell viability or ROS production in any of the PC12 phenotypes. Moreover, basal and stimulation-evoked intracellular calcium concentrations ($[Ca^{2+}]_i$) were not affected by acute or (sub-) chronic ELF-EMF exposure up to 1000 µT (Chapter 6, Figure 2 and 3).

The developing central nervous system (CNS) is very sensitive to external influences (Rice and Barone, 2000) and its function and development critically depend on many voltage-dependent processes (van Ooyen, 1994, Butz *et al.*, 2009, van Oss and van Ooyen, 1997). Therefore, we investigated the effects of chronic developmental ELF-EMF exposure in rat primary cortical cultures in Chapter 7. We demonstrate that a 7 day developmental ELF-EMF exposure up to 1000 µT does not affect basal $[Ca^{2+}]_i$, whereas depolarization and glutamate-evoked increases in $[Ca^{2+}]_i$ were significantly inhibited at high ELF-EMF intensities (1000 µT; Chapter 7, Figure 3), without affecting cell viability. Moreover, neurite length in cortical cultures exposed to 1000 µT ELF-EMF was increased, whereas it was unaffected at lower field strengths (Chapter 7, Figure 4). However, despite changes in calcium homeostasis and morphology, we were unable to demonstrate changes in the development of spontaneous electrical activity in exposed primary cortical cultures grown on MEA's, which suggests that effects of chronic, developmental ELF-EMF exposure on neuronal activity are probably limited.

The combined findings from Chapter 6 and 7 suggest that either the duration and/or timing of exposure is of crucial importance for the observed effects (at least on calcium homeostasis), as the other exposure characteristics (including field strength, frequency, and type of field) were kept constant between both studies. Long-term exposure during the developing phase may be more effective to induce ELF-EMF effects. As we used different cell models to assess ELF-EMF effects in Chapter 6 and 7, it cannot be excluded that the difference in cell models explains the difference in observed effects. However, this appears unlikely as previous studies in our lab have shown primary cortical cultures to be less sensitive than PC12 cells, at least to chemical exposures (Meijer *et al.*, 2015).

In line with our findings, acute or sub-chronic EMF exposure has been previously reported to have limited effect on calcium characteristics in undifferentiated neuronal (like) cells (Craviso *et al.*, 2002, Morabito *et al.*, 2010, Craviso *et al.*, 2003), although some effects were reported, mostly at high intensities (Lisi *et*

al., 2006, Barbier *et al.*, 1996). As for oxidative stress, several earlier studies did report increases in ROS production or (anti-) oxidative parameters after (sub-) chronic ELF-EMF exposure (Morabito *et al.*, 2010, Reale *et al.*, 2014, Di Loreto *et al.*, 2009, Park *et al.*, 2013), although others did not find ROS to be increased after chronic ELF-EMF exposure (Falone *et al.*, 2007), which is more in line with our findings.

As previously addressed in this thesis, ELF-EMF do theoretically not have enough energy to cause direct effects on cells (e.g. DNA damage or cell death). This is supported by many studies that find cell viability to be unaffected in different neuronal cells (or cell lines) after ELF-EMF exposure (de Groot *et al.*, 2014b, Pessina *et al.*, 2001, Morabito *et al.*, 2010, Reale *et al.*, 2014). Nevertheless, ELF-EMF are hypothesized to have modulatory effects (Otto and von Muhlendahl, 2007), e.g. to provide a co-stimulatory effect on a variety of strong (chemical or physical) cell stimulatory factors, e.g. activation of complex cell mechanisms (Tonini *et al.*, 2001, Santini *et al.*, 2009). This is interesting in light of our findings, as it could explain why timing of ELF-EMF exposure is so important; The differentiation processes activated during the development in rat primary cortical cultures could be considered as a strong cell stimulatory factor to which ELF-EMF exposure could be a co-stimulus.

In support of this hypothesis previous findings have shown growth rate and cell density to be affected in differentiating, but not in undifferentiated, neuroblastoma cells after 50 Hz EMF exposure (Tonini *et al.*, 2001). Additionally, chronic ELF-EMF exposure is found to effect (either increase or decrease) differentiation-evoked neurite outgrowth in the presence of a physiological or chemical stimulus (e.g. NGF or DMSO; Tonini *et al.*, 2001, Morabito *et al.*, 2010, Lisi *et al.*, 2006). Moreover, in line with Chapter 7, stimulation-evoked, but not basal $[Ca^{2+}]_i$ is affected by ELF-EMF exposure (Luo *et al.*, 2014, Piacentini *et al.*, 2008). Furthermore, the combined exposure to ELF-EMF and a chemical agent like melatonin, substance P or caffeine, can affect $[Ca^{2+}]_i$ (Liu *et al.*, 2008, Pessina *et al.*, 2001, Pirozzoli *et al.*, 2003), again demonstrating a co-stimulatory effects of ELF-EMF. Similarly, ELF-

EMF co-exposure with H_2O_2 increased cell oxidative activity by decreasing antioxidant catalase activity (Reale *et al.*, 2014). On the other hand, Morabito *et al* demonstrated effects on calcium homeostasis after ELF-EMF exposure in undifferentiated PC12 cells, but did not find NGF-differentiated PC12 cells to be affected. It is not clear if these PC12 cells were exposed during the differentiation process or after they had already been fully differentiated (Morabito *et al.*, 2010).

Clearly, biological effects of ELF-EMF are highly dependent on a variety of factors, the most important being the exposure parameters (i.e. electric and/or magnetic field, static or alternating, frequency, intensity, timing and duration of exposure; Otto and von Muhlendahl, 2007), the cell/animal model (intrinsic susceptibility of different cells or cell lines) and the investigated outcome (e.g. measuring techniques, sensitivity of the endpoint, etc.). Additionally, in *in vitro* or *in vivo* experiments, often a dose-response relationship between a certain biological effect and EMF exposure parameters cannot be established. Instead window-effects are often observed (Otto and von Muhlendahl, 2007), i.e. effects only at narrow exposure windows (see for example McFarlane *et al.*, 2000, Tonini *et al.*, 2001). Earlier, the National Radiological Protection Board concluded that results from different *in vitro* studies are often contradictory and that positive results can almost never be independently replicated. Moreover, they concluded that many of the effects involved exposures with flux densities greater than 100 μT and that ELF-EMF attributed effects tend to be small and their biological significance unclear (National Radiological Protection Board, 2004). Similarly, the size of the observed effects in Chapter 7 is small, especially when compared to the biological variation of the *in vitro* model system itself. If the “sensitive window” effects are also taken into consideration, this raises the question if actual ELF-EMF effects are measured, or if these can be explained by mere biological variation.

Nevertheless, when the findings from Chapter 6 and 7 are combined, we can conclude that acute and (sub-) chronic ELF-EMF exposure does not appear to

cause neurotoxic effects, whereas a developmental chronic exposure appears to affect cell morphology and calcium signaling at high exposure intensities (1000 μT).

8.3. Human risk assessment

In the research presented in the last two chapters of this thesis, we attempted to mimic the different human exposure scenarios to ELF-EMF by using *in vitro* models for the developing, adult and aging or stressed nervous system. Moreover, in our experiments a wide variety of field strengths were used. In this section, we attempt to translate our *in vitro* results to actual human exposures in order to assess the potential neurotoxic risks of ELF-EMF exposure.

To perform a risk assessment, several key steps need to be carried out, including the identification of the hazard and the population at risk. Hazard was characterized in Chapter 6 and 7 and compared with that from literature in Chapter 8.2. Our data identified only chronic developmental exposure at high intensity (1000 μT) as potentially hazardous to the nervous system. In this section, the others steps of the risk assessment will be dealt with in order to assess risk of ELF-EMF exposure for the (developing) human nervous system. Importantly, existing reduction measures are also taken into consideration.

8.3.1 ELF-EMF exposure

As briefly mentioned in previous chapters, common sources of ELF-EMF exposure include man-made sources involved in the use, generation and transportation of electricity, e.g. power plants, -lines and -cables. ELF-EMF also occur naturally, e.g. the earth's static magnetic field, the local buildup of electrical fields in the atmosphere associated with thunderstorms, or the Northern Lights (World Health Organization, 2007b). However, average background levels of naturally occurring EMF in the ELF range are very low; At 50 or 60 Hz the natural magnetic field is typically of the order of 10^{-6} μT (Polk, 1974). Exposure that results from man-made ELF-EMFs are usually several orders of magnitude higher and are therefore considered the dominant exposure source to time-varying magnetic fields.

Over the last decades, the growing demand for electricity, advancing technologies and changes in lifestyle have created more and more artificial sources of EMF, thus increasing human exposure to (ELF-) EMF. When describing EMF exposures, it is important to distinguish peak exposures from average (time-weighed) exposures. In reality, one can be exposed for a short time (*peak*) to a high field (e.g. at work or directly under a power line), whereas the rest of the time interval one is only exposed to background levels, resulting in low *average* individual exposure levels.

Residential exposure to power-frequency magnetic fields varies only slightly from country to country, depending on differences in power supply, wiring practices and electricity consumption per resident (IARC Working Group, 2002, World Health Organization, 2007b). Sources contributing to residential exposure are current-carrying wiring and electrical circuits, the use of appliances and the presence or absence of nearby power lines (IARC Working Group, 2002). The average chronic residential exposure ranges between 0.025–0.07 µT in Europa and 0.055–0.11 µT in the USA (IARC Working Group, 2002, World Health Organization, 2007b).

In close proximity to (overhead) transmission lines, magnetic fields reach maximum peak (magnetic flux) densities up to 10–30 µT (during peak demand). However, mean exposure levels are typically only a few µT. Notably, exposure levels decrease exponentially with increasing distance from the source and intensities three to four orders of magnitude lower are detected a few hundred meters from transmission lines (World Health Organization, 2007b, IARC Working Group, 2002). So, only few homes are actually exposed to fields from high-voltage power lines that are strong enough to potentially induce adverse health effects (IARC Working Group, 2002).

The main exposure source in home derives from electrical appliances. For most people, this is the largest exposure source overall, exceeding exposure at work and outside the home. When using certain appliances individuals can be exposed to ELF-EMF with intensities of several hundred µT (e.g. electrical can

opener, 5 cm from the source, Table 1). However, these are peak exposures, of which the intensity depends very much on the distance to the source (IARC Working Group, 2002, World Health Organization, 2007b). At a distance of 1 m, the exposure from electrical appliances is usually similar to background levels (IARC Working Group, 2002).

High exposures may also occur (often for shorter durations) in occupational settings. Occupational exposure intensities are commonly expressed as time-weighted average exposure during a x-hour workday and differ greatly between occupations. Time-weighted average exposures are for example lower for office workers than for electricians or welders (Table 2; NIOSH, 1996). The most common time-weighed personal exposure measurement at the workplace is 0.05 μT and it is rarely above 1 μT, although exposure intensities can reach approximately 10 μT at maximum (World Health Organization, 2007b, IARC Working Group, 2002). Notably, as many occupations involve the direct use of electrical appliances (e.g. electrical tools), high(er) peak exposures occur in occupational settings. For example, trunk exposures up to several hundreds of μT have been reported for welders using insulated welding cables that carry magnetic flux densities over 1000 μT at the cable surface (World Health Organization, 2007b).

Noteworthy, the research presented in Chapter 6 and 7 of this thesis focused on block-pulsed ELF-EMF, whereas the production and distribution of electricity are mainly associated with sinusoidal 50 Hz EMF. In pilot experiments at the beginning of this PhD-project, both sinusoidal and block-pulsed 50 Hz EMF (up to 1000 μT) were used side-by-side in acute experiments using the PC12 cell, resulting in similar (lack of) findings. As the biological effects of EMF exposure depend on factors like frequency and field strength, we decided to continue the rest of our experiments (chronic and developmental) with block-pulsed EMF. This added a third exposure characteristic, which is the slope of the wave, or dB/dt; The ratio of the amount of change in amplitude of the magnetic field (dB) and the time it takes to make that change (dt). As apparent from Figure 1, dB/dt is larger for block-pulsed waves, potentially

Table 1. Resultant broadband magnetic field calculated at 5, 50 and 100 cm from appliances. Table adjusted from (Preece et al., 1997).

	Strength of the magnetic field (μT) at distances from the surface of appliances computed from direct measurements					
Appliance type	*5 cm*	*± SD*	*50 cm*	*± SD*	*100 cm*	*± SD*
Television	2.69	1.08	0.26	0.11	0.07	0.04
Vacuum cleaner	39.53	74.58	0.78	0.74	0.16	0.12
Coffee maker	0.57	0.03	0.06	0.07	0.02	0.02
Clock radio	2.34	1.96	0.05	0.05	0.01	0.01
Can opener	145.70	106.23	1.33	1.33	0.20	0.21
Computer	1.82	1.96	0.14	0.07	0.04	0.02
Speaker	0.48	0.67	0.07	0.13	0.02	0.04
Hair dryer	17.44	15.56	0.12	0.10	0.02	0.02
Electric shaver	164.75	-	0.84	-	0.12	-

Table 2. Average exposures to magnetic fields during a work shift for typical workers who use electric equipment. For comparison, the table also lists worker exposures off the job. Table adjusted from (NIOSH, 1996).

	Average magnetic field exposure (μT) for different types of workers	
Type of worker	*Average daily median*	*Exposure range*
Office workers (no computers)	0.05	0.02 – 0.2
Office workers (with computers)	0.12	0.05 – 0.45
Machinists	0.19	0.06 – 2.76
Electric line workers	0.25	0.05 – 3.48
Electricians	0.54	0.08 – 3.40
Welders	0.82	0.17 – 9.6
Workers off the job (home, travel, etc.)	0.09	0.03 – 0.37

making the signal more capable of effecting neuronal cells, compared to sinusoidal waves. Although the frequency and magnetic flux densities for both signals are the same, we rationalize that block-pulsed EMF are a most worst-case exposure scenario for risk assessment.

8.3.2 Exposure guidelines

As previously discussed, ELF-EMF-induced electric fields and currents in the body can interact with electrically excitable tissues, especially in the (central) nervous system (International Commission on Non-Ionizing Radiation Protection, 2010, National Radiological Protection Board, 2004). As a result, ELF-EMF exposure should be limited to fields that induce electric field strengths that do not cause any possible acute, transient effects on nerve cell excitability. Currently, there are two international exposure guidelines that define ELF-EMF exposure limits (IEEE Standards Coordinating Committee 28, 2002, International Commission on Non-Ionizing Radiation Protection, 2010). Exposure limits vary per frequency range, between occupational and residential exposure and between body parts (e.g. head, torso, extremities). Moreover, they slightly differ between guidelines. In this chapter the most recent guidelines of the International Commission on Non-Ionizing Radiation Protection (ICNRP) will be used for risk assessment, as most countries have based their standards on the ICNIRP guidelines.

The ICNRP guidelines are based on so-called basic restrictions that concern nervous system responses caused by direct effects of induced electrical currents in excitable tissues. The induced internal electric fields in these basic restrictions vary per frequency and are set at 100 mV/m for occupational and 20 mV/m for residential exposure for 50 Hz EMF (International Commission on Non-Ionizing Radiation Protection, 2010). Using dosimetric calculations, based on realistic anatomic human models and measurements of the dielectric properties of human tissues, these basic restrictions are converted into external field strengths, which are the actual exposure reference levels for acute (peak) exposure. In the most recent 2010 ICNRP guidelines exposure reference levels are set at 1000 μT for occupational exposure and 200 μT

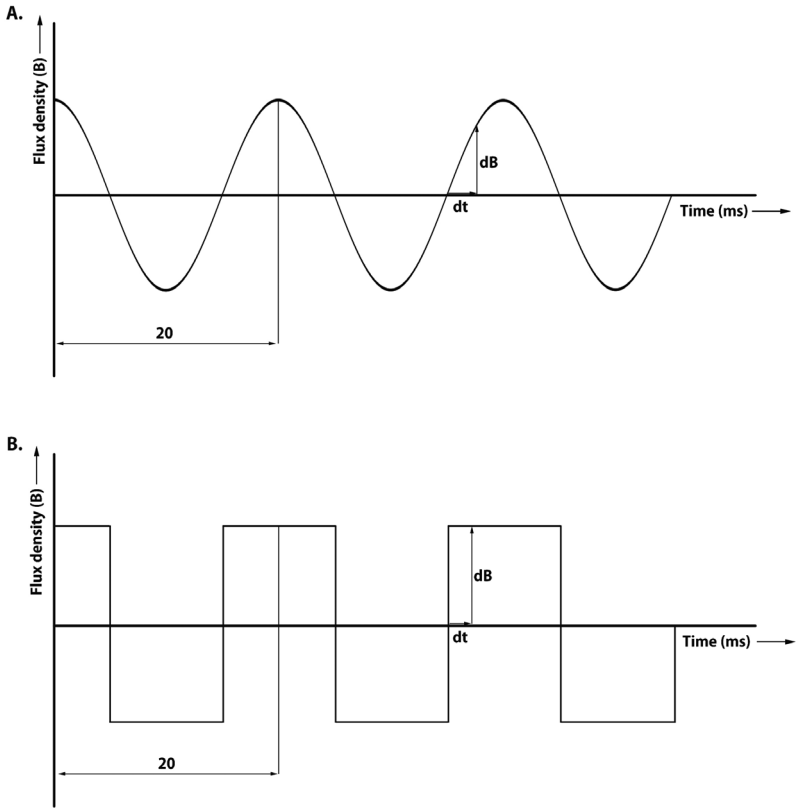

Figure 1. Schematic representation of a sinusoidal 50 Hz EMF **A**. and block-pulsed 50 Hz EMF **B**. signal, with on the x-axis the time in ms and on the y-axis the flux density B. The speed at which B changes (dB/dt) is higher for block-pulsed waves compared to sinusoidal waves as apparent from the steeper slope in the block-pulsed waves.

for residential exposure for 50 Hz EMF (International Commission on Non-Ionizing Radiation Protection, 2010). However, many countries, including the Netherlands, still use the 1998 ICNIRP guidelines in which exposure reference levels were set at 500 μT for occupational and 100 μT for residential exposure (see (International Commission on Non-ionizing Radiation Protection, 1998)).

ELF-EMF exposure reference levels concern the entire population and do not specifically address vulnerable groups, e.g. children. Dosimetric calculations for children and pregnant women or their unborn children have not been conducted extensively. Similar ELF-EMF exposures are hypothesized to cause higher internal electric field strength and current densities in adults than in children, because of differences in size and shape. However, in children, the nervous system is developing and brain tissue is more conductive than that of adults because of a higher water content and ion concentration (Kheifets *et al.*, 2005).

It should again be emphasized that the ICNIRP guidelines are based on evidence regarding acute effects only, as the ICNIRP concluded that there is no evidence to support chronic conditions related to ELF-EMF exposure (International Commission on Non-Ionizing Radiation Protection, 2010). Nevertheless, next to these reference levels, some countries have adopted additional measures to limit (chronic) ELF-EMF exposure for susceptible groups (e.g. children), based on the precautionary principle. For example, the Dutch government advices that it should preferably be avoided that new situations arise in which children are exposed (yearly average) to 50 Hz EMF above 0.4 μT because of the proposed association with childhood leukemia (Kennisplatform ElektroMagnetische Velden, 2009).

8.3.3 Risk assessment

In toxicology, risk is defined as hazard × exposure. Hence, when combining the findings from Chapter 6 and 7, the hazard of ELF-EMF regarding the nervous system is confined to chronic developmental exposure to high intensity fields (1000 μT). Evidently, a very large part of the population is chronically exposed to ELF-EMF in the 50 Hz range. However, when compared to the average residential exposure, which is 0.025–0.07 μT in Europe, 1000 μT is very high, i.e. approximately 10.000 times higher. Even in occupational settings where exposure can be higher, such high exposure intensities are unlikely to occur. Average occupational exposures are typically below 1 μT, even for electrical occupations (NIOSH, 1996, World Health Organization, 2007b). Although

higher average exposures are reported for welders, railway engine drivers and sewing machine operators, average exposures for these occupations are still below 10 μT (NIOSH, 1996, World Health Organization, 2007b).

As we found effects of developmental exposure to ELF-EMF, children (from embryonic life to adolescence, as this period is characterized by CNS growth and development) could be addressed as a susceptible group for the potential neurotoxic effects of high intensity ELF-EMF exposure. ELF-EMF exposure for children is similar to that of adults, or possibly even lower as younger children use appliances less and spend less time outside the home, and is close to average residential exposure. Moreover, as the precautionary principle tries to limit chronic ELF-EMF exposure in children to <0.4 μT, children are highly unlikely to receive high ELF-EMF exposure intensities as used in the research presented in Chapter 7.

Notably, susceptibility to ELF-EMF *in vivo* is predicted to be greater than *in vitro*, due to the larger number of interacting nerve cells and larger neural networks, at least for direct effects like nerve stimulation (National Radiological Protection Board, 2004). Nevertheless, because of the low chronic exposure and taking into account the present exposure limits, the risk of ELF-EMF exposure for neurotoxicity is limited, even when taking into consideration several safety factors on the currently investigated field strength of 1000 μT (to account for uncertainty in the data, e.g. for *in vitro* to *in vivo* extrapolation, etc.).

8.3.4 Risk perception and risk communication

Despite decades of research, there is still scientific controversy and concern amongst the public regarding the health impact of (ELF-) EMF (Otto and von Muhlendahl, 2007). Factors contributing to this controversy include the difficulties in interpreting and reproducing epidemiological findings and the lack of a dose-response relationship and biologically plausible mechanism(s) (Otto and von Muhlendahl, 2007). For the general public, the lack of proper communication of scientific results can be another important factor

contributing to the concern around ELF-EMF (Otto and von Muhlendahl, 2007). However, even if scientists establish a clear "risk" (or a lack thereof) of ELF-EMF exposure and communicated this to the general public, the perceived risk could still differ from the actual risk.

Risk perception depends on personal factors (i.e. age, sex, education, social and cultural background) of an individual (or a certain public), external factors (e.g. media, regulatory process, etc.) and the nature of the risk. Factors that determine the nature of the risk have been previously investigated and are summarized in Table 3 (adapted from World Health Organization, 2002, World

Table 3. Factors contributing to the magnitude of the perceived risk of environmental exposures (e.g. ELF-EMF), including relevant examples. Table based on (World Health Organization, 1999, World Health Organization, 2002).

Factors contributing to the magnitude of the perceived risk		
Increase risk perception	*Decrease risk perception*	*Example*
Involuntary exposure	Voluntary exposure	People feel much less at risk when the choice is theirs, e.g. smoking and the risk of cancer
Lack of personal control	Feeling of control over a situation	If people do not have any say in the installation of new powerlines, they tend to perceive the risk from such EMF facilities as high
Familiar exposure	Unfamiliar/exotic exposure	EMF is a relatively new, unfamiliar, or hard-to-comprehend technology which increases the perceived risk
Dreaded outcome	Not dreaded outcome	Disease outcomes such as cancer, severe and lingering pain, disability, or genetic threats to future generations are more highly feared.
Direct benefits from exposure	Indirect benefits from exposure	People without a mobile phone that are nevertheless exposed to radio frequency fields from mobile telephone base stations are less likely to accept the possible associated risks
Fair exposure	Unfair exposure	Unfairness may come from an uneven distribution of risk across the population and increases the perceived risk

Health Organization, 1999). For ELF-EMF exposure, especially the involuntary exposure, the lack of control (e.g. over installation of new power lines), the unfamiliarity to the technology and the possible association with a dreaded disease (i.e. leukemia in children) are all important factors contributing to the risk perception (World Health Organization, 1999).

Next to trying to evaluate if there is a hazard from EMF exposure (and the potential health impact thereof), it is almost equally important to investigate how the general public perceives the risk of ELF-EMF and manage this perception in a realistic manner.

8.4. Conclusions and recommendations for future research

The research presented in this thesis aimed at developing and characterizing (novel) *in vitro* models for neurotoxicity testing, with a special focus on developmental neurotoxicity. These models were used to investigate the *in vitro* neurotoxicity of exposure to 50 Hz extremely low frequency electromagnetic fields (ELF-EMF) and elucidate the underlying biological mechanisms. There are uncertainties and controversies with respect to ELF-EMF exposure and the research described in this thesis has been aimed to help resolve these.

- For evaluation of neurotoxicity of environmental exposures it is important to use appropriate cell models and to study both morphological and functional endpoints.
- Thorough characterization of any new model system is critical prior to using it for (developmental) neurotoxicity testing.
- Chemically stressed PC12 cells and mouse neural progenitor cells are promising models for aging/stressed and developing neuronal cells, respectively.
- ELF-EMF exposure has been linked to effects on the nervous system, although underlying mechanisms and dose-response relationships remain unknown.
- Acute and (sub-) chronic 50 Hz EMF exposure has no neurotoxic effects in an *in vitro* model for adult and aged or stressed neuronal cells.
- Calcium homeostasis and neurite outgrowth are potential sensitive targets for high intensity (1000 μT) chronic, developmental 50 Hz EMF exposure.
- Biological responses to ELF-EMF are highly dependent on a variety of factors. We found timing and intensity of exposure to be particular important for the vulnerability of the developing nervous system for 50 Hz EMF exposure.
- Residential and occupational chronic ELF-EMF exposures are generally at least four orders of magnitude below the high intensity used for the research presented in this thesis. Given the current ELF-EMF exposure and reference levels and taking into account experimental uncertainties such as poor reproducibility of effects, *in vitro-in vivo* extrapolation and window effects, we conclude that the neurotoxic potential of ELF-EMF exposure in humans is limited.
- Future research should primarily focus on reproducing present findings and confirm whether timing and intensity of exposure are indeed crucial exposure parameters, preferably using *in vitro* models (possibly of human origin) and techniques.

NEDERLANDSE SAMENVATTING

Inleiding

Het zenuwstelsel is een belangrijk en complex orgaansysteem. De voornaamste functie van het zenuwstelsel is het ontvangen en verzenden van signalen, ook wel neurotransmissie genoemd. Neuronen (zenuwcellen) zijn dan ook structureel en functioneel speciaal aangepast om deze taak te volbrengen. Neuronen hebben uitlopers, neurieten, om elektrische en chemische signalen te ontvangen en deze door te sturen naar andere neuronen. Naast neuronen bevat het zenuwstelsel ook andere cellen, zogenaamde gliacellen, die (onder andere) tot functie hebben de neuronen te voeden en ondersteunen.

Neuronale communicatie hangt voornamelijk af van de viabiliteit en structurele integriteit van de cellen in het zenuwstelsel, evenals van een goede regulatie van de mechanismen die ten grondslag liggen aan neurotransmissie. Een voorbeeld hiervan is de calcium homeostase. Calcium ionen (Ca^{2+}) zijn belangrijk bij bijna alle cellulaire processen, zoals de proliferatie, exciteerbaarheid, ontwikkeling en mobiliteit van cellen. De calcium homeostase wordt daarom streng gereguleerd en intracellulaire calcium concentraties ($[Ca^{2+}]_i$) worden laag gehouden door speciale controle mechanismen. In het zenuwstelsel is $[Ca^{2+}]_i$ met name essentieel voor de regulatie van neuronale communicatie, neuronale differentiatie en de uitgroei van neurieten.

Het zenuwstelsel is erg gevoelig en de regeneratieve capaciteiten van neuronen is gering. Elk negatief effect op de chemie, structuur en/of functie van het zenuwstelsel veroorzaakt door een bepaalde blootstelling wordt neurotoxiciteit genoemd. Deze blootstelling kan zowel chemisch (bijvoorbeeld pesticiden) als fysisch (bijvoorbeeld radioactieve straling) zijn. Neurotoxiciteit wordt voornamelijk *in vivo* (dierstudies) onderzocht. Dit is niet alleen ethisch bezwaarlijk, maar ook erg tijdrovend en duur. Een alternatief op *in vivo* experimenten zijn zogenaamde *in vitro* experimenten. Deze gebruiken cellulaire systemen en zorgen niet alleen voor proefdierreductie, maar kunnen ook inzicht geven in het functioneren van neuronale cellen en de mechanismes achter neurotoxiciteit van bepaalde blootstellingen. Verschillende *in vitro*

systemen voor het zenuwstelsel zijn ontwikkeld en de effecten van met name chemische blootstelling zijn daarin succesvol onderzocht. Fysische blootstellingen zijn echter lastiger te onderzoeken, met name wanneer deze te weinig energie bezitten om direct schadelijke effecten te veroorzaken. Een voorbeeld van een dergelijke fysische blootstelling zijn extreem laagfrequente elektromagnetische velden.

Elektromagnetische velden (EMV) ontstaan wanneer elektriciteit wordt gegenereerd, gedistribueerd of gebruikt. EMV bestaan uit een elektrisch en een magnetisch veld en de sterkte ervan wordt vaak uitgedrukt in (micro) Tesla (T of μT). EMV worden vaak ingedeeld aan de hand van hun frequentie en weergegeven in een elektromagnetisch spectrum, dat loopt van statische velden (zoals het aardmagnetisch veld) tot gammastraling. In dit proefschrift ligt de nadruk op EMV met een frequentie van 50 Hz, welke behoren tot de zogenaamde extreem laagfrequente (ELF-) EMV (0–300 Hz). Vanwege hun lage frequentie hebben deze velden weinig energie, maar kunnen zij diep in weefsels doordringen.

Context van dit proefschrift

Sinds in 1979 voor het eerst een studie gepubliceerd werd die een verband aantoonde tussen ELF-EMV en kinderleukemie, is er veel publieke en wetenschappelijke interesse in de mogelijke gezondheidseffecten van ELF-EMV. In de afgelopen decennia is in verschillende studies onderzoek gedaan naar de relatie tussen ELF-EMV en gezondheidseffecten, waaronder neurodegeneratieve ziekten (zoals Parkinson en Alzheimer). Het zenuwstelsel wordt gezien als mogelijk bijzonder gevoelig voor eventuele effecten van ELF-EMV omdat het een van nature gevoelig orgaansysteem is, maar ook omdat diens functie en ontwikkeling bovendien deels afhankelijk is van elektrische signalen. De resultaten van studies naar ELF-EMV effecten op het zenuwstelsel zijn echter niet eenduidig. Een relatie tussen ELF-EMV en effecten op het zenuwstelsel kan niet worden bevestigd, maar ook niet worden uitgesloten. Desondanks hebben de studies rondom kinderleukemie ervoor gezorgd dat het Internationale Agentschap voor Onderzoek naar Kanker (International

Agency For Research on Cancer [IARC]) ELF magnetische velden heeft geclassificeerd als “mogelijk carcinogeen voor mensen”. Het is echter niet bekend welke biologische mechanismen ten grondslag liggen aan eventuele ELF-EMV effecten en er lijkt geen duidelijke relatie te zijn tussen de mate van blootstelling aan EMV en de geobserveerde gezondheidseffecten.

Doel

Het doel van het onderzoek in dit proefschrift is tweeledig; het eerste deel (hoofdstuk 3 t/m 5) van dit proefschrift richt zich op de ontwikkeling en karakterisering van nieuwe *in vitro* cel modellen voor het onderzoeken van het zenuwstelsel, met speciale aandacht voor ontwikkelings-neurotoxiciteit. Deze modellen worden volgens in het tweede deel (hoofdstuk 6 en 7) van dit proefschrift toegepast om de neurotoxiciteit van 50 Hz ELF-EMV te bepalen op volwassen, verouderende en ontwikkelende zenuwcellen *in vitro*.

Overzicht van de hoofdstukken

In hoofdstuk 1 wordt de context van dit proefschrift geschetst. De opbouw en functie van het zenuwstelsel wordt kort toegelicht, extreem laagfrequente elektromagnetische velden worden geïntroduceerd en hun potentiele gezondheidseffecten worden uiteengezet. Aan het eind van het hoofdstuk wordt het doel van dit proefschrift gedefinieerd en de opbouw van de verschillende hoofdstukken toegelicht in de thesis outline. In hoofdstuk 2 worden vervolgens de cel systemen en onderzoekstechnieken toegelicht die in de verschillende onderzoeks-hoofdstukken gebruikt zijn.

Hoofdstuk 3 beschrijft de karakterisering van een nieuw cel model voor verouderde of gestreste zenuwcellen. Het gestreste of verouderde zenuwstelsel wordt onder andere gekenmerkt door oxidatieve schade (veroorzaakt door de verhoogde productie van reactieve zuurstofradicalen [ROS]) en is zeer gevoelig voor omgevingsfactoren, zoals chemische blootstellingen. Het onderzoek in dit hoofdstuk toont aan dat wanneer neuron-achtige cellen (pheochromocytoma cellen, ook wel PC12 cellen) chemisch-voorbehandeld worden met bepaalde stoffen, waaronder ijzer, deze PC12 cellen kenmerken

vertonen van veroudering. Zo hebben ze een verhoogde productie van ROS, een veranderde calcium homeostase en een verhoogde productie van α-synucleïne (een eiwit dat gerelateerd is aan de ziekte van Parkinson). Als proef op de som worden in dit hoofdstuk deze chemisch-voorbehandelde "verouderde" PC12 cellen blootgesteld aan een toxische stof en wordt gemeten hoe schadelijk dit is. Vergeleken met onbehandelde (naïeve) PC12 cellen zijn de chemisch-voorbehandelde cellen gevoeliger voor de toxische stof en daarmee een geschikt model om onderzoek te doen naar effecten van blootstellingen op verouderde of gestreste zenuwcellen.

Ook het ontwikkelende zenuwstelsel is erg gevoelig voor verstoringen van buitenaf. Onderzoek doen naar toxiciteit in een ontwikkelend systeem kent echter een aantal uitdagingen en wordt momenteel voornamelijk *in vivo* gedaan, met name in knaagdieren. Hoofdstuk 4 beschrijft de tekortkomingen van dit *in vivo* onderzoek en geeft eveneens een overzicht van de meest veelbelovende *in vitro* modelsystemen en onderzoekstechnieken die beschikbaar zijn om ontwikkelings-neurotoxiciteit te onderzoeken in cellulaire systemen. Het hoofdstuk benadrukt daarnaast dat het belangrijk is in dit type onderzoek heterogene cel modellen (die zowel neuronen als glia bevatten) te gebruiken en om naast de structuur en de viabiliteit van de cellen, ook hun functionaliteit te testen. Een kleine of tijdelijke verandering in de functionaliteit van een ontwikkelend systeem kan namelijk grote gevolgen hebben in een later stadium, ook zonder dat de cellen structureel zijn aangetast of niet meer levend zijn.

Voorbeelden van de in hoofdstuk 4 beschreven cel modellen voor het ontwikkelende zenuwstelsel zijn primaire kweken (zoals de rat corticale kweken in hoofdstuk 7) en stam- of progenitor cellen. In hoofdstuk 5 worden neuronale progenitor cellen uit de muis gekarakteriseerd als een modelsysteem om ontwikkelings-neurotoxiciteit in te onderzoeken. Deze cellen hebben stamcel-achtige eigenschappen en kunnen prolifereren als "sphere"-vormige groepjes cellen. Wij laten in dit hoofdstuk zien dat deze spheres kunnen worden aangezet tot differentiatie waarna de cellen in zo'n sphere zich gedurende 2 weken ontwikkelen tot een complex netwerk van neuronen en andere cellen van het

zenuwstelsel. Ook laten wij zien dat deze gedifferentieerde cellen niet alleen qua structuur, maar ook qua functie lijken op cellen in het zenuwstelsel. Zo hebben zij een calcium homeostasis die lijkt op die van neuronale cellen en worden zij spontaan elektrisch actief gedurende de ontwikkeling. Neuronale progenitor cellen zijn dus een veelbelovend model om ontwikkelings-neurotoxiciteit in te onderzoeken. Echter kent het gebruik van deze cellen ook nog tekortkomingen die moeten worden opgelost voordat deze cellen op voldoende grote schaal kunnen worden gebruikt. Daarnaast zullen de cellen nog verder moeten worden gekarakteriseerd en gevalideerd voordat zij in regulatoir onderzoek kunnen worden gebruikt.

Zoals eerder beschreven richt het tweede deel van dit proefschrift zich met name op de mogelijk neurotoxische effecten van extreem laagfrequente elektromagnetische velden (ELF-EMV) *in vitro*. In hoofdstuk 6 is het effect van acute en chronische blootstelling aan 50 Hz ELF-EMV onderzocht in onbehandelde, naïeve PC12 cellen en de in hoofdstuk 3 gekarakteriseerde chemisch-voorbehandelde PC12 cellen, een modelsysteem voor het verouderde zenuwstelsel. Hiertoe is het effect van 50 Hz ELF-EMV (veldsterktes 1-1000 µT) onderzocht op verschillende eindpunten die belangrijk zijn voor het functioneren van het zenuwstelsel, waaronder de viabiliteit, de productie van ROS en de calcium homeostase. De experimenten in dit hoofdstuk tonen aan dat 50 Hz ELF-EMV de viabiliteit van naïeve en chemisch-voorbehandelde PC12 cellen niet aantast. De productie van ROS en de calcium homeostase is eveneens onveranderd door de geteste blootstelling aan 50 Hz ELF-EMV. Acute en chronische blootstelling aan ELF-EMV in volwassen en verouderde neuronale cellen *in vitro* lijkt dus geen neurotoxische effecten te veroorzaken.

Hoofdstuk 7 beschrijft het onderzoek naar de effecten van chronische blootstelling aan 50 Hz ELF-EMV tijdens de ontwikkeling van het zenuwstelsel. Primaire corticale kweken uit ratten zijn in dit hoofdstuk gebruikt als modelsysteem voor het ontwikkelende zenuwstelsel. In tegenstelling tot de neuronale progenitor cellen uit hoofdstuk 5 zijn deze corticale kweken uitvoerig gekarakteriseerd en worden al decennia gebruikt in de neurotoxicologie. Het

onderzoek in dit hoofdstuk toont aan dat blootstelling aan 50 Hz ELF-EMV tijdens de ontwikkeling van de corticale kweken bij zeer hoge veldsterktes (1000 µT) de calciumhuishouding en de uitgroei van neurieten beïnvloed, zonder de viabiliteit van de cellen aan te tasten. Echter, de spontane elektrische activiteit in deze kweken, die erg afhankelijk is van een goede calciumhuishouding en netwerkstructuur (neurieten), wordt niet beïnvloed door ELF-EMV blootstelling tot en met 1000 µT. Hoewel 1000 µT een erg hoge blootstelling is, lijken op basis van dit hoofdstuk zowel de veldsterkte als de timing van de blootstelling kritisch te zijn voor het ontstaan van effecten door blootstelling aan ELF-EMV.

Conclusie

Het onderzoek in dit proefschrift heeft zich gericht op de ontwikkeling en karakterisering van nieuwe *in vitro* modelsystemen voor het testen van neurotoxiciteit. Deze modellen zijn vervolgens gebruikt om de neurotoxiciteit van ELF-EMV te onderzoeken. Er is veel onzekerheid en controversie omtrent blootstelling aan ELF-EMV en het onderzoek in dit proefschrift is erop gericht deze onduidelijkheden op te helderen.

In dit proefschrift zijn verschillende veldsterktes en blootstellingsscenario's getest in modelsystemen voor het volwassen, verouderde en ontwikkelende zenuwstelsel. De veldsterktes die daarvoor gebruikt zijn, zijn tot 10.000 maal hoger zijn dan de veldsterktes waar men normaliter dagelijks aan wordt blootgesteld. Het onderzoek toont aan dat enkel chronische blootstelling aan extreem hoge veldsterktes tijdens de ontwikkeling kleine effecten kan hebben op het zenuwstelsel.

Hoewel het onderzoek in dit proefschrift niet alle onduidelijkheden omtrent ELF-EMV blootstelling heeft opgehelderd, draagt het bij aan de kennis omtrent dit onderwerp. Uit dit proefschrift blijkt dat zowel de timing- als de veldsterkte van de blootstelling van invloed is voor het veroorzaken van effecten door ELF-EMV. Echter, op basis van hoofdstuk 6 en 7 van dit proefschrift, samen met de lage humane blootstelling, concluderen wij dat het neurotoxische potentieel van 50 Hz laagfrequente elektromagnetische velden zeer beperkt is.

REFERENCES

Ahlbom, A. (2001). Neurodegenerative diseases, suicide and depressive symptoms in relation to EMF. *Bioelectromagnetics*. Suppl 5, S132-S143.

Ahlbom, A., Day, N., Feychting, M., Roman, E., Skinner, J., Dockerty, J., Linet, M., McBride, M., Michaelis, J., Olsen, J. H., Tynes, T., and Verkasalo, P. K. (2000). A pooled analysis of magnetic fields and childhood leukaemia. *Br. J. Cancer.* 83, 692-698.

Ahlbom, I. C., Cardis, E., Green, A., Linet, M., Savitz, D., Swerdlow, A., and ICNIRP (International Commission for Non-Ionizing Radiation Protection) Standing Committee on Epidemiology. (2001). Review of the epidemiologic literature on EMF and Health. *Environ. Health Perspect.* 109 Suppl 6, 911-933.

Alberio, T., Lopiano, L., and Fasano, M. (2012). Cellular models to investigate biochemical pathways in Parkinson's disease. *FEBS J.* 279, 1146-1155.

Almeida, M., Han, L., Ambrogini, E., Weinstein, R. S., and Manolagas, S. C. (2011). Glucocorticoids and tumor necrosis factor alpha increase oxidative stress and suppress Wnt protein signaling in osteoblasts. *J. Biol. Chem.* 286, 44326-44335.

Andersen, S. L. (2003). Trajectories of brain development: point of vulnerability or window of opportunity? *Neurosci. Biobehav. Rev.* 27, 3-18.

Antonini, R. A., Benfante, R., Gotti, C., Moretti, M., Kuster, N., Schuderer, J., Clementi, F., and Fornasari, D. (2006). Extremely low-frequency electromagnetic field (ELF-EMF) does not affect the expression of alpha3, alpha5 and alpha7 nicotinic receptor subunit genes in SH-SY5Y neuroblastoma cell line. *Toxicol. Lett.* 164, 268-277.

Araque, A. and Navarrete, M. (2010). Glial cells in neuronal network function. *Philos. Trans. R. Soc. Lond. B. Biol. Sci.* 365, 2375-2381.

Arie, Y., Iketani, M., Takamatsu, K., Mikoshiba, K., Goshima, Y., and Takei, K. (2009). Developmental changes in the regulation of calcium-dependent neurite outgrowth. *Biochem. Biophys. Res. Commun.* 379, 11-15.

Asanuma, M., Miyazaki, I., and Ogawa, N. (2003). Dopamine- or L-DOPA-induced neurotoxicity: the role of dopamine quinone formation and tyrosinase in a model of Parkinson's disease. *Neurotox Res.* 5, 165-176.

Atchison, W. D. (1988). Effects of neurotoxicants on synaptic transmission: lessons learned from electrophysiological studies. *Neurotoxicol. Teratol.* 10, 393-416.

Azari, H., Sharififar, S., Rahman, M., Ansari, S., and Reynolds, B. A. (2011). Establishing embryonic mouse neural stem cell culture using the neurosphere assay. *J. Vis. Exp.* (47). pii: 2457.

Balassa, T., Varro, P., Elek, S., Drozdovszky, O., Szemerszky, R., Vilagi, I., and Bardos, G. (2013). Changes in synaptic efficacy in rat brain slices following extremely low-frequency magnetic field exposure at embryonic and early postnatal age. *Int. J. Dev. Neurosci.* 31, 724-730.

Bal-Price, A. K., Hogberg, H. T., Buzanska, L., Lenas, P., van Vliet, E., and Hartung, T. (2010). *In vitro* developmental neurotoxicity (DNT) testing: relevant models and endpoints. *Neurotoxicology.* 31, 545-554.

Barbier, E., Dufy, B., and Veyret, B. (1996). Stimulation of Ca^{2+} influx in rat pituitary cells under exposure to a 50 Hz magnetic field. *Bioelectromagnetics.* 17, 303-311.

Barclay, J. W., Morgan, A., and Burgoyne, R. D. (2005). Calcium-dependent regulation of exocytosis. *Cell Calcium.* 38, 343-353.

Bard, J. L., Kaufman, M. H., Dubreuil, C., Brune, R. M., Burger, A., Baldock, R. A., and Davidson, D. R. (1998). An internet-accessible database of mouse developmental anatomy based on a systematic nomenclature. *Mech. Dev.* 74, 111-120.

Barhoumi, R., Qian, Y., Burghardt, R. C., and Tiffany-Castiglioni, E. (2010). Image analysis of Ca^{2+} signals as a basis for neurotoxicity assays: promises and challenges. *Neurotoxicol. Teratol*. 32, 16-24.

Bellinger, D. C. (2012). Comparing the population neurodevelopmental burdens associated with children's exposures to environmental chemicals and other risk factors. *Neurotoxicology.* 33, 641-643.

Bernabo, N., Tettamanti, E., Russo, V., Martelli, A., Turriani, M., Mattoli, M., and Barboni, B. (2010). Extremely low frequency electromagnetic field exposure affects fertilization outcome in swine animal model. *Theriogenology.* 73, 1293-1305.

Berridge, M., Lipp, P., and Bootman, M. (1999). Calcium signalling. *Curr. Biol.* 9, R157-R159.

Blackman, C. F., Benane, S. G., House, D. E., and Pollock, M. M. (1993). Action of 50 Hz magnetic fields on neurite outgrowth in pheochromocytoma cells. *Bioelectromagnetics.* 14, 273-286.

Bolognin, S., Messori, L., and Zatta, P. (2009). Metal ion physiopathology in neurodegenerative disorders. *Neuromolecular Med.* 11, 223-238.

Bouwens, M., de Kleijn, S., Ferwerda, G., Cuppen, J. J., Savelkoul, H. F., and Kemenade, B. M. (2012). Low-frequency electromagnetic fields do not alter responses of inflammatory genes and proteins in human monocytes and immune cell lines. *Bioelectromagnetics.* 33, 226-237.

Brand, M. D. and Nicholls, D. G. (2011). Assessing mitochondrial dysfunction in cells. *Biochem. J.* 435, 297-312.

Breier, J. M., Gassmann, K., Kayser, R., Stegeman, H., De Groot, D., Fritsche, E., and Shafer, T. J. (2010). Neural progenitor cells as models for high-throughput screens of developmental neurotoxicity: state of the science. *Neurotoxicol. Teratol.* 32, 4-15.

Breier, J. M., Radio, N. M., Mundy, W. R., and Shafer, T. J. (2008). Development of a high-throughput screening assay for chemical effects on proliferation and viability of immortalized human neural progenitor cells. *Toxicol. Sci.* 105, 119-133.

Briz, V., Galofre, M., and Sunol, C. (2010). Reduction of glutamatergic neurotransmission by prolonged exposure to dieldrin involves NMDA receptor internalization and metabotropic glutamate receptor 5 downregulation. *Toxicol. Sci.* 113, 138-149.

Brumback, A. C., Lieber, J. L., Angleson, J. K., and Betz, W. J. (2004). Using FM1-43 to study neuropeptide granule dynamics and exocytosis. *Methods.* 33, 287-294.

Bunch, K. J., Keegan, T. J., Swanson, J., Vincent, T. J., and Murphy, M. F. (2014). Residential distance at birth from overhead high-voltage powerlines: childhood cancer risk in Britain 1962-2008. *Br. J. Cancer.* 110, 1402-1408.

Burr, S. A., and Ray, D. E. (2004). Structure-activity and interaction effects of 14 different pyrethroids on voltage-gated chloride ion channels. *Toxicol. Sci.* 77, 341-346.

Butz, M., Worgotter, F., and van Ooyen, A. (2009). Activity-dependent structural plasticity. *Brain Res. Rev.* 60, 287-305.

Buzanska, L., Sypecka, J., Nerini-Molteni, S., Compagnoni, A., Hogberg, H. T., del Torchio, R., Domanska-Janik, K., Zimmer, J., and Coecke, S. (2009). A human stem cell-based model for identifying adverse effects of organic and inorganic chemicals on the developing nervous system. *Stem Cells.* 27, 2591-2601.

Castano, A., Herrera, A. J., Cano, J., and Machado, A. (2002). The degenerative effect of a single intranigral injection of LPS on the dopaminergic system is prevented by dexamethasone, and not mimicked by rh-TNF-alpha, IL-1beta and IFN-gamma. *J. Neurochem.* 81, 150-157.

Caudle, W. M., Guillot, T. S., Lazo, C. R., and Miller, G. W. (2012). Industrial toxicants and Parkinson's disease. *Neurotoxicology.* 33, 178-188.

Ceccatelli, S., Tamm, C., Zhang, Q., and Chen, M. (2007). Mechanisms and modulation of neural cell damage induced by oxidative stress. *Physiol. Behav.* 92, 87-92.

Chadwick, W., Zhou, Y., Park, S. S., Wang, L., Mitchell, N., Stone, M. D., Becker, K. G., Martin, B., and Maudsley, S. (2010). Minimal peroxide exposure of neuronal cells induces multifaceted adaptive responses. *PLoS One.* 5, e14352.

Chen, Q., Lang, L., Wu, W., Xu, G., Zhang, X., Li, T., and Huang, H. (2013). A meta-analysis on the relationship between exposure to ELF-EMFs and the risk of female breast cancer. *PLoS One.* 8, e69272.

Chen, J., Liufu, C., Sun, W., Sun, X., and Chen, D. (2010). Assessment of the neurotoxic mechanisms of decabrominated diphenyl ether (PBDE-209) in primary cultured neonatal rat hippocampal neurons includes alterations in second messenger signaling and oxidative stress. *Toxicol. Lett.* 192, 431-439.

Cheng, A., Hou, Y., and Mattson, M. P. (2010b). Mitochondria and neuroplasticity. *ASN Neuro.* 2, e00045.

Chiappalone, M., Massobrio, P., and Martinoia, S. (2008). Network plasticity in cortical assemblies. *Eur. J. Neurosci.* 28, 221-237.

Ciejka, E., Kleniewska, P., Skibska, B., and Goraca, A. (2011). Effects of extremely low frequency magnetic field on oxidative balance in brain of rats. *J. Physiol. Pharmacol.* 62, 657-661.

Citri, A. and Malenka, R. C. (2008). Synaptic plasticity: multiple forms, functions, and mechanisms. *Neuropsychopharmacology.* 33, 18-41.

Clancy, B., Finlay, B. L., Darlington, R. B., and Anand, K. J. (2007). Extrapolating brain development from experimental species to humans. *Neurotoxicology.* 28, 931-937.

Clapham, D. E. (2007). Calcium signaling. *Cell.* 131, 1047-1058.

Coecke, S., Goldberg, A. M., Allen, S., Buzanska, L., Calamandrei, G., Crofton, K., Hareng, L., Hartung, T., Knaut, H., Honegger, P., Jacobs, M., Lein, P., Li, A., Mundy, W., Owen, D., Schneider, S., Silbergeld, E., Reum, T., Trnovec, T., Monnet-Tschudi, F., and Bal-Price, A. (2007). Workgroup report: incorporating *in vitro* alternative methods for developmental neurotoxicity into international hazard and risk assessment strategies. *Environ. Health Perspect.* 115, 924-931.

Cookson, M. R. (2009). alpha-Synuclein and neuronal cell death. *Mol. Neurodegener.* 4, 9.

Costa, L. G., Giordano, G., and Guizetti, M. (2011a). Chapter 13: *In vitro* approaches to developmental neurotoxicity. In *Reproductive and Developmental Toxicology*, 1st ed. (R. C. Gupta, Ed.), 159-166. Academic Press, San Diego, CA.

Costa, L. G., Giordano, G., and Guizetti, M. (2011b). *In Vitro* Neurotoxicology: Methods and Protocols. Methods in Molecular Biology - Volume 758, Humana Press, New York, NY.

Costa, L. G. (1998). Neurotoxicity testing: a discussion of *in vitro* alternatives. *Environ. Health Perspect.* 106 Suppl 2, 505-510.

Costin, G. E., Birlea, S. A., and Norris, D. A. (2012). Trends in wound repair: cellular and molecular basis of regenerative therapy using electromagnetic fields. *Curr. Mol. Med.* 12, 14-26.

Council of the European Union. (1999). Council recommendation of 12 July 1999 on the limitation of exposure of the general public to electromagnetic fields (0 Hz to 300 GHz). (1999/519/EC).

Craviso, G. L., Chatterjee, I., and Publicover, N. G. (2003). Catecholamine release from cultured bovine adrenal medullary chromaffin cells in the presence of 60 Hz magnetic fields. *Bioelectrochemistry.* 59, 57-64.

Craviso, G. L., Poss, J., Lanctot, C., Lundback, S. S., Chatterjee, I., and Publicover, N. G. (2002). Intracellular calcium activity in isolated bovine adrenal chromaffin cells in the presence and absence of 60 Hz magnetic fields. *Bioelectromagnetics.* 23, 557-567.

Crofton, K. M., Mundy, W. R., Lein, P. J., Bal-Price, A., Coecke, S., Seiler, A. E., Knaut, H., Buzanska, L., and Goldberg, A. (2011). Developmental neurotoxicity testing: recommendations for developing alternative methods for the screening and prioritization of chemicals. *ALTEX.* 28, 9-15.

Croom, E. L., Shafer, T. J., Evans, M. V., Mundy, W. R., Eklund, C. R., Johnstone, A. F., Mack, C. M., and Pegram, R. A. (2015). Improving *in vitro* to *in vivo* extrapolation by incorporating toxicokinetic measurements: a case study of lindane-induced neurotoxicity. *Toxicol. Appl. Pharmacol.* 283, 9-19.

Culbreth, M. E., Harrill, J. A., Freudenrich, T. M., Mundy, W. R., and Shafer, T. J. (2012). Comparison of chemical-induced changes in proliferation and apoptosis in human and mouse neuroprogenitor cells. *Neurotoxicology.* 33, 1499-1510.

Davila, J. C., Cezar, G. G., Thiede, M., Strom, S., Miki, T., and Trosko, J. (2004). Use and application of stem cells in toxicology. *Toxicol. Sci.* 79, 214-223.

de Groot, M. W., Dingemans, M. M., Rus, K. H., de Groot, A., and Westerink, R. H. (2014a). Characterization of calcium responses and electrical activity in differentiating mouse neural progenitor cells *in vitro*. *Toxicol. Sci.* 137, 428-435.

de Groot, M. W., Kock, M. D., and Westerink, R. H. (2014b). Assessment of the neurotoxic potential of exposure to 50Hz extremely low frequency electromagnetic fields (ELF-EMF) in naive and chemically stressed PC12 cells. *Neurotoxicology.* 44, 358-364.

de Groot, M. W. and Westerink, R. H. (2014). Chemically-induced oxidative stress increases the vulnerability of PC12 cells to rotenone-induced toxicity. *Neurotoxicology.* 43, 102-109.

de Groot, M. W., Westerink, R. H., and Dingemans, M. M. (2013). Don't judge a neuron only by its cover: neuronal function in *in vitro* developmental neurotoxicity testing. *Toxicol. Sci.* 132, 1-7.

de Kleijn, S., Bouwens, M., Verburg-van Kemenade, B. M., Cuppen, J. J., Ferwerda, G., and Hermans, P. W. (2011). Extremely low frequency electromagnetic field exposure does not modulate toll-like receptor signaling in human peripheral blood mononuclear cells. *Cytokine.* 54, 43-50.

Defranchi, E., Novellino, A., Whelan, M., Vogel, S., Ramirez, T., van Ravenzwaay, B., and Landsiedel, R. (2011). Feasibility Assessment of Micro-Electrode Chip Assay as a Method of Detecting Neurotoxicity *in vitro*. *Front. Neuroeng.* 4, 6.

Deitmer JW, Schild D. (2000). Calcium-Imaging, Protocolle und Ergebnisse. In: Ca^{2+} und pH, Ionenmessungen in Zellen und Geweben (Deitmer JW, Schild D, ed). 77-99. Spektrum Akademischer Verleger, Heidelberg.

Di Loreto, S., Falone, S., Caracciolo, V., Sebastiani, P., D'Alessandro, A., Mirabilio, A., Zimmitti, V., and Amicarelli, F. (2009). Fifty hertz extremely low-frequency magnetic field exposure elicits redox and trophic response in rat-cortical neurons. *J. Cell. Physiol.* 219, 334-343.

Dichter, M. A. (1978). Rat cortical neurons in cell culture: culture methods, cell morphology, electrophysiology, and synapse formation. *Brain Res.* 149, 279-293.

Dingemans, M. M., Heusinkveld, H.J., Bergman, Å, van den Berg, M., and Westerink, R. H. (2010a). Bromination pattern of hydroxylated metabolites of BDE-47 affects their potency to release calcium from intracellular stores in PC12 cells. *Environ. Health Perspect.* 118, 519-525.

Dingemans, M. M., van den Berg, M., Bergman, A., and Westerink, R. H. (2010b). Calcium-related processes involved in the inhibition of depolarization-evoked calcium increase by hydroxylated PBDEs in PC12 cells. *Toxicol. Sci.* 114, 302-309.

Donato, R., Miljan, E. A., Hines, S. J., Aouabdi, S., Pollock, K., Patel, S., Edwards, F. A., and Sinden, J. D. (2007). Differential development of neuronal physiological responsiveness in two human neural stem cell lines. *BMC Neurosci.* 8, 36.

Double, K. L., Gerlach, M., Youdim, M. B., and Riederer, P. (2000). Impaired iron homeostasis in Parkinson's disease. *J. Neural Transm. Suppl.* (60), 37-58.

Druwe, I., Freudenrich, T. M., Wallace, K., Shafer, T. J., and Mundy, W. R. (2015). Sensitivity of neuroprogenitor cells to chemical-induced apoptosis using a multiplexed assay suitable for high-throughput screening. *Toxicology.* 333, 14-24.

Duman, J. G., Chen, L., and Hille, B. (2008). Calcium transport mechanisms of PC12 cells. *J. Gen. Physiol.* 131, 307-323.

Dunlop, J., Bowlby, M., Peri, R., Vasilyev, D., and Arias, R. (2008). High-throughput electrophysiology: an emerging paradigm for ion-channel screening and physiology. *Nat. Rev. Drug Discov.* 7, 358-368.

Ek, C. J., Dziegielewska, K. M., Habgood, M. D., and Saunders, N. R. (2012). Barriers in the developing brain and neurotoxicology. *Neurotoxicology.* 33, 586-604.

Elhamdani, A., Brown, M. E., Artalejo, C. R., and Palfrey, H. C. (2000). Enhancement of the dense-core vesicle secretory cycle by glucocorticoid differentiation of PC12 cells: characteristics of rapid exocytosis and endocytosis. *J. Neurosci.* 20, 2495-2503.

Elhamdani, A., Palfrey, C. H., and Artalejo, C. R. (2002). Ageing changes the cellular basis of the "fight-or-flight" response in human adrenal chromaffin cells. *Neurobiol. Aging.* 23, 287-293.

Eriksson, C., Bjorklund, A., and Wictorin, K. (2003). Neuronal differentiation following transplantation of expanded mouse neurosphere cultures derived from different embryonic forebrain regions. *Exp. Neurol.* 184, 615-635.

Falone, S., Grossi, M. R., Cinque, B., D'Angelo, B., Tettamanti, E., Cimini, A., Di Ilio, C., and Amicarelli, F. (2007). Fifty hertz extremely low-frequency electromagnetic field causes changes in redox and differentiative status in neuroblastoma cells. *Int. J. Biochem. Cell Biol.* 39, 2093-2106.

Falone, S., Mirabilio, A., Carbone, M. C., Zimmitti, V., Di Loreto, S., Mariggio, M. A., Mancinelli, R., Di Ilio, C., and Amicarelli, F. (2008). Chronic exposure to 50Hz magnetic fields causes a significant weakening of antioxidant defence systems in aged rat brain. *Int. J. Biochem. Cell Biol.* 40, 2762-2770.

Fellin, T. (2009). Communication between neurons and astrocytes: relevance to the modulation of synaptic and network activity. *J. Neurochem.* 108, 533-544.

Feychting, M., Ahlbom, A., and Kheifets, L. (2005). EMF and health. *Annu. Rev. Public Health.* 26, 165-189.

Flaskos, J., Nikolaidis, E., Harris, W., Sachana, M., and Hargreaves, A. J. (2011). Effects of sub-lethal neurite outgrowth inhibitory concentrations of chlorpyrifos oxon on cytoskeletal proteins and acetylcholinesterase in differentiating N2a cells. *Toxicol. Appl. Pharmacol.* 256, 330-336.

Freire, C. and Koifman, S. (2012). Pesticide exposure and Parkinson's disease: epidemiological evidence of association. *Neurotoxicology.* 33, 947-971.

Frimat, J. P., Sisnaiske, J., Subbiah, S., Menne, H., Godoy, P., Lampen, P., Leist, M., Franzke, J., Hengstler, J. G., van Thriel, C., and West, J. (2010). The network formation assay: a spatially standardized neurite outgrowth analytical display for neurotoxicity screening. *Lab Chip* 10, 701-709.

Fritsche, E., Gassmann, K., and Schreiber, T. (2011). Neurospheres as a model for developmental neurotoxicity testing. *Methods Mol. Biol.* 758, 99-114.

Gandhi, S. and Abramov, A. Y. (2012). Mechanism of oxidative stress in neurodegeneration. *Oxid Med. Cell. Longev.* 2012, 428010.

Gao, H. M., Liu, B., Zhang, W., and Hong, J. S. (2003). Novel anti-inflammatory therapy for Parkinson's disease. *Trends Pharmacol. Sci.* 24, 395-401.

Garcia, S. J., Seidler, F. J., and Slotkin, T. A. (2005). Developmental neurotoxicity of chlorpyrifos: targeting glial cells. *Environ. Toxicol. Pharmacol.* 19, 455-461.

Garcia, A. M., Sisternas, A., and Hoyos, S. P. (2008). Occupational exposure to extremely low frequency electric and magnetic fields and Alzheimer disease: a meta-analysis. *Int. J. Epidemiol.* 37, 329-340.

Gassmann, K., Baumann, J., Giersiefer, S., Schuwald, J., Schreiber, T., Merk, H. F., and Fritsche, E. (2012). Automated neurosphere sorting and plating by the COPAS large particle sorter is a suitable method for high-throughput 3D *in vitro* applications. *Toxicol. In Vitro.* 26, 993-1000.

Gilgun-Sherki, Y., Melamed, E., and Offen, D. (2001). Oxidative stress induced-neurodegenerative diseases: the need for antioxidants that penetrate the blood brain barrier. *Neuropharmacology.* 40, 959-975.

Giordano, G., Kavanagh, T. J., and Costa, L. G. (2009). Mouse cerebellar astrocytes protect cerebellar granule neurons against toxicity of the polybrominated diphenyl ether (PBDE) mixture DE-71. *Neurotoxicology.* 30, 326-329.

Gomez, T. M. and Zheng, J. Q. (2006). The molecular basis for calcium-dependent axon pathfinding. *Nat. Rev. Neurosci.* 7, 115-125.

Gramowski, A., Jugelt, K., Weiss, D. G., and Gross, G. W. (2004). Substance identification by quantitative characterization of oscillatory activity in murine spinal cord networks on microelectrode arrays. *Eur. J. Neurosci.* 19, 2815-2825.

Gramowski, A., Schiffmann, D., and Gross, G. W. (2000). Quantification of acute neurotoxic effects of trimethyltin using neuronal networks cultured on microelectrode arrays. *Neurotoxicology* 21, 331-342.

Greene, L. A. and Tischler, A. S. (1976). Establishment of a noradrenergic clonal line of rat adrenal pheochromocytoma cells which respond to nerve growth factor. *Proc. Natl. Acad. Sci. USA.* 73, 2424-2428.

Greenland, S., Sheppard, A. R., Kaune, W. T., Poole, C., and Kelsh, M. A. (2000). A pooled analysis of magnetic fields, wire codes, and childhood leukemia. Childhood Leukemia-EMF Study Group. *Epidemiology.* 11, 624-634.

Gross, G. W., Harsch, A., Rhoades, B. K., and Gopel, W. (1997). Odor, drug and toxin analysis with neuronal networks *in vitro*: extracellular array recording of network responses. *Biosens. Bioelectron.* 12, 373-393.

Gross, G. W., Williams, A. N., and Lucas, J. H. (1982). Recording of spontaneous activity with photoetched microelectrode surfaces from mouse spinal neurons in culture. *J. Neurosci. Methods.* 5, 13-22.

Grynkiewicz, G., Poenie, M., and Tsien, R. Y. (1985). A new generation of Ca^{2+} indicators with greatly improved fluorescence properties. *J. Biol. Chem.* 260, 3440-3450.

Gubernator, N. G., Zhang, H., Staal, R. G., Mosharov, E. V., Pereira, D. B., Yue, M., Balsanek, V., Vadola, P. A., Mukherjee, B., Edwards, R. H., Sulzer, D., and Sames, D. (2009). Fluorescent false neurotransmitters visualize dopamine release from individual presynaptic terminals. *Science.* 324, 1441-1444.

Halliwell, B. (2006). Oxidative stress and neurodegeneration: where are we now? *J. Neurochem.* 97, 1634-1658.

Hardell, L. and Sage, C. (2008). Biological effects from electromagnetic field exposure and public exposure standards. *Biomed. Pharmacother.* 62, 104-109.

Harrill, J. A., Freudenrich, T. M., Robinette, B. L., and Mundy, W. R. (2011a). Comparative sensitivity of human and rat neural cultures to chemical-induced inhibition of neurite outgrowth. *Toxicol. Appl. Pharmacol.* 256, 268-280.

Harrill, J. A., Robinette, B. L., and Mundy, W. R. (2011b). Use of high content image analysis to detect chemical-induced changes in synaptogenesis *in vitro*. *Toxicol. In Vitro.* 25, 368-387.

Hausherr, V., van Thriel, C., Krug, A., Leist, M., and Schobel, N. (2014). Impairment of glutamate signaling in mouse central nervous system neurons *in vitro* by tri-ortho-cresyl phosphate at noncytotoxic concentrations. *Toxicol. Sci.* 142, 274-284.

Heikkila, T. J., Yla-Outinen, L., Tanskanen, J. M., Lappalainen, R. S., Skottman, H., Suuronen, R., Mikkonen, J. E., Hyttinen, J. A., and Narkilahti, S. (2009). Human embryonic stem cell-derived neuronal cells form spontaneously active neuronal networks *in vitro*. *Exp. Neurol.* 218, 109-116.

Hendriks, H. S., van Kleef, R. G., van den Berg, M., and Westerink, R. H. (2012). Multiple novel modes of action involved in the *in vitro* neurotoxic effects of tetrabromobisphenol-A. *Toxicol. Sci.* 128, 235-246.

Herbert, M. R. (2010). Contributions of the environment and environmentally vulnerable physiology to autism spectrum disorders. *Curr. Opin. Neurol.* 23, 103-110.

Hernandez, R. V., Navarro, M. M., Rodriguez, W. A., Martinez, J. L.,Jr, and LeBaron, R. G. (2005). Differences in the magnitude of long-term potentiation produced by theta burst and high frequency stimulation protocols matched in stimulus number. *Brain Res. Brain Res. Protoc.* 15, 6-13.

Heusinkveld, H. J., Molendijk, J., van den Berg, M., and Westerink, R. H. (2013). Azole fungicides disturb intracellular $Ca2^{+}$ in an additive manner in dopaminergic PC12 cells. *Toxicol. Sci.* 134, 374-381.

Heusinkveld, H. J., Thomas, G. O., Lamot, I., van den Berg, M., Kroese, A. B., and Westerink, R. H. (2010). Dual actions of lindane (gamma-hexachlorocyclohexane) on calcium homeostasis and exocytosis in rat PC12 cells. *Toxicol. Appl. Pharmacol.* 248, 12-19.

Heusinkveld, H. J. and Westerink, R. H. (2011). Caveats and limitations of plate reader-based high-throughput kinetic measurements of intracellular calcium levels. *Toxicol. Appl. Pharmacol.* 255, 1-8.

Hogberg, H. T., Sobanski, T., Novellino, A., Whelan, M., Weiss, D. G., and Bal-Price, A. K. (2011). Application of micro-electrode arrays (MEAs) as an emerging technology for developmental neurotoxicity: evaluation of domoic acid-induced effects in primary cultures of rat cortical neurons. *Neurotoxicology.* 32, 158-168.

Hojevik, P., Sandblom, J., Galt, S., and Hamnerius, Y. (1995). $Ca2^{+}$ ion transport through patch-clamped cells exposed to magnetic fields. *Bioelectromagnetics.* 16, 33-40.

Hondebrink, L., Meulenbelt, J., Meijer, M., van den Berg, M., and Westerink, R. H. (2011a). High concentrations of MDMA ('ecstasy') and its metabolite MDA inhibit calcium influx and depolarization-evoked vesicular dopamine release in PC12 cells. *Neuropharmacology.* 61, 202-208.

Hondebrink, L., Meulenbelt, J., van Kleef, R. G., van den Berg, M., and Westerink, R. H. (2011b). Modulation of human $GABA_A$ receptor function: a novel mode of action of drugs of abuse. *Neurotoxicology* 32, 823-827.

Hondebrink, L., Meulenbelt, J., Rietjens, S. J., Meijer, M., and Westerink, R. H. (2012). Methamphetamine, amphetamine, MDMA ('ecstasy'), MDA and mCPP modulate electrical and cholinergic input in PC12 cells. *Neurotoxicology.* 33, 255-260.

Hondebrink, L., Meulenbelt, J., Timmerman, J. G., van den Berg, M., and Westerink, R. H. (2009). Amphetamine reduces vesicular dopamine content in dexamethasone-differentiated PC12 cells only following L-DOPA exposure. *J. Neurochem.* 111, 624-633.

Howard, A. S., Fitzpatrick, R., Pessah, I., Kostyniak, P., and Lein, P. J. (2003). Polychlorinated biphenyls induce caspase-dependent cell death in cultured embryonic rat hippocampal but not cortical neurons via activation of the ryanodine receptor. *Toxicol. Appl. Pharmacol.* 190, 72-86.

Hug, K., Roosli, M., and Rapp, R. (2006). Magnetic field exposure and neurodegenerative diseases-recent epidemiological studies. *Soz. Praventivmed.* 51, 210-220.

Hung, C. W., Chen, Y. C., Hsieh, W. L., Chiou, S. H., and Kao, C. L. (2010). Ageing and neurodegenerative diseases. *Ageing Res. Rev.* 9 Suppl 1, S36-S46.

IARC Working Group. (2002). Non-Ionizing Radiation, Part 1: Static and Extremely Low-Frequency (ELF) Electric and Magnetic Fields. Available as pdf at: http://monographs.iarc.fr/ENG/Monographs/vol80/mono80.pdf

IEEE Standards Coordinating Committee 28. (2002). IEEE standard for safety levels with respect to human exposure to electromagnetic fields, 0-3 kHz, IEEE - The Institute of Electrical and Electronics Engineers (IEEE Std C95.6-2002). Available as pdf at: http://ieeexplore.ieee.org

International Commission on Non-Ionizing Radiation Protection. (2010). Guidelines for limiting exposure to time-varying electric and magnetic fields (1 Hz to 100 kHz). *Health Phys.* **99,** 818-836.

International Commission on Non-ionizing Radiation Protection. (1998). Guidelines for limiting exposure to time-varying electric, magnetic, and electromagnetic fields (up to 300 GHz). International Commission on Non-Ionizing Radiation Protection. *Health Phys.* **74,** 494-522.

Ivancsits, S., Pilger, A., Diem, E., Jahn, O., and Rudiger, H. W. (2005). Cell type-specific genotoxic effects of intermittent extremely low-frequency electromagnetic fields. *Mutat. Res.* **583,** 184-188.

Jakubowski, W. and Bartosz, G. (2000). 2,7-Dichlorofluorescin Oxidation and Reactive Oxygen Species: what does it measure? *Cell Biol. Int.* **24,** 757-760.

Janac, B., Tovilovic, G., Tomic, M., Prolic, Z., and Radenovic, L. (2009). Effect of continuous exposure to alternating magnetic field (50 Hz, 0.5 mT) on serotonin and dopamine receptors activity in rat brain. *Gen. Physiol. Biophys.* **28 Spec No,** 41-46.

Jiang, H., Luan, Z., Wang, J., and Xie, J. (2006). Neuroprotective effects of iron chelator Desferal on dopaminergic neurons in the substantia nigra of rats with iron-overload. *Neurochem. Int.* **49,** 605-609.

Johansen, C. (2004). Electromagnetic fields and health effects-epidemiologic studies of cancer, diseases of the central nervous system and arrhythmia-related heart disease. *Scand. J. Work Environ. Health.* **30 Suppl 1,** 1-30.

Johnstone, A. F., Gross, G. W., Weiss, D. G., Schroeder, O. H., Gramowski, A., and Shafer, T. J. (2010). Microelectrode arrays: a physiologically based neurotoxicity testing platform for the 21st century. *Neurotoxicology.* **31,** 331-350.

Jurga, M., Lipkowski, A. W., Lukomska, B., Buzanska, L., Kurzepa, K., Sobanski, T., Habich, A., Coecke, S., Gajkowska, B., and Domanska-Janik, K. (2009). Generation of functional neural artificial tissue from human umbilical cord blood stem cells. *Tissue Eng. Part C. Methods.* **15,** 365-372.

Kavet, R., Stuchly, M. A., Bailey, W. H., and Bracken, T. D. (2001). Evaluation of biological effects, dosimetric models, and exposure assessment related to ELF electric- and magnetic-field guidelines. *Appl. Occup. Environ. Hyg.* **16,** 1118-1138.

Kennisplatform ElektroMagnetische Velden. (2009). Hoogspanningslijnen en kinderleukemie. Kennisbericht 2009-004. Herziening 2014. Available as pdf at: http://www.kennisplatform.nl/

Kheifets, L., Ahlbom, A., Crespi, C. M., Draper, G., Hagihara, J., Lowenthal, R. M., Mezei, G., Oksuzyan, S., Schuz, J., Swanson, J., Tittarelli, A., Vinceti, M., and Wunsch Filho, V. (2010a). Pooled analysis of recent studies on magnetic fields and childhood leukaemia. *Br. J. Cancer.* **103,** 1128-1135.

Kheifets, L., Bowman, J. D., Checkoway, H., Feychting, M., Harrington, J. M., Kavet, R., Marsh, G., Mezei, G., Renew, D. C., and van Wijngaarden, E. (2009). Future needs of occupational epidemiology of extremely low frequency electric and magnetic fields: review and recommendations. *Occup. Environ. Med.* **66,** 72-80.

Kheifets, L., Renew, D., Sias, G., and Swanson, J. (2010b). Extremely low frequency electric fields and cancer: assessing the evidence. *Bioelectromagnetics.* **31,** 89-101.

Kheifets, L., Repacholi, M., Saunders, R., and van Deventer, E. (2005). The sensitivity of children to electromagnetic fields. *Pediatrics.* **116,** e303-13.

Kheifets, L. and Shimkhada, R. (2005). Childhood leukemia and EMF: review of the epidemiologic evidence. *Bioelectromagnetics.* **Suppl 7,** S51-9.

Khvotchev, M., Dulubova, I., Sun, J., Dai, H., Rizo, J., and Sudhof, T. C. (2007). Dual modes of Munc18-1/SNARE interactions are coupled by functionally critical binding to syntaxin-1 N terminus. *J. Neurosci.* **27,** 12147-12155.

Kim, H. J., Jung, J., Park, J. H., Kim, J. H., Ko, K. N., and Kim, C. W. (2013). Extremely low-frequency electromagnetic fields induce neural differentiation in bone marrow derived mesenchymal stem cells. *Exp. Biol. Med. (Maywood).* **238,** 923-931.

Kodandaramaiah, S. B., Franzesi, G. T., Chow, B. Y., Boyden, E. S., and Forest, C. R. (2012). Automated whole-cell patch-clamp electrophysiology of neurons *in vivo*. *Nat. Methods.* **9,** 585-587.

Komaki, A., Khalili, A., Salehi, I., Shahidi, S., and Sarihi, A. (2014). Effects of exposure to an extremely low frequency electromagnetic field on hippocampal long-term potentiation in rat. *Brain Res.* **1564,** 1-8.

Kraft, A. D. (2015). The use of glial data in human health assessments of environmental contaminants. *Toxicology.* **333,** 127-136.

Kuegler, P. B., Zimmer, B., Waldmann, T., Baudis, B., Ilmjarv, S., Hescheler, J., Gaughwin, P., Brundin, P., Mundy, W., Bal-Price, A. K., Schrattenholz, A., Krause, K. H., van Thriel, C., Rao, M. S., Kadereit, S., and Leist, M. (2010). Markers of murine embryonic and neural stem cells, neurons and astrocytes: reference points for developmental neurotoxicity testing. *ALTEX.* **27,** 17-42.

Kurkowska-Jastrzebska, I., Litwin, T., Joniec, I., Ciesielska, A., Przybylkowski, A., Czlonkowski, A., and Czlonkowska, A. (2004). Dexamethasone protects against dopaminergic neurons damage in a mouse model of Parkinson's disease. *Int. Immunopharmacol.* **4,** 1307-1318.

Leclerc, C., Neant, I., and Moreau, M. (2011). Early neural development in vertebrates is also a matter of calcium. *Biochimie.* **93,** 2102-2111.

Lefew, W. R., McConnell, E. R., Crooks, J. L., and Shafer, T. J. (2013). Evaluation of microelectrode array data using Bayesian modeling as an approach to screening and prioritization for neurotoxicity testing. *Neurotoxicology.* **36,** 34-41.

Lein, P., Locke, P., and Goldberg, A. (2007). Meeting report: alternatives for developmental neurotoxicity testing. *Environ. Health Perspect.* **115,** 764-768.

Leong, S. L., Cappai, R., Barnham, K. J., and Pham, C. L. (2009). Modulation of alpha-synuclein aggregation by dopamine: a review. *Neurochem. Res.* **34,** 1838-1846.

Lesuisse, C. and Martin, L. J. (2002). Long-term culture of mouse cortical neurons as a model for neuronal development, aging, and death. *J. Neurobiol.* **51,** 9-23.

Li, C. Y., Lee, W. C., and Lin, R. S. (1998). Risk of leukemia in children living near high-voltage transmission lines. *J. Occup. Environ. Med.* **40,** 144-147.

Li, P., McLaughlin, J., and Infante-Rivard, C. (2009). Maternal occupational exposure to extremely low frequency magnetic fields and the risk of brain cancer in the offspring. *Cancer Causes Control.* **20,** 945-955.

Liburdy, R. P., Callahan, D. E., Harland, J., Dunham, E., Sloma, T. R., and Yaswen, P. (1993). Experimental evidence for 60 Hz magnetic fields operating through the signal transduction cascade. Effects on calcium influx and c-MYC mRNA induction. *FEBS Lett.* **334,** 301-308.

Lin, M. T. and Beal, M. F. (2006). Mitochondrial dysfunction and oxidative stress in neurodegenerative diseases. *Nature.* **443,** 787-795.

Lisi, A., Ledda, M., Rosola, E., Pozzi, D., D'Emilia, E., Giuliani, L., Foletti, A., Modesti, A., Morris, S. J., and Grimaldi, S. (2006). Extremely low frequency electromagnetic field exposure promotes differentiation of pituitary corticotrope-derived AtT20 D16V cells. *Bioelectromagnetics.* **27,** 641-651.

Liu, T., Wang, S., He, L., and Ye, K. (2008). Chronic exposure to low-intensity magnetic field improves acquisition and maintenance of memory. *Neuroreport.* **19,** 549-552.

Lohmann, C. (2009). Calcium signaling and the development of specific neuronal connections. *Prog. Brain Res.* **175,** 443-452.

Luk, K. C., Kehm, V., Carroll, J., Zhang, B., O'Brien, P., Trojanowski, J. Q., and Lee, V. M. (2012). Pathological alpha-synuclein transmission initiates Parkinson-like neurodegeneration in nontransgenic mice. *Science.* **338,** 949-953.

Luo, F. L., Yang, N., He, C., Li, H. L., Li, C., Chen, F., Xiong, J. X., Hu, Z. A., and Zhang, J. (2014). Exposure to extremely low frequency electromagnetic fields alters the calcium dynamics of cultured entorhinal cortex neurons. *Environ. Res.* **135,** 236-246.

Mack, C. M., Lin, B. J., Turner, J. D., Johnstone, A. F., Burgoon, L. D., and Shafer, T. J. (2014). Burst and principal components analyses of MEA data for 16 chemicals describe at least three effects classes. *Neurotoxicology.* **40,** 75-85.

Magnani, E. and Bettini, E. (2000). Resazurin detection of energy metabolism changes in serum-starved PC12 cells and of neuroprotective agent effect. *Brain Res. Brain Res. Protoc.* **5,** 266-272.

Mains, R. E. and Patterson, P. H. (1973). Primary cultures of dissociated sympathetic neurons. I. Establishment of long-term growth in culture and studies of differentiated properties. *J. Cell Biol.* **59,** 329-345.

Mattson, M. P. and Kater, S. B. (1987). Calcium regulation of neurite elongation and growth cone motility. *J. Neurosci.* **7,** 4034-4043.

Mattsson, M. O. and Simko, M. (2012). Is there a relation between extremely low frequency magnetic field exposure, inflammation and neurodegenerative diseases? A review of *in vivo* and *in vitro* experimental evidence. *Toxicology.* **301,** 1-12.

McConnell, E. R., McClain, M. A., Ross, J., Lefew, W. R., and Shafer, T. J. (2012). Evaluation of multi-well microelectrode arrays for neurotoxicity screening using a chemical training set. *Neurotoxicology.* **33,** 1048-1057.

McFarlane, E. H., Dawe, G. S., Marks, M., and Campbell, I. C. (2000). Changes in neurite outgrowth but not in cell division induced by low EMF exposure: influence of field strength and culture conditions on responses in rat PC12 pheochromocytoma cells. *Bioelectrochemistry.* **52,** 23-28.

Meijer, M., Brandsema, J. A., Nieuwenhuis, D., Wijnolts, F. M., Dingemans, M. M., and Westerink, R. H. (2015). Inhibition of voltage-gated calcium channels after subchronic and repeated exposure of PC12 cells to different classes of insecticides. *Toxicol. Sci.* **147,** 607-617.

Miller, G. W. (2014). Improving reproducibility in toxicology. *Toxicol. Sci.* **139,** 1-3.

Moors, M., Rockel, T. D., Abel, J., Cline, J. E., Gassmann, K., Schreiber, T., Schuwald, J., Weinmann, N., and Fritsche, E. (2009). Human neurospheres as three-dimensional cellular systems for developmental neurotoxicity testing. *Environ. Health Perspect.* **117,** 1131-1138.

Morabito, C., Guarnieri, S., Fano, G., and Mariggio, M. A. (2010). Effects of Acute and Chronic Low Frequency Electromagnetic Field Exposure on PC12 Cells during Neuronal Differentiation. *Cell. Physiol. Biochem.* **26,** 947-958.

Mundy, W. R., Robinette, B., Radio, N. M., and Freudenrich, T. M. (2008). Protein biomarkers associated with growth and synaptogenesis in a cell culture model of neuronal development. *Toxicology* **249,** 220-229.

National Institute of Environmental Health Sciences. (2002). EMF: Electric and Magnetic Fields Associated with the Use of Electric Power. Available as pdf at: http://www.niehs.nih.gov/

National Radiological Protection Board. (2004). Review of the scientific evidence for limiting exposure to electromagnetic fields (0-300 GHz). Documents of the NRPB. Volume 15, No. 3. Available as pdf at: http://www.elettra2000.it/

National Research Council. (2007). Toxicity Testing in the 21st Century: A Vision and a Strategy. The National Academies Press, Washington, DC. Available online at: http://www.nap.edu/read/11970/chapter/1

Neher, E. and Sakaba, T. (2008). Multiple roles of calcium ions in the regulation of neurotransmitter release. *Neuron.* **59,** 861-872.

Nicolas, J., Hendriksen, P. J., van Kleef, R. G., de Groot, A., Bovee, T. F., Rietjens, I. M., and Westerink, R. H. (2014). Detection of marine neurotoxins in food safety testing using a multielectrode array. *Mol. Nutr. Food Res.* **58,** 2369-2378.

NIOSH. (1996). National Institute for Occupational Safety and Health, National Institute of Environmental Health Sciences, US Department of Energy. Questions and answers - EMF in the workplace. Electric and magnetic fields associated with the use of electric power. NIOSH Publication No. 96-129. Available online at: http://www.cdc.gov/niosh/docs/96-129/

Novellino, A., Scelfo, B., Palosaari, T., Price, A., Sobanski, T., Shafer, T. J., Johnstone, A. F., Gross, G. W., Gramowski, A., Schroeder, O., Jugelt, K., Chiappalone, M., Benfenati, F., Martinoia, S., Tedesco, M. T., Defranchi, E., D'Angelo, P., and Whelan, M. (2011). Development of micro-electrode array based tests for neurotoxicity: assessment of interlaboratory reproducibility with neuroactive chemicals. *Front. Neuroeng.* **4,** 4.

Obeso, J. A., Rodriguez-Oroz, M. C., Goetz, C. G., Marin, C., Kordower, J. H., Rodriguez, M., Hirsch, E. C., Farrer, M., Schapira, A. H., and Halliday, G. (2010). Missing pieces in the Parkinson's disease puzzle. *Nat. Med.* **16,** 653-661.

Obien, M. E., Deligkaris, K., Bullmann, T., Bakkum, D. J., and Frey, U. (2015). Revealing neuronal function through microelectrode array recordings. *Front. Neurosci.* **8,** 423.

OECD. (2007). Guideline for testing of chemicals, No. 426 "Developmental Neurotoxicity Study." Available online at: http://www.oecd-ilibrary.org/docserver/download/9742601e.pdf?expires=1451512549&id=id&accname=guest&checksum=39A3C124D-738D318C6027523D912079B

OECD. (1997). Guideline for testing of chemicals, No. 424 "Neurotoxicity Study in Rodents." Available online at: http://www.oecd-ilibrary.org/docserver/download/9742401e.pdf?expires=1451512700&id=id&accname=guest&checksum=1F07E9661D-1A69539B519520B3B2CE97

Otto, M. and von Muhlendahl, K. E. (2007). Electromagnetic fields (EMF): do they play a role in children's environmental health (CEH)? *Int. J. Hyg. Environ. Health.* **210,** 635-644.

Pall, M. L. (2013). Electromagnetic fields act via activation of voltage-gated calcium channels to produce beneficial or adverse effects. *J. Cell. Mol. Med.* **17,** 958-965.

Pancrazio, J. J., Keefer, E. W., Ma, W., Stenger, D. A., and Gross, G. W. (2001). Neurophysiologic effects of chemical agent hydrolysis products on cortical neurons *in vitro*. *Neurotoxicology* **22**, 393-400.

Park, J. E., Seo, Y. K., Yoon, H. H., Kim, C. W., Park, J. K., and Jeon, S. (2013). Electromagnetic fields induce neural differentiation of human bone marrow derived mesenchymal stem cells via ROS mediated EGFR activation. *Neurochem. Int.* **62,** 418-424.

Pasquale, V., Massobrio, P., Bologna, L. L., Chiappalone, M., and Martinoia, S. (2008). Self-organization and neuronal avalanches in networks of dissociated cortical neurons. *Neuroscience.* **153,** 1354-1369.

Pennings, J. L., Theunissen, P. T., and Piersma, A. H. (2012). An optimized gene set for transcriptomics based neurodevelopmental toxicity prediction in the neural embryonic stem cell test. *Toxicology.* **300,** 158-167.

Pessina, G. P., Aldinucci, C., Palmi, M., Sgaragli, G., Benocci, A., Meini, A., and Pessina, F. (2001). Pulsed electromagnetic fields affect the intracellular calcium concentrations in human astrocytoma cells. *Bioelectromagnetics.* **22,** 503-510.

Piacentini, R., Ripoli, C., Mezzogori, D., Azzena, G. B., and Grassi, C. (2008). Extremely low-frequency electromagnetic fields promote *in vitro* neurogenesis via upregulation of Ca(v)1-channel activity. *J. Cell. Physiol.* **215,** 129-139.

Pirozzoli, M. C., Marino, C., Lovisolo, G. A., Laconi, C., Mosiello, L., and Negroni, A. (2003). Effects of 50 Hz electromagnetic field exposure on apoptosis and differentiation in a neuroblastoma cell line. *Bioelectromagnetics.* **24,** 510-516.

Polk, C. (1974). Sources, propagation, amplitude, and temporal variation of extremely low frequency (0-100 Hz) electromagnetic fields. In: Biological and clinical effects of low frequency magnetic and electric fields (J. G. Llaurado, A. Sances, and J. H. Battoclettie, Eds.) 21-48. Charles C. Thomas, Springfield, Illinois.

Pravettoni, E., Bacci, A., Coco, S., Forbicini, P., Matteoli, M., and Verderio, C. (2000). Different localizations and functions of L-type and N-type calcium channels during development of hippocampal neurons. *Dev. Biol.* **227,** 581-594.

Preece, A. W., Kaune, W., Grainger, P., Preece, S., and Golding, J. (1997). Magnetic fields from domestic appliances in the UK. *Phys. Med. Biol.* **42,** 67-76.

Radio, N. M., Freudenrich, T. M., Robinette, B. L., Crofton, K. M., and Mundy, W. R. (2010). Comparison of PC12 and cerebellar granule cell cultures for evaluating neurite outgrowth using high content analysis. *Neurotoxicol. Teratol.* **32,** 25-35.

Radio, N. M. and Mundy, W. R. (2008). Developmental neurotoxicity testing *in vitro*: models for assessing chemical effects on neurite outgrowth. *Neurotoxicology.* **29,** 361-376.

Radio, N. M., Breier, J. M., Shafer, T. J., and Mundy, W. R. (2008). Assessment of chemical effects on neurite outgrowth in PC12 cells using high content screening. *Toxicol. Sci.* **105,** 106-118.

Raha, S. and Robinson, B. H. (2000). Mitochondria, oxygen free radicals, disease and ageing. *Trends Biochem. Sci.* **25,** 502-508.

Rampersad, S. N. (2012). Multiple applications of Alamar Blue as an indicator of metabolic function and cellular health in cell viability bioassays. *Sensors (Basel).* **12,** 12347-12360.

Reale, M., Kamal, M. A., Patruno, A., Costantini, E., D'Angelo, C., Pesce, M., and Greig, N. H. (2014). Neuronal cellular responses to extremely low frequency electromagnetic field exposure: implications regarding oxidative stress and neurodegeneration. *PLoS One.* **9,** e104973.

Repetto, G., del Peso, A., and Zurita, J. L. (2008). Neutral red uptake assay for the estimation of cell viability/cytotoxicity. *Nat. Protoc.* **3,** 1125-1131.

Rice, D. and Barone, S.,Jr. (2000). Critical periods of vulnerability for the developing nervous system: evidence from humans and animal models. *Environ. Health Perspect.* **108 Suppl 3,** 511-533.

Ringler, S. L., Aye, J., Byrne, E., Anderson, M., and Turner, C. P. (2008). Effects of disrupting calcium homeostasis on neuronal maturation: early inhibition and later recovery. *Cell. Mol. Neurobiol.* **28,** 389-409.

Robinette, B. L., Harrill, J. A., Mundy, W. R., and Shafer, T. J. (2011). *In vitro* assessment of developmental neurotoxicity: use of microelectrode arrays to measure functional changes in neuronal network ontogeny. *Front. Neuroeng.* **4,** 1-9.

Rusanescu, G., Qi, H., Thomas, S. M., Brugge, J. S., and Halegoua, S. (1995). Calcium influx induces neurite growth through a Src-Ras signaling cassette. *Neuron.* **15,** 1415-1425.

Ruszkiewicz, J. and Albrecht, J. (2015). Changes in the mitochondrial antioxidant systems in neurodegenerative diseases and acute brain disorders. *Neurochem. Int.* **88,** 66-72.

Santini, M. T., Rainaldi, G., and Indovina, P. L. (2009). Cellular effects of extremely low frequency (ELF) electromagnetic fields. *Int. J. Radiat. Biol.* **85,** 294-313.

Saunders, R. D. and Jefferys, J. G. (2007). A neurobiological basis for ELF guidelines. *Health Phys.* **92,** 596-603.

Schreiber, T., Gassmann, K., Götz, C., Hübenthal, U., Moors, M., Krause, G., Merk, H. F., Nguyen, N. H., Scanlan, T. S., Abel, J., Rose, C. R., and Fritsche, E. (2010). Polybrominated diphenyl ethers induce developmental neurotoxicity in a human *in vitro* model: evidence for endocrine disruption. *Environ. Health Perspect.* **118,** 572-578.

Schuz, J., Lagorio, S., and Bersani, F. (2009). Electromagnetic fields and epidemiology: an overview inspired by the fourth course at the International School of Bioelectromagnetics. *Bioelectromagnetics.* **30,** 511-524.

Seiler, A., Oelgeschlager, M., Liebsch, M., Pirow, R., Riebeling, C., Tralau, T., and Luch, A. (2011). Developmental toxicity testing in the 21st century: the sword of Damocles shattered by embryonic stem cell assays? *Arch. Toxicol.* **85,** 1361-1372.

Shafer, T. J. and Atchison, W. D. (1991). Transmitter, ion channel and receptor properties of pheochromocytoma (PC12) cells: a model for neurotoxicological studies. *Neurotoxicology.* **12,** 473-492.

Shin, O. H., Rizo, J., and Sudhof, T. C. (2002). Synaptotagmin function in dense core vesicle exocytosis studied in cracked PC12 cells. *Nat. Neurosci.* **5,** 649-656.

Shulman, J. M., De Jager, P. L., and Feany, M. B. (2011). Parkinson's disease: genetics and pathogenesis. *Annu. Rev. Pathol.* **6,** 193-222.

Sieron, A., Brus, R., Szkilnik, R., Plech, A., Kubanski, N., and Cieslar, G. (2001). Influence of alternating low frequency magnetic fields on reactivity of central dopamine receptors in neonatal 6-hydroxydopamine treated rats. *Bioelectromagnetics.* **22,** 479-486.

Sieron, A., Labus, L., Nowak, P., Cieslar, G., Brus, H., Durczok, A., Zagzil, T., Kostrzewa, R. M., and Brus, R. (2004). Alternating extremely low frequency magnetic field increases turnover of dopamine and serotonin in rat frontal cortex. *Bioelectromagnetics*. **25,** 426-430.

Slotkin, T. A., and Seidler, F. J. (2008). Developmental neurotoxicants target neurodifferentiation into the serotonin phenotype: Chlorpyrifos, diazinon, dieldrin and divalent nickel. *Toxicol. Appl. Pharmacol*. **233,** 211-219.

Slotkin, T. A. and Seidler, F. J. (2010). Diverse neurotoxicants converge on gene expression for neuropeptides and their receptors in an *in vitro* model of neurodifferentiation: effects of chlorpyrifos, diazinon, dieldrin and divalent nickel in PC12 cells. *Brain Res.* **1353,** 36-52.

Slotkin, T. A., Seidler, F. J., Wu, C., MacKillop, E. A., and Linden, K. G. (2009). Ultraviolet photolysis of chlorpyrifos: developmental neurotoxicity modeled in PC12 cells. *Environ. Health Perspect*. **117,** 338-343.

Snyder, A. M. and Connor, J. R. (2009). Iron, the substantia nigra and related neurological disorders. *Biochimica et Biophysica Acta (BBA)-General Subjects.* **1790,** 606-614.

Spencer, C. I., Li, N., Chen, Q., Johnson, J., Nevill, T., Kammonen, J., and Ionescu-Zanetti, C. (2012). Ion channel pharmacology under flow: automation via well-plate microfluidics. *Assay Drug Dev. Technol.* **10,** 313-324.

Stiegler, N. V., Krug, A. K., Matt, F., and Leist, M. (2011). Assessment of chemical-induced impairment of human neurite outgrowth by multiparametric live cell imaging in high-density cultures. *Toxicological Sciences.* **121,** 73-87.

Tang, F., Dent, E. W., and Kalil, K. (2003). Spontaneous calcium transients in developing cortical neurons regulate axon outgrowth. *J. Neurosci.* **23,** 927-936.

Taylor, S. C. and Peers, C. (2000). Three distinct $Ca^{(2+)}$ influx pathways couple acetylcholine receptor activation to catecholamine secretion from PC12 cells. *J. Neurochem.* **75,** 1583-1589.

Taylor, S. C. and Peers, C. (1999). Store-operated Ca^{2+} influx and voltage-gated Ca^{2+} channels coupled to exocytosis in pheochromocytoma (PC12) cells. *J. Neurochem.* **73,** 874-880.

Teepen, J. C. and van Dijck, J. A. (2012). Impact of high electromagnetic field levels on childhood leukemia incidence. *Int. J. Cancer.* **131,** 769-778.

Tonini, R., Baroni, M. D., Masala, E., Micheletti, M., Ferroni, A., and Mazzanti, M. (2001). Calcium protects differentiating neuroblastoma cells during 50 Hz electromagnetic radiation. *Biophys. J.* **81,** 2580-2589.

Uttara, B., Singh, A. V., Zamboni, P., and Mahajan, R. T. (2009). Oxidative stress and neurodegenerative diseases: a review of upstream and downstream antioxidant therapeutic options. *Curr. Neuropharmacol.* **7,** 65-74.

Valdivia, P., Martin, M., LeFew, W. R., Ross, J., Houck, K. A., and Shafer, T. J. (2014). Multi-well microelectrode array recordings detect neuroactivity of ToxCast compounds. *Neurotoxicology.* **44,** 204-217.

Vallotton, P., Lagerstrom, R., Sun, C., Buckley, M., Wang, D., De Silva, M., Tan, S. S., and Gunnersen, J. M. (2007). Automated analysis of neurite branching in cultured cortical neurons using HCA-Vision. *Cytometry A.* **71,** 889-895.

VanDemark, K. L., Guizzetti, M., Giordano, G., and Costa, L. G. (2009). Ethanol inhibits muscarinic receptor-induced axonal growth in rat hippocampal neurons. *Alcohol Clin. Exp. Res.* **33,** 1945-1955.

van der Mark, M., Brouwer, M., Kromhout, H., Nijssen, P., Huss, A., and Vermeulen, R. (2012). Is pesticide use related to Parkinson disease? Some clues to heterogeneity in study results. *Environ. Health Perspect.* **120,** 340-347.

van Ooyen, A. (1994). Activity-dependent neural network development. *Network: Computation in Neural Systems.* **5,** 401-423.

van Oss, C. and van Ooyen, A. (1997). Effects of inhibition on neural network development through activity-dependent neurite outgrowth. *J. Theor. Biol.* **185,** 263-280.

van Pelt, J., Vajda, I., Wolters, P. S., Corner, M. A., and Ramakers, G. J. (2005). Dynamics and plasticity in developing neuronal networks *in vitro*. *Prog. Brain Res.* **147,** 173-188.

van Pelt, J., Wolters, P. S., Corner, M. A., Rutten, W. L., and Ramakers, G. J. (2004). Long-term characterization of firing dynamics of spontaneous bursts in cultured neural networks. *IEEE Trans. Biomed. Eng.* **51,** 2051-2062.

van Thriel, C., Westerink, R. H., Beste, C., Bale, A. S., Lein, P. J., and Leist, M. (2012). Translating neurobehavioural endpoints of developmental neurotoxicity tests into *in vitro* assays and readouts. *Neurotoxicology.* **33,** 911-924.

Vergara, X., Kheifets, L., Greenland, S., Oksuzyan, S., Cho, Y. S., and Mezei, G. (2013). Occupational exposure to extremely low-frequency magnetic fields and neurodegenerative disease: a meta-analysis. *J. Occup. Environ. Med.* **55,** 135-146.

Visan, A., Hayess, K., Sittner, D., Pohl, E. E., Riebeling, C., Slawik, B., Gulich, K., Oelgeschläger, M., Luch, A., and Seiler, A. E. (2012). Neural differentiation of mouse embryonic stem cells as a tool to assess developmental neurotoxicity *in vitro*. *Neurotoxicology*. **33,** 1135-1146.

Wallace, K., Strickland, J. D., Valdivia, P., Mundy, W. R., and Shafer, T. J. (2015). A multiplexed assay for determination of neurotoxicant effects on spontaneous network activity and viability from microelectrode arrays. *Neurotoxicology.* **49,** 79-85.

Walleczek, J. (1992). Electromagnetic field effects on cells of the immune system: the role of calcium signaling. *FASEB J.* **6,** 3177-3185.

Walsh, K., Megyesi, J., and Hammond, R. (2005). Human central nervous system tissue culture: a historical review and examination of recent advances. *Neurobiol. Dis.* **18,** 2-18.

Wang, D., Lagerstrom, R., Sun, C., Bishof, L., Valotton, P., and Gotte, M. (2010). HCA-vision: Automated neurite outgrowth analysis. *J. Biomol. Screen.* **15,** 1165-1170.

Weick, J. P., Liu, Y., and Zhang, S. C. (2011). Human embryonic stem cell-derived neurons adopt and regulate the activity of an established neural network. *Proc. Natl. Acad. Sci. USA.* **108,** 20189-20194.

Wertheimer, N. and Leeper, E. (1979). Electrical wiring configurations and childhood cancer. *Am. J. Epidemiol.* **109,** 273-284.

Westerink, R. H. S. (2004). Exocytosis: using amperometry to study presynaptic mechanisms of neurotoxicity. *Neurotoxicology.* **25,** 461-470.

Westerink, R. H. (2013). Do we really want to REACH out to *in vitro*? *Neurotoxicology.* **39,** 169-172.

Westerink, R. H. (2006). Targeting exocytosis: ins and outs of the modulation of quantal dopamine release. *CNS Neurol. Disord. Drug Targets.* **5,** 57-77.

Westerink, R. H., de Groot, A., and Vijverberg, H. P. (2000). Heterogeneity of catecholamine-containing vesicles in PC12 cells. *Biochem. Biophys. Res. Commun.* **270,** 625-630.

Westerink, R. H. and Ewing, A. G. (2008). The PC12 cell as model for neurosecretion. *Acta Physiol. (Oxf).* **192,** 273-285.

Westerink, R. H., Klompmakers, A. A., Westenberg, H. G., and Vijverberg, H. P. (2002). Signaling pathways involved in Ca^{2+}- and Pb^{2+}-induced vesicular catecholamine release from rat PC12 cells. *Brain Res.* **957,** 25-36.

Westerink, R. H. and Vijverberg, H. P. (2002). $Ca^{(2+)}$-independent vesicular catecholamine release in PC12 cells by nanomolar concentrations of $Pb^{(2+)}$. *J. Neurochem.* **80,** 861-873.

Winneke, G. (2011). Developmental aspects of environmental neurotoxicology: lessons from lead and polychlorinated biphenyls. *J. Neurol. Sci.* **308,** 9-15.

Wolff, C., Fuks, B., and Chatelain, P. (2003). Comparative study of membrane potential-sensitive fluorescent probes and their use in ion channel screening assays. *J. Biomol. Screen.* **8,** 533-543.

Wood, C., Williams, C., and Waldron, G. J. (2004). Patch clamping by numbers. *Drug Discov. Today.* **9,** 434-441.

Woodman, R. and Lockette, W. (2009). Alpha-methyltyrosine inhibits formation of reactive oxygen species and diminishes apoptosis in PC12 cells. *Brain Res.* **1296,** 137-147.

World Health Organization. (2007a). "Electromagnetic fields and public health" - Exposure to extremely low frequency fields. *Fact sheet 322*. Available online at: http://www.who.int/peh-emf/publications/facts/fs322/en/

World Health Organization. (2007b). Extremely low frequency fields. *Environmental Health Criteria Monograph No. 238*. Available as pdf at: http://www.who.int/peh-emf/publications/Complet_DEC_2007.pdf?ua=1

World Health Organization. (2002). Establishing a dialogue on risks from electromagnetic fields. Radiation and Environmental Health Department Of Protection Of The Human Environment World Health Organization, Geneva, Switzerland. Available as pdf at: http://apps.who.int/medicinedocs/documents/s17317e/s17317e.pdf

World Health Organization. (1999). EMF Risk Perception and Communication. Available as pdf at: http://www.who.int/peh-emf/publications/reports/ottawa.pdf

Yankner, B. A., Lu, T., and Loerch, P. (2008). The aging brain. *Annu. Rev. pathmechdis. Mech. Dis.* **3,** 41-66.

Yla-Outinen, L., Heikkila, J., Skottman, H., Suuronen, R., Aanismaa, R., and Narkilahti, S. (2010). Human cell-based micro electrode array platform for studying neurotoxicity. *Front. Neuroeng.* **3,** pii: 111.

You, J. M., Yun, S. J., Nam, K. N., Kang, C., Won, R., and Lee, E. H. (2009). Mechanism of glucocorticoid-induced oxidative stress in rat hippocampal slice cultures. *Can. J. Physiol. Pharmacol.* **87,** 440-447.

Zhang, Y., Ding, J., Duan, W., and Fan, W. (2005). Influence of pulsed electromagnetic field with different pulse duty cycles on neurite outgrowth in PC12 rat pheochromocytoma cells. *Bioelectromagnetics.* **26,** 406-411.

Zhang, Y., Liu, X., Zhang, J., and Li, N. (2015). Short-term effects of extremely low frequency electromagnetic fields exposure on Alzheimer's disease in rats. *Int. J. Radiat. Biol.* **91,** 28-34.

Zhong, C., Zhao, T. F., Xu, Z. J., and He, R. X. (2012). Effects of electromagnetic fields on bone regeneration in experimental and clinical studies: a review of the literature. *Chin. Med. J. (Engl).* **125,** 367-372.

Zimmer, B., Kuegler, P. B., Baudis, B., Genewsky, A., Tanavde, V., Koh, W., Tan, B., Waldmann, T., Kadereit, S., and Leist, M. (2011a). Coordinated waves of gene expression during neuronal differentiation of embryonic stem cells as basis for novel approaches to developmental neurotoxicity testing. *Cell Death Differ.* **18,** 383-395.

Zimmer, B., Schildknecht, S., Kuegler, P. B., Tanavde, V., Kadereit, S., and Leist, M. (2011b). Sensitivity of dopaminergic neuron differentiation from stem cells to chronic low-dose methylmercury exposure. *Toxicol. Sci.* **121,** 357-367.

Zurich, M. G., Honegger, P., Schilter, B., Costa, L. G., and Monnet-Tschudi, F. (2004). Involvement of glial cells in the neurotoxicity of parathion and chlorpyrifos. *Toxicol. Appl. Pharmacol.* **201,** 97-104.

DANKWOORD

Dankwoord

En dan is het zover, ik ben aangekomen bij (zeer waarschijnlijk) het meest gelezen deel van mijn proefschrift: het dankwoord. Na 4,5 jaar is het tijd om een warm nest te verlaten en uit te vliegen, maar niet zonder eerst iedereen te bedanken, voor *alles*. Wie mij kent weet dat ik nooit echt om woorden verlegen zit, maar nu schieten woorden toch tekort en ben ik bang iemand te vergeten… Maar ik ga m'n best doen!

Allereerst wil ik Martin en Remco bedanken, promotor en copromotor. Martin, bedankt voor alle vrijheid en voor het vertrouwen dat je in Remco en mij stelde om dit project tot een succesvol einde te brengen. Je input op met name de introductie en de discussie van dit proefschrift is waardevol geweest. Remco, bedankt dat de drempel van jouw kamer zo laag is, dat ik soms bijna naar binnen leek te vallen. Je vertrouwen, steun, (soms plagerige) humor en harde werken hebben me geholpen een zelfstandig onderzoeker te worden. Zonder jou was de reis heel anders geweest. Ik hoop dat we in de toekomst nog vaker samen zullen werken, ik zal je mailtjes op bizarre tijdstippen missen!

Alle (voormalig) neurotox collega's: Aart, Gina, Fiona, Milou, Hester H., Harm, Marieke, Laura, Alfons en alle neurotox studenten die in de afgelopen jaren mee hebben gelopen in onze groep. Bedankt voor alles wat mijn AiO tijd heeft gemaakt tot wat die is geweest: de lunches met Italiaanse broodjes, neurotox-uitjes, BBQ's, pizza-meetings en borrels. Aart, al jouw macro's, technisch hoogstandjes, noodoplossingen voor de ELF-EMV exposure unit en adviezen over de statistiek zijn onmisbaar geweest. Wat moet een lab zonder een Aart?! Gina, voor jou geldt eigenlijk hetzelfde. Bedankt voor alle gezellige gesprekken, het gezamenlijk mopperen, je hulp op het lab, het ontelbare aantal cortex isolaties (samen met Fiona) waar ik gebruik van mocht maken en de experimenten die je van me overnam toen ik het toch echt niet allemaal alleen kon doen. Fiona, ik ben blij dat je halverwege m'n AiO tijd bij neurotox bent gekomen. Ik heb veel gezellige uren met je doorgebracht op de labs en

ben héél blij dat je voorlopig nog bij neurotox aan het werk blijft. Milou, mede dankzij jou is dit proefschrift twee mooie hoofdstukstukken rijker. Bedankt voor de samenwerking, ik heb veel van je geleerd, over de wetenschap en over mezelf. Je gaf me (misschien onbewust) het vertrouwen dat ik als AiO ook best mama kon zijn. Laura, Harm, Hester H. en Marieke, mede neurotox-AiO's, het was fijn om dit samen met jullie te doen. Drie goede voorbeelden gingen me voor (bedankt voor jullie mooie voorbeeld-proefschriften) en Marieke, jij zult me snel volgen, zet 'm op!

(ex) Roommates: Hester P., Jessica, Hester H. Marieke, Soheil, Harm en Annick. Thanks for sharing every moment of success, happiness, deadline stress, disappointment or pure frustration. Thank you for multiplying happiness and for making my burdens easier to bear. Soheil, you never complain and are always kind and interested, it's nice to keep seeing you at the DDW building now and then! I wish you all the best in your final year as a PhD student. Hester H., jij versierde onze kamer tijdens Pasen, Halloween, Sinterklaas en Kerstmis, bedankt dat je het altijd meer "thuis" liet voelen. Veel succes met je nieuwe baan. Hester P., wat leuk om een oud-studiegenoot tegen te komen als AiO op het IRAS. Bedankt voor jouw nuchtere kijk op dingen, je humor en alle uitjes, etentjes en AiO bijeenkomsten die je (mede-) organiseerde! Succes met de laatste loodjes. Marieke, wij deelden niet alleen de AiO-kamer, maar ook vele kamers tijdens congressen. SOT 2014 was daarvan wel het hoogtepunt (bedankt nog dat je zelfs op de grond wilde slapen om mij een bed te geven)! Karin en Maarke, geen roomies, maar soms voelde dat wel bijna zo. Karin, bedankt dat je 5,5 jaar geleden zo enthousiast was over je werk dat ik ook graag op "jouw werk" wilde gaan werken. Maarke, jouw brede interesse en in mijn ogen ongelimiteerde geheugen voor details vind ik heel bijzonder. Ik ben blij dat ook jij bijna bij de eindstreep bent!

Rob, bedankt voor al je hulp met de vele IF-stainings. Ik kon altijd bij jou terecht voor advies, hulp bij het kleuren of een gezellig praatje achter de microscoop. Jan, we spraken soms bijna een andere taal, maar zonder jouw spoelen waren hoofdstuk 6 en 7 er niet geweest. Bedankt voor je hulp en

geduldige uitleg omtrent EMV. Ook anderen die me op wat voor manier dan ook geholpen hebben met mijn onderzoek: heel erg bedankt!

Alle andere Tox-AiO's en Tox-collega's: ik ga jullie niet allemaal bij naam noemen, want dan ben ik bang iemand te vergeten die óók een woordje verdiend. Iedereen bedankt voor de klets-momentjes in de gang, bij de waterkoker, tijdens de lunch en de koekjes op woensdag, maar ook voor gezelligheid tijdens de labuitjes, congressen, etentjes en feestjes. Door jullie interesse in mijn project en in mij als persoon heb ik me altijd op mijn plek gevoeld op het IRAS.

Mijn studenten, Marjolijn, Katinka en Gerike. Bedankt voor jullie inzet en geduld, ik heb zoveel van jullie geleerd. Jullie enthousiasme en harde werken gaven me nieuwe energie als ik die zelf even kwijt was. Marjolijn, mijn eerste student! Ik ben zo blij dat je na je bachelor scriptie nog terug wilde komen voor een master stage. Hoofdstuk 6 was zonder jouw harde werken nooit afgekomen. Katinka, jij werkte hard en zelfstandig; onze MEA-pionier in hoofdstuk 5! Hopelijk zie ik je af en toe nog eens op Anne's verjaardag. Gerike, ondanks dat je maar kort bij ons was, hoop ik dat de stage je veel heeft geleerd over wat je wilt doen in de toekomst.

Al mijn nieuwe collega's bij Farmacologie, het UMC en Nutricia Research: bedankt voor het warme welkom, wat fijn dat jullie zo enthousiast zijn. Als het labuitje, de lunches en borrels indicatief zijn voor hoe gezellig jullie zijn, dan ga ik de komende 1,5 jaar een ontzettend leuke tijd tegemoet!

Lotte, twee AiO's in één vriendschap maakt het nóg moeilijker elkaar regelmatig te zien of spreken. Bedankt dat je zo trouw en geïnteresseerd bent en voor alle keren dat je naar het IRAS kwam fietsen om samen te lunchen of thee te drinken om bij te kletsen, soms last minute of op rare momenten, zodat experimenten tóch door konden gaan. Ik verheug me op jouw promotie (en de vrije ruimte in ons beiden agenda's die daar hopelijk op volgt)!

Alle vrienden bij wie ik kan ontspannen en genieten; van lekkere kippies en BBQ's in de tuin tot urenlange gesprekken op de app of berichtjes op Facebook. Eline, Nanda en Quirine, we zien elkaar niet vaak, maar als we elkaar zien is het altijd goed. Ik geniet van onze vriendschappen!

Lieve Christiaan en Anne, Richard en Marlon, Fransje en Ralph. Wat moet ik zonder jullie? Bedankt voor al jullie gezelligheid, voor het delen van leuke en moeilijke momenten. Voor het luisteren en jullie interesse, maar ook zeker ook voor alle onvergetelijke SinterChrissen, etentjes, feestjes, drankjes en gewoon jullie berichtjes op de app. Laten we nog lang samen blijven!

Ladies: Anique, Marlous en Marlon, bedankt dat we ondanks onze drukke agenda's toch altijd tijd vinden om thee te drinken, te bonen, naar de film te gaan, te eten, te shoppen, of gewoon samen te zijn. Ik kan alles met jullie delen, jullie vriendschap is me heel dierbaar. Marlon, lieve drollie, ik ben zo blij dat je de kaft van mijn proefschrift wilde ontwerpen. Je hebt mijn verwachtingen overtroffen!

Mijn lieve schoonfamilie: Jan en Anke, Jasper en Ilona (met Sanna en Tibbe), Iris en Roel (met Marijn en binnenkort nog een neefje of nichtje), Elsa en Max, Erwin en Eefje. Wat zijn jullie een fijne, gezellige, soms drukke maar altijd lieve familie, ik ben blij dat ik deel uit mag maken van jullie gezin. Elsa en Anke, bedankt dat jullie zo goed voor Lise zorgen, zo kon ik onbezorgd mama en AiO zijn. Laten we een goed feestje vieren!

Lieve broers en zussen: Hans en Kim, Saskia en Corinne; Maarten en Anne-Marie, Jorte, Lobke, Jip en Noor; Carolijn en Albert, Sascha; Hanneke en Cees; en Gijs en Jente. Ooms en tantes, (achter-) neven en nichten: bedankt voor jullie gezelligheid, jullie interesse in mijn project en voor het begrip als ik ergens niet bij kon zijn (omdat ik "te druk" was). Wat heb ik een fijne familie! Tante Herma, bedankt voor alle winkel momentjes, je bezorgdheid, interesse en dat je zo trots op me bent. Ik weet zeker dat oom Jo meekijkt en ook trots op me is!

Gijs en Richard, mijn paranimfen, bedankt dat jullie meteen ja zeiden, ook zonder te weten wat dat precies inhield. Door jullie had ik het gevoel dat ik het niet allemaal alleen hoefde te doen. Wat fijn dat jullie planningen maakten, meedachten over locaties en dj's en zelfs jullie stropdassen wilden matchen met mijn outfit. Met jullie aan mijn zijde ga ik vandaag zelfverzekerd mijn verdediging tegemoet.

Lieve papa en mama, het is zover: ik ga promoveren! Bedankt voor jullie vertrouwen en interesse, al jullie hulp met het nakijken van stukken (jullie verdien allebei een punt van het eindcijfer) en voor het meedenken over moeilijke vraagstukken of dilemma's binnen (of buiten) mijn onderzoek. Ik denk niet dat er veel mensen zijn wiens beide ouders zoveel van hun proefschrift zullen begrijpen als jullie van het mijne. Maar ook bedankt voor jullie liefde en alle mogelijkheden die jullie mij hebben geboden. Bedankt dat jullie mij ontlasten als dat nodig is en zo goed zorgen voor mijn kleine Lise. Het is fijn te weten dat er goed voor haar gezorgd wordt als ik druk aan het werk ben. Ik weet dat jullie als kritische wetenschappers zelfs nog graag achter de opponententafel hadden gezeten, maar ik hoop dat jullie vandaag op de eerste rij vooral zullen genieten als trotse ouders!

Allerliefste Thomas, je had gelijk: het is allemaal goed gekomen! Jij hebt daar altijd in geloofd en mij daar stug van overtuigd als ik het niet meer zag zitten. Wat bof ik dat het eten zo vaak al klaar stond, je nooit boos was als ik later thuis kwam dan ik had beloofd en dat je begrijpt waarom het allemaal zo belangrijk voor me is. Bedankt dat je er altijd voor me bent en je je leven met mij (en inmiddels ons) wilt delen. Ik heb je lief!

Allerliefste Lise, van alle prestaties over de afgelopen 4,5 jaar, ben ik op jou het meest trots. Mama is nu klaar met promoveren, het is tijd voor een feestje: Hiep Hiep, Hoeraaaa!

Martje

ABOUT THE AUTHOR

Martje de Groot

Martje de Groot was born on October 1st, 1987 in Delft and grew up in Sassenheim and Zeist. After her graduation from secondary school at the Christelijk Lyceum Zeist (Zeist, The Netherlands) in 2005, she started her study Pharmacy at Utrecht University (Utrecht, The Netherlands). During her bachelor pharmacy she did an internship at the department of toxicology and applied pharmacology at TNO Quality of Life (Zeist, The Netherlands). She obtained her bachelor degree (cum laude) in 2008 and started a master Drug Innovation at Utrecht University that same year. During her master, Martje did her internships at the department of Psychopharmacology (Utrecht University, The Netherlands) and at the department of Immune Therapeutics, Schering-Plough (Oss, The Netherlands). Martje obtained her master degree (cum laude) at the end of 2010. From January 2011 until June 2015, she worked as a PhD student under supervision of Dr. Remco H.S. Westerink and Prof. Dr. Martin van den Berg on the research presented in this thesis, which was part of the larger ZonMw funded project "Electromagnetic fields and Health" ("Elektromagnetische velden en gezondheid"). During her PhD study, she also completed several postgraduate courses of the postgraduate education in toxicology (PET) program to obtain a registration as European registered toxicologist. Martje is currently working as a post-doc at the department of Pharmacology (Utrecht University, The Netherlands) on the NWO funded project "Prenatal maternal infection: how diet influences behaviour in the offspring".

Training, Conferences and Prizes

Training

Experimental Neurophysiology Course, 2011, The Graduate School of Neurosciences Amsterdam Rotterdam (ONWAR), VU University Amsterdam, the University of Amsterdam and the Erasmus medical center (1,4 ECTS).

Supervising Research Course, 2011, Centre for Education and Learning, Utrecht University (1,5 ECTS).

How to deal with magnetic field exposure in the workplace, 2011, Institute for Risk Assessment Sciences, Universiteit Utrecht (2 day short course).

Food Toxicology and Food Safety, 2011, Postgraduate Education in Toxicology (P.E.T.) course, Wageningen University (1,5 ECTS).

Toxicological Risk Assessment, 2011, Postgraduate Education in Toxicology (P.E.T.) course, Wageningen University (3 ECTS).

Medical and Forensic Toxicology, 2012, Postgraduate Education in Toxicology (P.E.T.) course, Universiteit Utrecht (2 ECTS).

Organ Toxicology, 2012, Postgraduate Education in Toxicology (P.E.T.) course, Radboud University Nijmegen (1,5 ECTS).

Risk Communatication, 2012, Postgraduate Education in Toxicology (P.E.T.) course, Utrecht University (1,5 ECTS).

Molecular Toxicology, 2012, Postgraduate Education in Toxicology (P.E.T.) course, VU University Amsterdam (1,5 ECTS).

Ecotoxicology, 2013, Postgraduate Education in Toxicology (P.E.T.) course, Wageningen University (3 ECTS).

Workshop career perspectives, 2014, Graduate School of Life Sciences, UMC Utrecht, Utrecht University (0,3 ECTS).

Epidemiology, 2015, Postgraduate Education in Toxicology (P.E.T.) course, Utrecht University (1,5 ECTS).

Conference abstracts

de Groot, M.W.G.D.M. and Westerink, R.H.S. *In vitro* assessment of the neurotoxic potential of acute exposure to 50 Hz Extremely Low Frequency Electromagnetic Fields in PC12 cells. Poster presentation at the annual meeting of the Dutch Society of Toxicology (NVT), 2011, Zeist, The Netherlands.

de Groot, M.W.G.D.M. and Westerink, R.H.S. Acute exposure to 50 Hz Extremely Low Frequency Electromagnetic Fields does not affect Ca^{2+}-homeostasis in four different PC12 cell models. Poster presentation at the annual meeting of the Dutch Society of Toxicology (NVT), 2012, Zeist, The Netherlands.

de Groot, M.W.G.D.M. and Westerink, R.H.S. Chemically-induced aging of PC12 cells to study *in vitro* neurodegeneration. Oral presentation at the annual meeting of the Dutch Society of Toxicology (NVT), 2013, Zeist, The Netherlands.

de Groot, M.W.G.D.M. and Westerink, R.H.S. Chemically-induced aging of PC12 cells to study *in vitro* neurodegeneration. Poster presentation at the annual meeting of the Society of Toxicology (SOT), 2013, San Antonio, Texas, USA.

de Groot, M.W.G.D.M. and Westerink, R.H.S. Chemically-induced aging of PC12 cells to study *in vitro* neurodegeneration. Poster presentation at the bi-annual meeting of the International Neurotoxicology Association (INA), 2013, Egmond aan Zee, The Netherlands.

de Groot, M.W.G.D.M., Dingemans, M.M.L, Rus, K.H., de Groot, A., and Westerink, R.H.S. Development of calcium responses and electrical activity in differentiating mouse neural progenitor cells *in vitro*. Poster presenation at the annual meeting of the Society of Toxicology (SOT), 2014, Phoenix, Arizona, USA.

de Groot, M.W.G.D.M., Dingemans, M.M.L., Rus, K.H., de Groot, A., and Westerink, R.H.S. Development of calcium response and electrical activity in differentiating mouse neural progenitor cells *in vitro*. Oral presentation at bi-annual meeting of the European Society of Toxicology *In Vitro* (ESTIV), 2014, Egmond aan Zee, The Netherlands.

de Groot, M.W.G.D.M., Kock, M.D.M., and Westerink, R.H.S. Assessment of the neurotoxic potential of 50 Hz extremely low frequency electromagnetic fields in naïve and chemically stressed PC12 cells. Oral and poster presenation at the annual meeting of the Dutch Society of Toxicology (NVT), 2014, Veldhoven, The Netherlands.

de Groot, M.W.G.D.M., van Kleef, R.G.D.M., de Groot, A. and Westerink, R.H.S. Assessment of the neurotoxic potential of developmental exposure to 50 Hz extremely low frequency electromagnetic fields (ELF-EMF) in primary rat cortical cultures. Oral presenatation at the annual meeting of the Dutch Society of Toxicology (NVT), 2015, Soesterberg, The Netherlands.

Prizes

1st Prize for best debator at the annual meeting of the Dutch Society for Toxicology (Nederlandse Vereniging voor Toxicologie [NVT]), 2012, Woudenberg, The Netherlands.

3rd Prize for Best Scientific Poster (Chemically-induced aging of PC12 cells to study *in vitro* neurodegeneration) at the bi-annual meeting of the International Neurotoxicology Association (INA), 2013, Egmond aan Zee, The Netherlands.

2nd Prize for best Young Scientist Oral Presentation (Development of calcium response and electrical activity in differentiating mouse neural progenitor cells *in vitro*) at the bi-annual meeting of the European Society of Toxicology *In Vitro* (ESTIV), 2014, Egmond aan Zee, The Netherlands.

1st Prize for Best Oral Presentation (Assessment of the neurotoxic potential of developmental exposure to 50 Hz extremely low frequency electromagnetic fields [ELF-EMF] in primary rat cortical cultures) at the annual meeting of the Dutch Society for Toxicology (Nederlandse Vereniging voor Toxicologie [NVT]), 2015, Soesterberg, The Netherlands.

List of Publications

de Groot, M.W.G.D.M., Westerink, R.H.S, Dingemans, M.M.L. (2013). Don't judge a neuron only by its cover: neuronal function in *in vitro* developmental neurotoxicity testing. *Toxicol. Sci*. **132**; 1-7

de Groot, M.W.G.D.M., Dingemans, M.M.L., Rus, K.H., de Groot, A., Westerink, R.H.S. (2014) Characterization of calcium response and electrical activity in differentiating mouse neural progenitor cells *in vitro*. *Toxicol. Sci.* **137**(2); 428-35

de Groot, M.W.G.D.M., Kock, M.D., Westerink, R.H. (2014). Assessment of the neurotoxic potential of exposure to 50 Hz extremely low frequency electromagnetic fields (ELF-EMF) in naïve and chemically stressed PC12 cells. *Neurotoxicology.* **44**; 358-64

de Groot, M.W.G.D.M. and Westerink, R.H.S. (2014). Chemically-induced aging of PC12 cells to study *in vitro* neurodegeneration. *Neurotoxicology.* **43**; 102-9

de Groot, M.W.G.D.M., van Kleef, R.G.D.M., de Groot, A., Westerink R.H.S. (2015). *In vitro* developmental neurotoxicity following chronic exposure to 50 Hz extremely low frequency electromagnetic fields (ELF-EMF) in primary rat cortical cultures. *Toxicol. Sci*. advance online acces: doi: 10.1093/toxsci/kfv242

In this thesis, novel model systems for *in vitro* neurotoxicity testing were developed and characterized, with a special focus on developmental neurotoxicity. These model systems were used to investigate the *in vitro* neurotoxicity of exposure to 50 Hz extremely low frequency electromagnetic fields (ELF-EMF). Using different and sensitive *in vitro* models for adult, aging/stressed and developing neuronal cells, the potential neurotoxic effects of a variety of EMF exposure scenarios and field strengths were thoroughly investigated. At the same time, the use of *in vitro* models allowed for the investigation of the biological mechanisms underlying any observed effects.

Universiteit Utrecht
Institute for Risk Assessment Sciences